University of Stavanger

Faculty of Science and Technology

MASTER'S THESIS

Study program/Specialization: Master´s degree in Biological Chemistry	Spring semester, 2020 Open access
Writer: Nabeela Zaman	…… (Writer's signature)
Faculty supervisors: Cathrine Lillo, Maria Terese Creighton External supervisor(s):	
Thesis title: Methylation of PP2A in Arabidopsis – Stress tolerance and gene expression analysis	
Credits (ECTS): 60	
Key words: *Arabidopsis thaliana*, PP2A, Catalytic subunit, LCMT1, Sulfur deficiency, Stress tolerance, Salt stress, Oxidative stress, Gene expression analysis.	Pages: 80 Stavanger, 15/06/2020 Date/year

Methylation of PP2A in Arabidopsis – Stress tolerance and gene expression analysis

University of Stavanger

Faculty of Science and Technology

Master's degree in Biological Chemistry

June, 2020

Nabeela Zaman

Acknowledgment

I would like to express my deepest gratitude to my supervisors, Professor Cathrine Lillo and Dr. Maria Terese Creighton for giving me the opportunity to work in this interesting project. I am grateful to Prof. Cathrine Lillo for her excellent supervision, valuable advice and suggestions throughout the writing of my thesis. I want to specially thank Dr. Maria Terese Creighton for her continuous help and guidance in the laboratory. I greatly appreciate her for being so patient and support me every time.

My sincere thank goes to Dr. Behzad Heidari, Dr. Dugassa Nemie-Feyissa and PhD student Irina O. Averkina for always being willing to help if needed and also for creating an enjoyable working environment.

Finally, but not the least, I would like to thank my family for all the encouragements and supports through ups and downs, specially Ashraf for being with me in all situations.

I dedicate this thesis to my parents for their unconditional love. Thank you for giving me strength. I miss you every day.

Abstract

PP2A is a highly conserved enzyme complex in eukaryotes that is involved in various signal transduction pathways including hormone-regulated pathways in plants. This enzyme is composed of catalytic C, scaffolding A, and regulatory B subunit. The PP2A activity is regulated by methylation of terminal amino acid leucine in the catalytic subunit C. Leucine carboxyl methyl transferase 1 (LCMT1) is an enzyme that methylates PP2A by using S-adenosyl-L-methionine (SAM) as methyl donor. The *lcmt1* mutant, where the LCMT1 enzyme is knocked out possesses unmethylated PP2A-C. This mutant still grows almost as WT under standard growth conditions, yet with some phenotypic differences such as more elongated leaves and earlier flowering than WT. However, as this regulatory mechanism, e.g., methylation of PP2A, is conserved from yeast to mammals and different species of plants, it is believed to be crucial for plant survival under certain types of stresses. We here investigated the importance of PP2A methylation in *Arabidopsis thaliana* under competitive conditions and evaluated certain genes that strongly influenced by the methylation status of PP2A-C. The oxidative stress devastatingly stunted the growth of *lcmt1*, whereas the root lengths of the mutant were more significantly affected than WT under high salt stress. The differences between WT and *lcmt1* regarding the morphological responses toward nutrient deficiency or toxicity were striking. The root lengths of the mutant were remarkably inhibited under sulfur deficiency and sulfur toxicity, whereas withdrawal of three important nutrients such as Mg, S and Cl crucially impaired both shoot weight and root length of the mutant compared to WT Arabidopsis. Our analysis of several genes involved in the Fe assimilation pathway and sulfur uptake pointed out some fascinating facts related to the defensive capability of the mutant under stress. We noticed a comparatively lower expression of Sulfate transporter 1;2 (*SULTR1;2)* and Sulphur deficiency induced 1 (*SDI1)* genes in *lcmt1*, when compared with WT upon sulfur depletion, which indicated less sulfur uptake by the mutant. Furthermore, Fe superoxide dismutase 1 (*FSD1*) was up-regulated and Protein phosphatase 2A subunit A2 (*PP2AA2*) was down-regulated in the *lcmt1* mutant during sulfur depletion, hence showed higher ROS production and weaker PP2A-A2 subunit, respectively, when compared to WT.

Abbreviations

½ MS medium	Half strength Murashige and Skoog medium
ABA	Abscisic acid
BHLH100	Basic helix-loop-helix type 100
Bp	Base pairs
cDNA	Complementary DNA
FRO	Ferric reduction oxidase family
FSD1	Fe superoxide dismutase 1
IRT1	Iron-regulated transporter 1
LCMT-1	Leucine carboxyl methyltransferase 1 enzyme
NA	Nicotianamine
NAS	Nicotianamine synthase family
PKs	Protein kinases
PP2A	Protein phosphatase 2A
PP2AA2	Protein phosphatase type 2A subunit A2
PP2Ac	Protein phosphatase type 2A catalytic subunit
PPP	Phosphoserine/phosphothreonine specific protein phosphatase
PTP	Phospho-tyrosine phosphatase
RCN1	ROOTS CURL IN NAPHTHYLPHTHALAMIC ACID1
ROS	Reactive oxygen species
RT-PCR	Real-time polymerase chain reaction
S	Sulfur
SBI1	Suppressor of brassinosteroid insensitive 1
SDI1	Sulphur deficiency induced 1
SE	Standard error
SULTR1;2	Sulfate transporter 1;2
WT	Wild type
WT	Wild type

Table of Contents

Acknowledgment I
Abstract II
Abbreviations III
1 Introduction 1
1.1 Reversible protein phosphorylation 1
1.2 Protein Phosphatases 2
1.3 Ser/Thr phosphoprotein phosphatases 2
1.4 Protein Phosphatase 2A 3
1.4.1 PP2A Structure 3
1.4.2 PP2A subunits 4
1.5 Regulatory subunits 6
1.6 Leucine carboxyl methyl transferase 1 (LCMT1) 7
1.7 Sulfur in plant 7
1.7.1 Sulfur starvation 8
1.7.2 The genes involved in sulfur starvation 8
1.8 Abiotic Stress 9
1.8.1 Salt Stress 9
1.8.2 Oxidative stress 10
1.9 Objectives of the Present Study 12
2 Materials and Methods 13
2.1 Plant material 13
2.2 Solutions and media 13
2.2.1 Hoagland solution 13
2.2.2 ½ MS (Murashige and Skoog) solution 14
2.3 Other materials 15
2.4 Transfer of seedling to vermiculite 15
2.5 Transfer of seedling to rockwool 16
2.6 Surface sterilization of seeds 16
2.7 Stress tolerance experiment 16
2.7.1 Sulfur experiment 16

2.7.2 NaCl experiment 16
2.7.3 H_2O_2 experiment 17
2.7.4 Chlorophyll assay 17
2.8 Gene expression analysis 17
2.8.1 RNA extraction 17
2.8.2 cDNA synthesis 19
2.8.3 In-gel analysis 20
2.8.4 Real-time PCR 22
3 Results 23
3.1 Phenotype 23
3.1.1 Arabidopsis transferred in vermiculite 23
3.1.2 Arabidopsis transferred in rockwool 25
3.2 Stress experiments 26
3.2.1 Sulphur experiment 26
3.2.2 NaCl experiment 29
3.2.3 H_2O_2 experiment 32
3.3 Gene expression analysis 36
3.3.1 In-gel analysis 36
3.3.2 Real-time PCR 44
4 Discussion 49
4.1 S-deficiency induced chlorosis 49
4.2 Effects of S-deficiency in absence of methylation 50
4.3 Arabidopsis seedlings grown in Hoagland media 50
4.4 Arabidopsis response to salt stress 51
4.5 H_2O_2 induced oxidative stress 52
4.6 In-gel gene expression analysis of Arabidopsis 53
4.7 Gene expression analysis by RT-PCR 54
4.8 Confounding variables and sources of errors 55
5 Conclusion and future perspective 57
5.1 Conclusion 57
5.2 Future perspective 57

6 References 58
APPENDIX 69
A. Phenotypic difference between WT and *lcmt1* 69
A.1 Arabidopsis grown in vermiculite 69
A.2. Arabidopsis grown in rockwool 71
B. Stress experiments 72
B.1. Sulphur experiment 72
B.2. NaCl experiment 73
B.3. H_2O_2 experiment 76
C. Gene expression analysis 78
C.1. In-gel analysis 78
C.2. Real-time PCR 79

1 Introduction

1.1 Reversible protein phosphorylation

Proteins undergo post-translational modification by reversible protein phosphorylation. The post-translational modification of protein is a major mechanism to regulate the diverse cellular processes and is performed by a protein kinase and a phosphoprotein phosphatase (Meimoun et al., 2007; Zolnierowicz and Bollen, 2000).

The reversible protein phosphorylation is regulated by the interplay of protein kinases (PKs) and protein phosphatases (Okamura et al., 2017). In the protein phosphorylation process, protein kinase enzyme transfers the terminal phosphate group of adenosine triphosphate (ATP) to a specific amino acid side chain on a target protein (Alberts et al., 2013). In the dephosphorylation process, the phosphoester bond becomes hydrolyzed and the phosphate group from the target protein is removed by protein phosphatases (Luan, 2003).

The reversible protein phosphorylation mainly alters the structural conformation of proteins which ultimately leads to changes in protein cellular localization, activation, deactivation as well as stability of the protein (Olsen et al., 2006; Pesaresi et al., 2011; Humphrey et al., 2015). Intracellular signal transduction and enzymatic activity are also impacted by these biological processes.

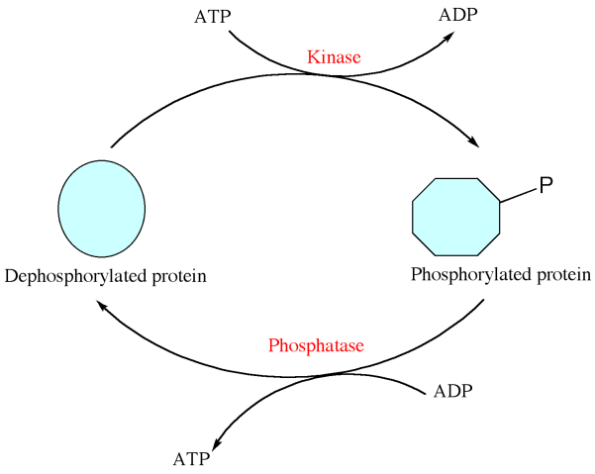

Figure 1.1. Schematic diagram of phosphorylation and dephosphorylation process. In the reaction, protein kinases transfer the phosphate group of ATP to the target protein, while protein phosphatases remove the phosphate from the protein. The conformational changes in protein structure due to phosphorylation and dephosphorylation is shown in the diagram. The figure is obtained from Raimi et al., 2014.

In eukaryotes, about one-third of proteins are modified by reversible phosphorylation process (Cohen, 2001; Olsen et al., 2006; Pesaresi et al., 2011). Some amino acids are prone to post-translational phosphorylation including serine, threonine, tyrosine, arginine, lysine, aspartate, glutamate, histidine, and cysteine (Moorhead et al., 2009). About 1125 protein kinases and 150 protein phosphatases are encoded in the genome of *Arabidopsis thaliana* to control the phosphorylation status (Kerk et al., 2008). However, the functions of protein kinases are recognized for a long time, protein phosphatases are much less studied than protein kinases (DeLong, 2006; Brautigan, 2013; Uhrig et al., 2013b).

1.2 Protein Phosphatases

Protein phosphatases are signal transducing enzymes that catalyze dephosphorylation reactions through different enzymatic mechanisms. Eukaryotic protein phosphatases can be divided into four gene families that are serine/threonine specific phospho-protein phosphatases (PPP), Mg^{2+} dependent protein phosphatases (PPM/PP2C), phospho-tyrosine phosphatases (PTP) and Asp-based phosphatases (Kerk et al., 2008; Lillo et al., 2014). Protein phosphatases are structurally and evolutionary varied from each other whereas, all the protein kinases share similar motifs and folded structures (Kerk et al., 2002).

1.3 Ser/Thr phosphoprotein phosphatases

The Ser/Thr phosphoprotein phosphatases (PPPs) are responsible for 80% of protein phosphatase activity in eukaryotic cells and are further divided into sub-groups such as PP1, PP2/PP2A, PP3/PP2B, PP4, PP5, PP6, PP7, PPKL/Kelch and bacterial like protein phosphatases (Uhrig et al., 2013a,b; Maselli et al., 2014).

PPPs play a major role in modulating the activity and specificity of catalytic subunits, targeting the enzymes to specific locations and cellular signaling in plants. There are 26 genes that encode the catalytic subunits of Arabidopsis Ser/Thr phosphoprotein phosphatases (Farkas et al., 2007; Figure 1.2).

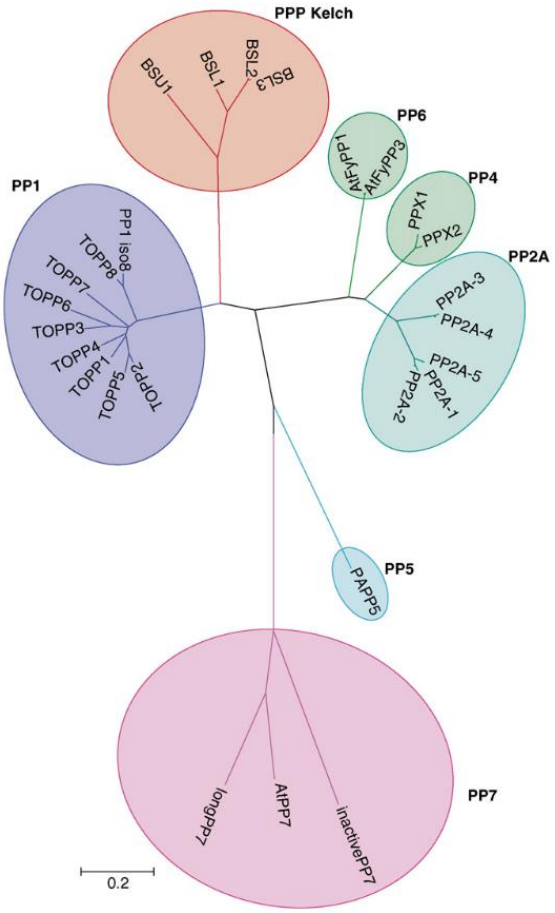

Figure 1.2. Family tree of PPP catalytic subunits in Arabidopsis. The bar represents 0.2 amino acid substitutions per site in the primary structure. The figure is obtained from Farkas et al., 2007.

1.4 Protein Phosphatase 2A

Among the subgroups of Ser/Thr phosphoprotein phosphatases (PPPs), PP2A is a major phosphatase and conserved throughout eukaryotes. It is mainly composed of catalytic C, structural A (also called scaffolding subunit) and regulatory B-type subunits. As PP2A is involved in regulation of many cellular processes, the deregulation of this enzyme can be observed in several diseases such as cancer and Alzheimer's disease in human (Janssens and Goris, 2001; Sontag, 2001). Protein phosphatase 2A is involved in a wide range of external and internal signals. It is known to involve in signal transduction pathways of several hormones in plants such as abscisic acid, ethylene, and auxin (Antolín-Llovera et al., 2011).

1.4.1 PP2A Structure

PP2A is a heterotrimer that is composed of a catalytic C, scaffolding A, and regulatory B subunit. The different catalytic C subunits are 97% identical and the scaffolding A subunits are 85%

identical, in human (Janssens et al., 2008). The three subunits are the building blocks of various PP2A complexes and each of them has their isoforms which are encoded by distinct genes. In the heterotrimer complex of PP2A, the catalytic subunit (36 kDa) is associated with either regulatory A subunit (65 kDa) or together with a third variable B-subunit (Farkas et al., 2007).

The genome of Arabidopsis encodes 5 C, 3 A and 17 B subunits which make up to 255 different combinations in the PP2A complex (Kerk et al., 2002; Wang et al., 2007). Among all the subunits, both the scaffolding A and catalytic C subunits are highly conserved in all eukaryotes. On the other hand, B subunits are more diverse and responsible for subcellular localization and substrate specificity of different holoenzymes (Janssens et al., 2008).

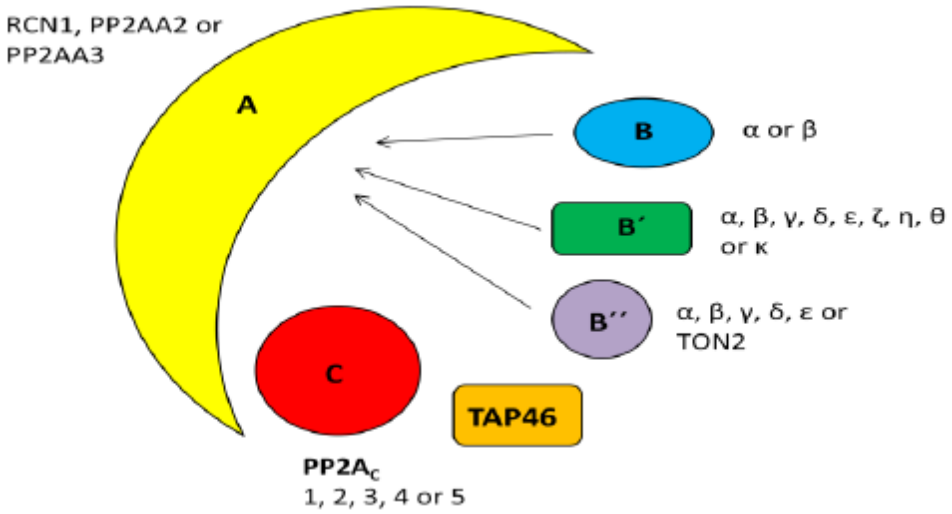

Figure 1.3. Structure of PP2A in Arabidopsis. A: scaffolding subunit , B: variable regulatory subunits (B, B´ and B´´), C: catalytic subunit, A subunits are encoded by three genes (RCN1, PP2AA2, PP2AA3); the B subunits are encoded by two related genes (α and β), the B´ subunits are encoded by nine related genes (α, β, γ, δ, ε, ζ, η, θ and κ); the B´´ subunits are encoded by six related genes (α, β, γ, δ, ε and TON2) and TAP46 is an unrelated regulatory subunit. C subunits are encoded by five genes (PP2AC-1, 2, 3, 4 and 5); The figure is based on Janssens and Goris, 2001; Farkas et al., 2007; Amundsen, 2011.

1.4.2 PP2A subunits

1.4.2.1 Catalytic subunits

The PP2A catalytic subunit C has similarity with other Ser/Thr protein phosphatase such as PP1, PP4 and PP6 catalytic subunits. (Moorhead et al., 2009). In Arabidopsis, there are five genes that encode PP2A catalytic subunits (PP2Ac) (Kerk et al., 2002; He et al., 2004). Based on identity among protein sequences, PP2Ac proteins are grouped into two subfamilies that are subfamily I

and subfamily II. PP2A-C1, PP2A-C2 and PP2A-C5 belong to subfamily I, while PP2A-C3 and PP2A-C4 belong to subfamily II. (Perez-Callejon et al., 1998).

The C2 is involved in abscisic acid (ABA) signaling and seed germination rate when exposed to ABA (Pernas et al., 2007). In addition to this, mutant and PP2A inhibitor studies showed that C2 involves in actin-binding proteins and causes reorganization of the actin/cytoskeleton structure.

The PP2A-C5 is related to brassinosteroids (BRZ) signaling (Tang et al., 2011). A recent study revealed that this subunit has a positive effect on plant response to salt stresses. That study showed that overexpression of PP2A-C5 increases tolerance of both seedling and vegetative stages of Arabidopsis to several salt treatments. On the other hand, the mutant *PP2A-C5* leads to hypersensitivity towards those salt treatments. Therefore, hampered root growth of seedlings and generally smaller plants are produced by the loss of functional C5 mutant (Hu et al., 2016).

Generally, in Arabidopsis, a single gene knockout of catalytic subunit does not have any visible effect on plant phenotype but *pp2a-c2* knockout reduces the germination rate of the plant (Pernas et al., 2007; Heidari et al., 2011; Ballesteros et al., 2013). However, double knockout, triple knockout or knockout of all the members in either of the two subfamilies causes a serious effect on the plant. For example, a homozygous double knockout of c3 and c4 stops root development and the plant died at the seedling stage. The root growth is severely dwarfed in triple knockout c1 × c2 × c5 mutant but clear roots and leaves are present (Ballesteros et al., 2013).

The catalytic subunits (C) of PP2A are involved in defense signaling and plant stress. This subunit also thought to be involved in gibberellin signaling (Janssens et al., 2008).

1.4.2.2 Scaffolding subunits

There are three scaffolding subunits A1/RCN1, A2 and A3 in Arabidopsis. These subunits are found in both cytoplasm and nucleus according to their different functions (Tran et al., 2012). They are composed of 15 tandemly repeated HEAT motifs that bind with the catalytic C and regulatory B subunits and form a hook-like architecture. Each HEAT-motif repeat consists of a loosely conserved 39-residue sequence that folds into two antiparallel α helices. Adjacent α-helices are connected by an intra repeat loop (Farkas et al., 2007; Groves et al., 1999; Mumby, 2007).

RCN1 (roots curl in NPA) acts as a regulator of auxin transport and gravitropism. It increases the sensitivity of naphthylphthalamic acid (NPA). This subunit of PP2A is a positive transducer of early ABA signaling. The *a1/rcn1* mutant has a 50% reduction of protein phosphatase activity when assayed with phosphohistone or phosphorylase as substrates (Deruere et al., 1999). This mutant involves in insensitivity of abscisic acid (ABA) during seed germination. It also results in guard cell responses and gene expression, reduction of PP2A activity, leading to defects in apical hook formation as well as in root and hypocotyl elongation (Garbers et al., 1996; Kwak et al., 2002).

RCN1 gene has no functional ability in *eer1* (enhanced ethylene response 1) mutant. *In vitro,* RCN1 gene interacts with PP2A-1 catalytic subunit and binds with a negative regulator of ethylene signaling, CTR1 kinase which is possibly a substrate of PP2A (Larsen and Cancel, 2003).

Mutations in PDF1 and PDF2 genes show slight phenotypic changes in plants. However, double mutants including *rcn1* and either *pdf1* or *pdf2* results in severe deficiencies such as abnormal embryogenesis, defective radial cell expansion, dwarfing and sterility that indicates that RCN1 plays a crucial role in the regulation of PP2A activity (Zhou et al., 2004).

1.5 Regulatory subunits

The regulatory B-type subunit is the most variable subunit of PP2A holoenzyme. Based on the molecular weight and domains it can be classified into three families that are unrelated to each other in sequence, called B (55-kD), B′(52- to 74-kD) and B′′(72- to 130-kD) (Terol et al., 2002). Distinct genes encode various structurally related isoforms within each family of regulatory subunit. In Arabidopsis, two related genes (α and β) encode B subunit, nine related genes (α, β, γ, δ, ε, ζ, η, θ and κ) encode B′ as well as six related genes (α, β, γ, δ, ε and TON2) encode B′′ (Farkas et al., 2007). The α and β genes of B′ subunit contain putative nuclear targeting sequences whereas γ gene produces alternatively spliced transcripts. Structural studies of PP2A holoenzymes revealed that there is an exposed concave surface on the B subunit which is suggested to be a major determinant in substrate recognition (Mumby, 2007).

The active B/B55 play a crucial role in Arabidopsis and it cannot be replaced by other subunits during growth and development. PP2A 55-kDa B subunit isoforms contain five degenerate WD-40 repeats (Farkas et al., 2007). A single knockout of α or β gene appears as normal whereas a homozygous double knockout (b55α × b55β) can be lethal (Heidari et al., 2011).

The nine members of B′ subunit are divided into three subgroups α, η, κ (Terol et al., 2002; Farkas et al., 2007). The B′α and B′β are 85% identical and 96% similar at the amino acid level and expressed evenly at all developmental stages and tissues (Winter et al., 2007). It has been revealed that double knockout of B′α and B′β causes malformations like dwarfism and severely reduced seed set (Jonassen et al., 2011; Tang et al., 2011). Besides B′α and B′β, B′γ is the most studied gene of the group. The knockdown of B′γ causes yellow spots in mature Arabidopsis leaves under normal light. This gene also influences the flowering time of the plant. The *b′γ* mutant has late flowering as compared to the WT (Heidari et al., 2013).

Relatively little research has been conducted on B″ subunit. The expression levels of B″ subunit varied. The expression level of B″δ, B″ε and TON2 is relatively high in most of the organs including leaves, whereas in mature pollen, the level of expression is very low (Winter et al., 2007). B″α involves in inducing seedling roots and stress responses (Farkas et al., 2007). Exception from other encoding genes of B″ subunit, TON2 is the most studied. *TON2* mutant causes reduced growth of the plant from the seedling stage and throughout the life cycle (Torres-Ruiz and Jurgens, 1994; Camilleri et al., 2002).

1.6 Leucine carboxyl methyl transferase 1 (LCMT1)

Carboxymethylation of the terminal amino acid (leucine) in the catalytic subunit of PP2A influences the assembly and properties of the full complex. (Janssens et al., 2008). Leucine carboxyl methyl transferase 1 (LCMT1) extensively methylates the conserved leucine in the C-terminal end of the PP2A by using S-adenosyl-L-methionine as methyl donor which is also called SAM or AdoMet (De Baere et al., 1999; Kalhor et al., 2001; Wu et al., 2011; Tsai et al., 2011). This methylation controls the PP2A activity (Wu et al., 2000; Stanevich et al., 2011). The presence of unmethylated PP2A-C almost entirely in the cytosol fraction was found in Arabidopsis whereas only methylated PP2A-C had been found in the microsomal fraction. If the LCMT1 is knocked out from Arabidopsis plants, methylated PP2A-C is absent, and only unmethylated PP2A-C is present in both microsomal and cytosolic fractions. This finding indicates that active LCMT1 methylate all PP2A-C in microsomes (Wu et al., 2011).

The enzymes, LCMT1 (Leucine carboxyl methyl transferase 1), mediating methylation of PP2A have been studied mainly in animals and yeast but a very little in plants (Lillo et al., 2014). Some mammalian studies revealed that LCMT1 is necessary in cells for their normal progression through mitosis (Lee and Pallas, 2007) and downregulation of LCMT1 activity is associated with conditions such as Alzheimer's disease (Sontag et al., 2014) and Parkinson's disease (Park et al., 2016). On the other hand, embryonic lethality can be caused in mice due to loss of LCMT1 function (Lee and Pallas, 2007). In addition to this, deletion of LCMT1 (called PPM1) is linked toward severe growth defects in Saccharomyces cerevisiae (Wu et al., 2000; Wei et al., 2001; Castermans et al., 2012).

It was estimated that about 50% to 90% of Leu-309 in PP2Ac is methylated in plants (Kalhor et al., 2001; Wu et al., 2011, Chen et al., 2014). Lack of methylation is observed in LCMT1 null mutant known as suppressor of brassinosteroid insensitive 1 (*sbi11*) or *lcmt1*. It indicates that in Arabidopsis, SBI1/LCMT1 is the primary PP2Ac methylating enzyme (Wu et al., 2011). A study suggested that there are 80% to 90% of PP2Ac is methylated in Arabidopsis and unmethylated PP2Ac form is 5 to 10-fold more abundant in the *sbi11* mutant than in wild-type Arabidopsis (Wu et al., 2011). Interestingly, lack of methylation in Arabidopsis seems to not be detrimental to plant development, as the *lcmt1* or *sbi11* mutant is viable and shows minimal morphological defects (Chen et al., 2014; Wu et al., 2011).

1.7 Sulfur in plant

The essential elements are the intrinsic components in the structure or metabolism of a plant or whose absence causes severe abnormalities in plant growth, development, and reproduction. Essential elements for the plant can be divided into four basic groups according to their biochemical role and physiological function in the plant. Regarding this classification, Nitrogen and Sulfur remain in the first group (Taiz and Zeiger, 2010). In this project, sulfur starvation was investigated on Arabidopsis WT and mutant *lcmt1*.

Sulfur is found in amino acids such as cystine, cysteine and methionine. It is also a constituent of several coenzymes and vitamins such as coenzyme A, S-adenosylmethionine, biotin, vitamin B_1 and pantothenic acid which are essential for metabolism of the plant (Taiz and Zeiger, 2010). Most of the plants absorb sulfur in the sulfate form (SO_4^{--}) through their roots. It has an important role in the protein structure and enzymatic functions. Sulfur metabolites provide protection against some stresses such as oxidative stress, heavy metals, and xenobiotics. The secondary sulfur compounds also provide resistance against pathogens and herbivory. Apart from these, sulfur has a key role in chlorophyll formation and protein production in the plants. Overall, adequate and balanced sulfur nutrition is necessary for the growth, quality, and health of the plants (Zhao et al., 2008).

1.7.1 Sulfur starvation

Sulfur deficiency is similar to nitrogen deficiency as both of them are constituents of proteins. When the sulfur level decreases below the optimal level, visual changes appear in the plants. During sulfur deficiency, chlorosis and anthocyanin accumulation can occur. When chlorosis arises, the leaves become pale-yellow or light-green and this symptom first appears in the younger leaves in most species. Nonetheless, in many plant species, sulfur chlorosis may occur simultaneously in all leaves, or even initially in older leaves. The plants having sulfur starvation, are short with slender stalks as well as their growth is retarded (Taiz and Zeiger, 2010).

1.7.2 The genes involved in sulfur starvation

Sulfur is absorbed by the plants from soil in the form of sulfate. In Arabidopsis, SULTR1;2 is a high-affinity sulfate transporter that is present in the root epidermis and cortex. This protein is responsible for taking up sulfate from the soil. The absorbed sulfate is then transported to the shoots and metabolized to cysteine through reductive assimilation. The transcript level of *SULTR1;2* is increased during sulfur deficiency (-S) (Kimura et al., 2019). The model plant Arabidopsis uses the sulfate to produce sulfur-rich secondary metabolites, glucosinolates (GSLs) and proteins. GSLs act as an important defense compound against pathogens and its synthesis is controlled by several MYB transcription factors during sulfur sufficient condition (+S). When sulfur is limiting (-S), sulfur deficiency-induced gene, *SDI1* is strongly induced and acts as a negative regulator of GSL biosynthesis. In this case, plants prioritize the growths over defense by this mechanism under sulfur deficiency (Arabi et al., 2016).

In plants, Fe and S both are essential nutrients for plant growth and yield. There is a cross-regulation mechanism between the assimilation pathway of Fe and S. In the cellular membrane of mitochondria and chloroplast, Fe mainly conjugates with S to form Fe-S clusters. Thus, simultaneously reduced S in the form of cysteine and chelated Fe are required for the biosynthesis of Fe-S clusters. As e result, the genes involved in the Fe assimilation pathway are co-related with S sufficiency or deficiency in the plant (Forieri et al., 2013). In this study, several genes of Fe

assimilation pathway were tested in S deficient WT and *lcmt1* as they indirectly involve in S starvation.

The reduction-based strategy (strategy I) is followed by the plants of *Arabidopsis thaliana* to cope with Fe deficiency. In the strategy I, Fe (III) chelates are reduced at the root surface to form soluble Fe^{2+} by plasma membrane ferric chelate reductase enzyme. The soluble Fe^{2+} is then transported by a Fe^{2+} transporter from the rhizosphere into the root cell. In Arabidopsis, the *FRO2* gene from the ferric reductase oxidase (FRO) family encodes the ferric chelate reductase and *IRT1* encodes the major high-affinity iron transporter. The *IRT1* transport Fe^{2+} through the plasma membrane of the roots to cytosol (Robinson et al., 1999; Vert et al., 2002; Jeong and Connolly, 2009; Brumbarova et al., 2014). The other genes of the FRO family are also responsible for Fe (III) reduction in different locations of Arabidopsis, e.g., *FRO7* reduces Fe^{3+} in the chloroplast. The role of *FRO3* is still unclear but it is predicted to have roles in Fe import to mitochondria of plants (Sperotto et al., 2014). The *FRO4* encodes a ferric chelate reductase that is expressed at low levels in roots, shoots and cotyledons. Another gene *BHLH100* serves as a key regulator of Fe-deficiency and is involved in the Fe distribution in plants.

Nicotianamine is a Fe chelator that binds with Fe and involves in metal translocation in plants. It is synthesized from S-adenosyl L-methionine by nicotianamine synthase (NAS) in most of the tissues of plants (Cassin et al., 2009). The regulation of *NAS* genes is important for metal acquisition, distribution and tolerance (Koen et al., 2013). In Arabidopsis, the genes of *NAS* family, e.g., *NAS1*, *ATNAS2* and *ATNAS4*, act as the sensor for physiological iron status.

1.8 Abiotic Stress

The complex environment where plants grow and reproduce is composed of various abiotic (non-living) chemical and physical factors. Any environmental condition that affects the ability of plant growth, development and production below the optimal levels is called abiotic stress (Rahnama et al., 2010; Quados, 2011). The abiotic factors include air quality and air flow, light intensity, temperature, water availability, mineral nutrients and trace element concentrations, salinity. These factors are needed for plants to grow and develop normally. The fluctuation of essential environmental factors outside of their normal ranges leads to negative biochemical and physiological consequences for plants which are called stress situation (Taiz and Zeiger, 2010). The response to the stress depends on some factors such as type, level and duration of stress as well as affected organ or tissue of the plants (Cramer et al., 2011).

In this project, salt stress and oxidative stress were investigated on Arabidopsis WT and *lcmt1* mutant.

1.8.1 Salt Stress

Salt stress refers to an excessive exposure of plants to salt. This stress has two components such as nonspecific osmotic stress and specific ion effects. The osmotic stress leads to water deficits.

On the other hand, the ion effects cause accumulation of toxic ions that disturb nutrient acquisition and is responsible for cytotoxicity (Munns and Tester, 2008). According to the adaptation to salt stress, the plants are termed as halophytes (salty) and glycophytes (sweet). The plants that are not adapted to salt stress are called glycophytes (Taiz and Zeiger, 2010).

During the salt stress, plants undergo various physiological changes such as nutrient imbalance, membrane interruption, increased amount of reactive oxygen species (ROS), reduced and altered photosynthetic activity, impaired ability to detoxify ROS and decreased stomatal aperture (Sharma and Dubey, 2005; Tanou et al., 2009; Gupta and Huang, 2014). Excessive sodium in the plant cell causes osmotic stress which ultimately leads to cell death (Shrivastava and Kumar, 2015). The impaired photosynthetic ability due to excess salt decreases leaf area, chlorophyll content as well as stomatal conductance (Sharma et al., 2012). Apart from these, high salt stress also inhibits the ability of plants to absorb nutrients which ultimately leads the plants towards death (Shrivastava and Kumar, 2015).

1.8.1.1 Salt stress induced ion toxicity

Inside the cytosol, certain ions disturb the nutrient status of the plant during salt stress and cause cytotoxicity. As the ions move to the shoot in the transpiration stream, the whole plants are affected by them (Munns and Tester, 2008). The salt at high concentrations denature the protein and destabilize the membrane by reducing the hydration of these macromolecules. Apoplastic Na^+ inhibits the uptake of K^+ which is necessary for plant growth and development (Gupta and Huang, 2014). The high concentration of salt and reduced level of K^+ trigger the accumulation of ROS which causes various cell damages in the plant. Further, elevated Na^+ is also responsible for displacing Ca^{2+} from the sites on the cell wall and reducing its activity in the apoplast which results in an increased level of Na^+ influx (Epstein and Bloom, 2005; Apse and Blumwald, 2007). Ca^{2+} activates the Na^+ detoxification via efflux across the plasma membrane. Since the availability of Ca^{2+} in the cytosol is also reduced for Na^+ influx, the detoxification of Na^+ is also blocked (Taiz and Zeiger, 2010).

Plants possess a variety of biochemical mechanisms during elevated salt concentration such as ion exclusion, altered photosynthesis, compatible solute synthesis, modifications in membrane structures as well as increasing antioxidants and plant hormones (Parida and Das, 2005).

1.8.2 Oxidative stress

The oxidative stress can be caused by the accumulation of reactive oxygen species (ROS), which damage plant cells before elimination (Limon Pacheco et al., 2017; Xie et al., 2019). ROS are the molecules having low molecular weight and at high concentration, they cause oxidative damage to proteins, lipids, RNA and DNA. ROS associated oxidative stress destroys cellular and metabolic functions which ultimately lead to cell death (Taiz and Zeiger, 2010). Singlet O_2, superoxide radical ($O_2^{\bullet-}$), hydrogen peroxide (H_2O_2), nitric oxide (NO•) and hydroxyl radical (•OH) are crucial for oxidative stress (Apel and Hirt, 2004). Among these, hydrogen peroxide is a non-radical

weak acid which is a stable molecule compared to other reactive oxygen species (Hernández et al., 2001; Noctor et al., 2016). In this project, hydrogen peroxide was used for oxidative stress on Arabidopsis WT and *lcmt1*.

In plant cells, lipids and proteins are the major targets of oxidative damage. ROS causes lipid peroxidation when it reaches above threshold. Lipid peroxidation produces lipid-derived radicals that react and damage the proteins and DNA. Peroxidation of polyunsaturated fatty acids present in membrane phospholipids can cause chain breakage which results in membrane fluidity and permeability. The oxidative stress in proteins leads to modification of site-specific amino acid, peptide chain fragmentation, aggregation of cross-linked reaction products as well as proteolysis. Several studies revealed that a certain degree of oxidative damage produces extensively cross-linked and aggregated products that inhibit proteases and cause degradation of other oxidized proteins (Sharma et al., 2012). Oxidative modification on proteins leads to carbonylation which is responsible for dangerous effects such as covalent intermolecular cross-linking, cleavage and changing the rate of protein degradation (Tanou et al., 2009).

Oxidative damage of DNA can cause changes in the encoded proteins which lead to malfunctions or complete inactivation of the encoded proteins. It also causes deoxyribose oxidation, strand breakage, removal of nucleotides from DNA and other modifications in DNA. These types of changes in the nucleotides of one strand cause mismatches with the nucleotides of another strand of DNA (Sharma et al., 2012).

The antioxidative mechanism of plant maintains a balance between ROS production and ROS scavenging (Apel and Hirt, 2004). Perhaps, various environmental stresses such as extreme temperature, salt stress, dehydration, high light, and ion toxicity cause an imbalance between ROS production and scavenging which leads to oxidative damage of macromolecules and signaling dysfunction (Taiz and Zeiger, 2010). In Arabidopsis, the Fe superoxide dismutase 1 (*FSD1*) gene provides cellular defense against reactive oxygen species by converting the superoxide (O^{2-}) radical into hydrogen peroxide (H_2O_2) and molecular oxygen (O_2) (Myouga et al., 2008).

1.9 Objectives of the Present Study

PP2A is a highly conserved phosphatase throughout the eukaryotes. It has a crucial role in the regulation of cellular process, signal transduction pathways of several hormones and response of the plant to environmental stress (Janssens and Goris, 2001; Sontag, 2001). PP2A is regulated by carboxymethylation of C-terminal amino acid (leucine) by LCMT1 (Leucine carboxyl methyl transferase 1) enzyme. This methylation of PP2A is believed to be essential for the survival of plants under certain types of stresses. Recently, the methylation status of PP2A-C was shown to be influenced by environmental stressors such as salt, flooding, and nutrient deprivation, e.g., Nitrogen and Iron deficiency (Creighton et al., 2017). The main objectives of the present study were:

- To investigate the necessity of *LCMT1* gene and associated methylation of PP2A under various environmental conditions such as salt stress, oxidative stress (H_2O_2) and deprivation of nutrient (sulfur).
- To identify the genes strongly influenced by the PP2A methylation level.

2 Materials and Methods

2.1 Plant material

Arabidopsis thaliana ecotype Columbia was used as wild type in the present study. The *Arabidopsis thaliana* single mutant T-DNA insert line *lcmt1* (SALK_079466) (Alonso, 2003) was obtained from the European Arabidopsis Stock Centre in Nottingham, UK. The WT and *lcmt1* seeds were sown directly in the regular soil and stratified at 4^0C for 2-3 days, then transferred to artificial 12 h light room at 22^0C. The plants were watered two to three times a week. The plants were transferred from soil after 25 days to vermiculite and rockwool.

2.2 Solutions and media

2.2.1 Hoagland solution

The Hoagland solutions (Hoagland and Arnon, 1950) were made with 2 mM MgSO4, 10 mM $MgSO_4$, 2 mM $MgCl_2$, 10 mM $MgCl_2$ and without $MgSO_4$ and $MgCl_2$ (Showed in tables 2.1 and 2.2). The micronutrients are showed in table 2.3. A Hoagland media was prepared by adding 0.7% agar (VWR International, Italy) and 1% sucrose in the Hoagland solution. The pH of the solution was adjusted to 5.8 before autoclaving.

Table 2.1. Composition of Hoagland solution (Hoagland and Arnon, 1950) with different concentrations of sulfur.

Nutrient solution with Fe-EDTA pH 6	**mL to make 1x concentrated nutrient solution/L**	**Final concentration/L**
KH_2PO_4 (1M)	1 mL	1 mM
KNO_3 (1M)	5 mL	5 mM
$Ca(NO_3)_2$:$4H_2O$ (1M)	5 mL	10 mM NO_{3-} 5 mM Ca^{2+}
$MgSO_4$:7 H_2O (1M)	10, 2, and 0 mL	10, 2, 0 mM
Fe-EDTA 1%	1 mL	27 μM
Micronutrients	1 mL	

Table 2.2. Composition of Hoagland solution (Hoagland and Arnon, 1950) with different concentrations of $MgCl_2$.

Nutrient solution without SO4	1x solution/L	Final concentration/L
$MgCl_2 \cdot 6\ H_2O$ (1M)	10, 2 and 0 mL	10, 2 and 0 mM

Table 2.3. Composition of micronutrients of Hoagland solution (Hoagland and Arnon, 1950).

Micronutrients/L	1 x Stock solution Final concentration/L
H_3BO_3	46 µM
$MnC1_2$:4 H_2O	9 µM
$CuSO_4$:5 H_2O	0.36 µM
ZnSO4:7 H_2O	0.76 µM
$Na_2M_oO_4$:H_2O	0.12 µM

2.2.2 ½ MS (Murashige and Skoog) solution

A ½ MS media (Murashige and Skoog, 1962) was prepared by adding 0.7% agar (VWR International, Italy) and 1% sucrose in ½ MS solution. The pH of the solution was adjusted to 5.8 before autoclaving. The composition of ½ MS media is shown in table 2.4.

Table 2.4. Composition of ½ MS nutrient solution (Murashige and Skoog, 1962).

MS stock solutions	MS medium salts	½ MS	Final concentration
A: KNO_3 FW: 101.10	A: KNO_3	10 mL	9.4 mM
B: NH_4NO_3 FW: 80.04	B: NH_4NO_3	6.5 mL	9.7 mM
C: $MgSO_4$ $7H_2O$ FW: 246.47	C: $MgSO_4$ $7H_2O$	5 mL	750 µM
D: KH_2PO_4 FW: 136.09	D: KH_2PO_4	10 mL	1.3 mM
E: $CaCl_2$ $2H_2O$ FW: 147.01	E: $CaCl_2$*$2H_2O$	5 mL	1.5 mM
Fe/EDTA:			
Na_2EDTA	Fe/EDTA	25 mL	34 µM

FW: 372.2368			
$FeSO_4$ $7H_2O$ FW: 278.0146			25 µM
Minor I:	Minor I	5 mL	
$ZnSO_4$ $7H_2O$ 287.541			16 µM
H_3BO_3 FW: 61.83			50 µM
$MnSO_4$ $4H_2O$ FW: 223.0618			5 µM
Minor II:	Minor II	5 mL	
Na_2MoO_4 $2H_2O$ FW: 241.95			0.5 µM
$CuSO_4$ $5H_2O$ FW: 249.69			0.06 µM
$CoCl_2$ $6H_2O$ FW: 237.93			0.06 µM
KI FW: 166.00			2.5 µM
Sucrose		10 g	1%
	Agar	7 g	0.7%
	Water	Up to 1 L	

2.3 Other materials

The enzymes, reagents and commercial kits used in this study are mentioned with their respective methods in the text.

2.4 Transfer of seedling to vermiculite

Wild type and *lcmt1* seedlings grown in soil at 12 h light, were transferred to vermiculite and moistened the vermiculite with different concentrations of $MgSO_4$ and $MgCl_2$. Then the trays placed in 8 h light for 5 weeks. Each seedling was watered with 50 mL of corresponding Hoagland nutrient solutions in every week and growth changes were monitored. After 5 weeks, the plants were harvested from vermiculite and weight of roots and shoots were measured. Then the WT and *lcmt1* roots and shoots both that treated with different concentrations of Hoagland solutions in vermiculite were wrapped in foil papers and stored at -80^0 C for In-gel gene expression analysis.

2.5 Transfer of seedling to rockwool

Wild type and *lcmt1* seedlings grown in soil at 12 h light, were transferred to rockwool as same as vermiculite. The seedlings (5 WT and 5 *lcmt1* per treatment) were treated with Hoagland solutions of 2 mM $MgSO_4$ (control) and 2 mM $MgCl_2$ (125 mL of each solution per seedling) at the beginning. Then the plants placed in 8 h light for 5 weeks. In every week, 50 mL of corresponding Hoagland nutrient solutions were given to each of the seedlings and growth changes were monitored. After 5 weeks, the plants were harvested from rockwool and weight of shoots were measured. Then both WT and *lcmt1* shoots for 2 mM $MgSO_4$ (control) and 2 mM $MgCl_2$ were stored at -80^0 C for further gene expression analysis. The gene expression analysis was performed via real-time PCR using Taq-Man assays.

2.6 Surface sterilization of seeds

Arabidopsis seeds were placed into Eppendrof tubes (0.1 mL or less) and mixed with 1 mL ethanol (95%) containing 0.1 % Ca-hypochlorite and one drop of Tween-20. After shaking and 4 min incubation, the supernatant was removed. The seeds were washed with 1 mL of 95 % ethanol twice and left to air-dry overnight sterile hood. The ethanol was well removed after washing. After drying the tubes were closed and sealed with para-film.

2.7 Stress tolerance experiment

2.7.1 Sulfur experiment

In this study, both WT and *lcmt1* Arabidopsis seeds were sowed on Hoagland nutrient media with different concentrations of $MgSO_4$ and $MgCl_2$. The Hoagland media was prepared by adding 0.7% of plant agar (made in Ducheta, hoaslem, The Netherlands) and 1% sucrose in 1x concentrated Hoagland solutions. The pH of this solution was adjusted to 5.8. Then both WT and *lcmt1* sterilized seeds were sown on those agar plates and kept the plates in dark room at 4^0 C for 3 d. After that, the plates with seeds were placed vertically in 16 h light for 5 d until germination. At the end, the germinated seeds were transferred into new plates containing different concentrations of Hoagland media and kept in 16 h light room for additional 7 d. After 7 d, the root lengths and shoot weights were measured. In addition to this, chlorophyll content was also determined.

2.7.2 NaCl experiment

WT and *lcmt1* seeds sowed on square Petri dishes with ½ MS media. The plates were placed in dark place at 4^0C for 3 d and then kept at 16 h light for 5 d until germination. After 5 d, both WT and mutant seedlings were transferred to new media plates containing ½ MS media and different concentrations (25 mM, 50 mM, 75 mM, 100 mM and control without NaCl) of NaCl stress. Here, 3 replicates were made for the control and each concentration of NaCl. Then the plates were kept

vertically at 16 h light for additional 7 d. After this period, root length and shoot weight were measured as well as chlorophyll content was determined.

2.7.3 H_2O_2 experiment

WT and *lcmt1* seeds sowed on small round Petri dishes with ½ MS media. The plates were placed in dark place at 4^0C for 3 d and then kept at 16 h light for 5 d until germination. After 5 d, both WT and mutant seedlings were transferred to new small round media plates containing ½ MS media and different concentrations (0.5 mM, 1 mM, 1.5 mM, 2 mM and control without H_2O_2) of H_2O_2 stress. Here, 3 replicates were made for the control and each concentration of H_2O_2. Then the plates were kept vertically at 16 h light for additional 7 d, then root length and shoot weight were measured as well as chlorophyll assay was performed after the period.

2.7.4 Chlorophyll assay

The WT and *lcmt1* shoots treated with different stress (Sulfur, chloride, salt or H_2O_2) were pasted in mortar with 2000 µL 95% ethanol. The solutions were centrifuged at maximum speed for 2 min. After centrifugation, 300 µL of each supernatant was diluted with 1200 µL of ethanol. The absorbance was determined at 654 nm and chlorophyll content was calculated by using the following formula: Chlorophyll content = ($Absorbance_{654}$ × 25.1 × 5) × 2 µg/mL.

2.8 Gene expression analysis

The RNA isolation and cDNA synthesis were performed with WT and *lcmt1* plants, grown on vermiculite (roots and shoots) as well as rockwool (shoots) at 8 h light and treated with 2 mM $MgSO_4$ and 2 mM $MgCl_2$.

2.8.1 RNA extraction

Preparation of samples

The plant samples were crushed with liquid nitrogen by using a mortar and pestle. Less than 100 mg of frozen tissue was transferred to a nitrogen cooled 2 mL Eppendorf tube. In this case, there were in total 4 samples such as WT roots, WT shoots, *lcmt1* roots and *lcmt1* shoots for each of the $MgSO_4$ and $MgCl_2$ treatment.

Preparation of lysis buffer

A fresh amount of Lysis Buffer containing 1% of 2-mercaptoethanol was needed for each purification procedure before beginning the lysis and homogenization steps. For this, 500 µL buffer was prepared for per <100 mg sample.

DNase treatment preparations

The PureLink® DNase was Resuspended by dissolving in 550 µL RNase–Free Water (supplied with PureLink® DNase) (Invitrogen, Carlsbad, USA) and stored at -20°C from before.

Preparation of PureLink® DNase for on-column treatment

DNase I incubation mix solution was prepared to remove genomic DNA. In this case, 80 µL of this solution was prepared per sample. The composition of mix solution is given in the table 2.5. The following components was supplied with PureLink® DNase (Invitrogen, Carlsbad, USA)

Table 2.5. Composition of DNase for on-column treatment.

Components	**Amount**
10X DNase I Reaction Buffer	8 µL
Resuspended DNase	10 µL
RNase Free Water	62 µL

RNA isolation initiation

In the fume hood, 500 µL lysis buffer was added per sample and the samples were vortexed vigorously for 45 s and incubated at room temperature for 3 min. The samples were transferred to homogenizer (supplied with PureLink^{TM} RNA Mini Kit) and spun for 2 min. the homogenizers were removed and 250 µL of ethanol (96-100%) was added in each tube. The solutions were mixed by vortex and transferred the sample (up to 700 µL) including any precipitate to the spin cartridge (supplied with PureLink^{TM} RNA Mini Kit) assembled in a collection tube. The tubes were spun for 15 s and then the flow through were discarded. This process was repeated until the samples were processed.

Removal of genomic DNA

In the spin cartridges, 350 µL wash buffer I was added and spun for 15 s. After spinning, the flow through in collection tubes were discarded and the Spin Cartridges were inserted into new collection tubes. In addition to this, 80 µL DNase 1 incubation mix solution was added to the center of the membrane and incubated at room temperature for 15 min.

Wash and elute

In the washing procedure, 350 µL wash buffer I was added to the membrane followed by centrifugation for 15 s at 12 000 x g. Then the collection tubes with flow through were discarded and new collection tubes were inserted. In the spin cartridge, 500 µL wash buffer II with ethanol was added and centrifuged at 12,000 x g for 15 s. The procedure of adding wash buffer II with ethanol, centrifuging for 15 s and discarding the collection tubes were repeated. After this, the spin cartridges were inserted into new collection tubes as before and centrifuged at 12,000 × g for 1 min to dry the membrane with bound RNA. In the center of the spin cartridges, 40 µL RNase–Free Water was added after discarding the collection tubes and inserting the spin cartridges into

recovery tubes. Then the tubes incubated at room temperature for 1 min and centrifuged at ≥12,000 x g for 1 min. The concentration and quality of elute RNA was assessed by Nanodrop (Thermo Scientific™ NanoDrop 2000 Wilmington, DE, USA). In NanoDrop, the ratio of absorbances at 260 nm and 280 nm (A260/A280) as well as 260 nm and 230 nm (A260/ A230) are used to assess the purity of RNA. If the ratio of absorbance is ~2.0 for RNA at A260/A280, the RNA is generally considered as "pure" and indicates lower presence of protein, phenol or other contaminants that absorb strongly at or near 280 nm. In addition to this, A260/ A230 ratio is used as a secondary measure of nucleic acid purity. In general, the value ~2.2 for RNA at A260/ A230 ratio is considered as "pure" RNA and indicates lower presence of contaminants (Carbohydrates, phenols, guanidine) which absorb at 230 nm. After getting the purity assessment of RNA from NanoDrop, the RNA samples were stored at -80^{0}C.

2.8.2 cDNA synthesis

A PCR was run to synthesize cDNA from purified RNA. The protocol of SuperScript™ IV VILO™ Master Mix (without ezDNase enzyme treatment) (Thermo Fisher Scientific, USA) was followed to prepare RT control reaction mix and run the PCR. After PCR, the synthesized cDNA was stored at -20^{0}C to perform gene expression analysis. The components of RT control reaction mix and thermal conditions for PCR are listed in table 2.6 and 2.7, respectively.

Table 2.6. Components of RT control reaction mix to run PCR.

Components	**RT reaction**
SuperScript™ IV VILO™ Master Mix	4 µL
Template RNA (1µg total RNA used)	Varied (according to concentrations of different RNA sampless)
Nuclease-free water	to 20 µL

Table 2.7. Thermal cyclic conditions for PCR.

Steps	**T, ^{0}C**	**Time, min**
Anneal primers	25	10
Reverse transcribe RNA	50	10
Inactivate enzyme	85	5

2.8.3 In-gel analysis

A Polymerase chain reaction (PCR) was performed with both roots and shoots of WT and *lcmt1* grown on vermiculite at 8 h light and treated with 2 mM $MgSO_4$ and 2 mM $MgCl_2$ in order to determine expression of some specific genes. The experimented genes and the primer combinations are listed in the following table 2.8 and description of these gene are presented in Appendix (Table C.1).

Table 2.8. Primers of genes used in the PCR.

Gene	Forward primer 5'to 3'	Reverse primer 5' to 3'	Product size, bp
IRT1	CACCAGCAAGAACGCAGTTG	TCCAGCGGAGCATGCATTTA	445 635 (genomic)
BHLH 100	TGGCCTTGCGGAGATCATAG	TCGAAGAAACTGTCGACGCA	439 700 (genomic)
FRO2	TTGCTACCGGCAATGGGATT	AACTTATGCCGACGTGGAGG	322 754 (genomic)
FRO3	ATCACTTCCAACCGACGGAG	TCTAATCGCCGGGAATGTGG	361 968 (genomic)
FRO7	GTGTGGAGGGACCTTATGGC	CTCCAACATCCACACTCCCC	795 1166 (genomic)
FRO4	GGCAACATCTGTTGGGCCTT	GAGGCTGACATATCCAGTGGG	944 1460 (genomic)
CAP	TGGGGTGGGACCCTTAAGAT	TTGCACATCCCAACCTCTCC	278
NAS1	CGTGCTTACCCACGGATACA	ACGAGGTTTGAAGCGAGTGT	388
ATNAS2	AAGTTCCACCTCCCCAACAC	CAAGCTTACGTGCGATGACC	397
ATNAS4	CGACGTTGTGTTCTTGGCTG	TTAGCACCTGCGAACTCCTC	366
ACTIN	TCCCAGTGTTGTTGGTAGGC	CAGTAAGGTCACGTCCAGCA	467 545 (genomic)

The PCR was run according to the protocol of Thermo Scientific DreamTaq DNA Polymerase (Thermo Scientific). The components that were used to prepare one PCR mix and the thermal conditions are represented in table 2.8 and 2.9, respectively.

Table 2.9. Components of PCR mix to run the PCR by using Thermo Scientific DreamTaq DNA Polymerase.

Components	**Volume (per sample)**	**Final conc**
10*Dream taq buffer Dntp mix 2.5 mM of each Forward primer (10 μM) Reverse Primer (10 μM) Dream taq polymerase 5 U/μL Water DNA Template	1.0 μL 0.4 μL 0.5 μL 0.5 μL 0.1 μL 6,5 μL 1.0 μL	1x 0.1 mM of each 0.5 μM 0.5 μM 0.05 U Variable 50 ng/μL
Final volume	10 μL	

Table 2.10. Thermal conditions for PCR with Thermo Scientific DreamTaq DNA Polymerase.

Step	**T, ^{0}C**	**Time**	**Number of cycles**
Initial denaturation	95	3 min	
Denaturnation	95	30 s	
Annealing	55	30 s	34
Extension	72	1 min/kb	
Final extension	72	5 min	

Gel run and gene expression analysis

The cDNA samples of WT and *lcmt1* roots and shoots obtained by PCR, were run into a gel to study the amount of gene expression. The gel was made by using 1% Agarose bioreagent (Sigma-Aldrich). After casting the gel, 1μL gel red (BIOLINE) was mixed with 5μL Hyperladder 1kb (BIOLINE) to make the ladder. In addition to this, 1 μL gel red (BIOLINE) and 2 μL 5X DNA loading buffer were mixed with each cDNA samples. All the samples were centrifuged for few seconds before inserting into the gel. In each well 10 μL of the PCR mixture was added. Then the gel was run at 80 V for 40 min, using 1X TAE as the running buffer. However, the band images were obtained from ChemiDoc^{TM} Touch imaging system (BIO-RAD) and the band intensities were measured by using ImageJ software (https://imagej.nih.gov/ij/index.html).

2.8.4 Real-time PCR

In this study, Taq-Man assay was used to perform real time PCR and analyze gene expression for some specific genes. The TaqMan primers of analyzed genes are listed in table 2.11 and description of those genes are listed in Appendix (Table C.2). Each well of an optical-96-well reaction plate (Applied Biosystems, USA) was filled with 18 µL real-time PCR reaction mix (showed in table 2.12) (Applied Biosystem) together with 2 µL diluted cDNA sample (5 ng/µL). The gene amplification and analysis were performed using the Applied Biosystems 7300 Real-Time PCR System (Applied Biosystems, USA). The thermal cycling profile is displayed in table 2.13.

Table 2.11. List of TaqMan primers (Applied Biosystems, USA).

Gene	Accession number	TaqMan ID
FSD1	At4g25100	At02238153_g1
SULTR1;2	At1g78000	At02250682_g1
NAS1	AT5g04950	At02181318_s1
SDI1	At5g48850	At02318365_m1
PP2AA2	AT3G25800	At02280306_g1
UBC35	AT1G78870	At02612351_g1

Table 2.12. Real-time PCR reaction mix (Applied Biosystems, USA).

Component	Volume (µL)
TaqMan® Fast Advancrd Master Mix	10.0
TaqMan primer	1.0
Water	7.0
Total volume	18

Table 2.13. Thermal-cycling profile of real time PCR.

Step	Temperature, ^{0}C	Time	Number of cycles
Hold	50	2 min	
Hold	95	20 s	
Denature	95	3 s	40
Aneal/Extend	60	30 s	

3 Results

3.1 Phenotype

3.1.1 Arabidopsis transferred in vermiculite

Arabidopsis WT and *lcmt1* were harvested from vermiculite after treating them with regular Hoagland solution (2 mM $MgSO_4$) and Hoagland solution with 2 mM $MgCl_2$ at an 8 h light/16 h darkness scheme. This experiment was done 4 times with different incubation periods such as 5 weeks, 2 weeks, 4 weeks and 3 weeks, respectively. Pictures of the plants were taken with and without vermiculite, e.g. vermiculite was still attached to the roots after harvesting or carefully removed to identify the phenotypic differences between WT and *lcmt1* (Appendix; figure A.1, A.2, A.3 and A.4). The weight of roots and shoots for both WT and mutant were measured in each experiment except the last experiment which had 3 weeks incubation period. Bar diagrams are made from the root weights (Figure 3.1) and shoot weights (Figure 3.2) of both WT and *lcmt1*.

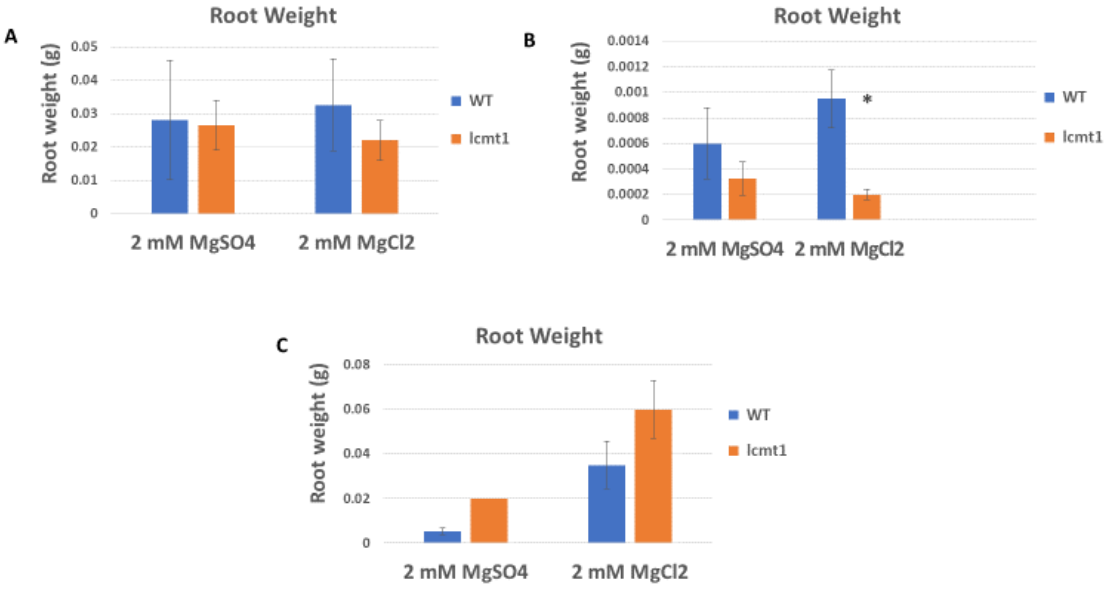

Figure 3.1. Root weight assay performed with Arabidopsis WT and *lcmt1* in vermiculite. The plants (5 WT and 5 mutants per treatment) were treated with regular Hoagland solution (2 mM $MgSO_4$) and Hoagland solution with 2 mM $MgCl_2$ at 8 h light/ 16 h dark cycle. **A.** Root weights of WT and *lcmt1* harvested from vermiculite, after 5 weeks of incubation. Three WT and mutants were taken for both treatments. **B.** Root weights of WT and *lcmt1* harvested from vermiculite, after 2 weeks of incubation. Four representative plants were taken from both WT and mutant in each treatment. **C.** Root weights of WT and *lcmt1* harvested from vermiculite, after 4 weeks of incubation. Here 3 WT and 1 *lcmt1* were taken for 2 mM $MgSO_4$; 3 WT and 3 *lcmt1* were taken for 2 mM $MgCl_2$. SE is given as vertical bars. P-values below 0.05 is denoted by * where WT is significantly different from *lcmt1*.

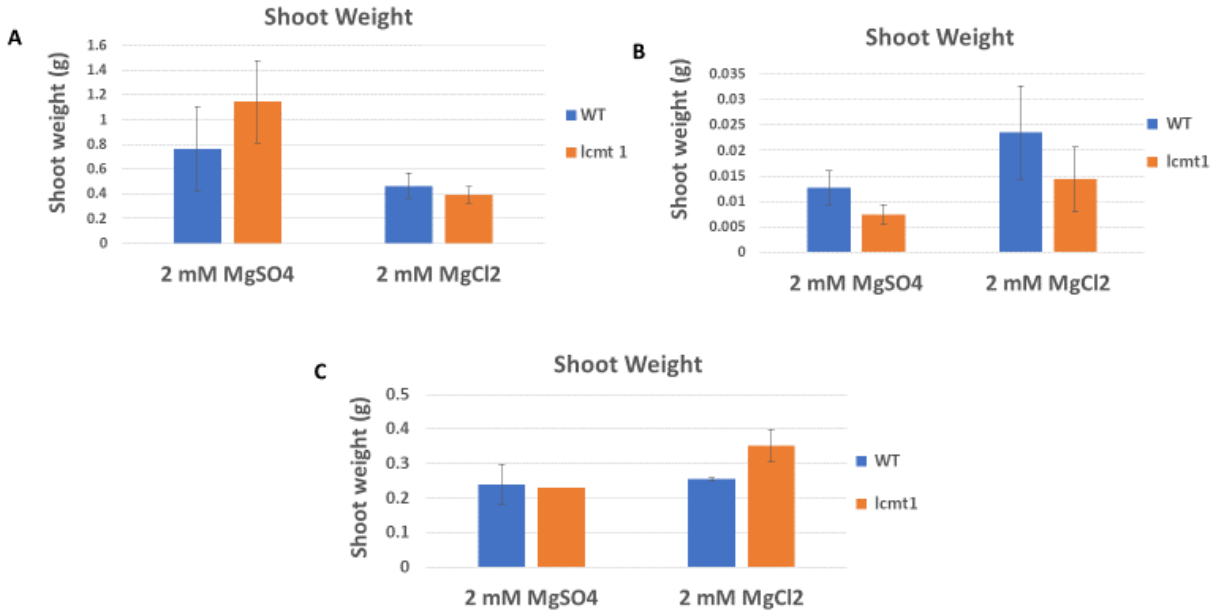

Figure 3.2. Shoot weight assay performed with Arabidopsis WT and *lcmt1* in vermiculite. The plants (5 WT and 5 mutants per treatment) were treated with regular Hoagland solution (2 mM $MgSO_4$) and Hoagland solution with 2 mM $MgCl_2$ at 8 h light/ 16 h dark cycle. **A.** Shoot weights of WT and *lcmt1* harvested from vermiculite, after 5 weeks of incubation. Three WT and mutants were taken for both treatments. **B.** Shoot weights of WT and *lcmt1* harvested from vermiculite, after 2 weeks of incubation. Four representative plants were taken from both WT and mutant in each treatment. **C.** Shoot weights of WT and *lcmt1* harvested from vermiculite, after 4 weeks of incubation. Here 3 WT and 1 *lcmt1* were taken for 2 mM $MgSO_4$; 3 WT and 3 *lcmt1* were taken for 2 mM $MgCl_2$. SE is given as vertical bars.

The effects on root weight between WT and *lcmt1* were not significantly different in the first assay (5 weeks incubation, Figure 3.1 A) in presence of either 2 mM $MgSO_4$ or 2 mM $MgCl_2$. In the second assay (2 weeks incubation, Figure 3.1 B), the root weight of mutant was significantly lower than WT in presence of 2 mM $MgCl_2$ (P-value = 0.0085), whereas no significant effect on root weights was seen in 2 mM $MgSO_4$ treatment. In the third assay (4 weeks incubation, Figure 3.1 C), there was no significant difference in root weight between WT and *lcmt1* for any of the treatments. Here, only 1 *lcmt1* was counted in 2 mM $MgSO_4$ treatment as the rest of the *lcmt1* were died. The tendency of root weight between WT and *lcmt1* was kind of similar in both first and second assay (Figure 3.1 A and B), e.g. root weight of *lcmt1* was lower than WT in both treatments. On the other hand, in the third assay (Figure 3.1 C), the root weight of *lcmt1* seemed to be higher than WT in both $MgSO_4$ and $MgCl_2$ treatments.

The effect on shoot weight between WT and mutant was not significant in any of the assessments (Figure 3.2 A, B and C) in presence of either Hoagland solution with $MgSO_4$ or $MgCl_2$. The shoot weights of WT and *lcmt1* seemed to randomly vary between them in all the repetitions.

The root and shoot weights of WT and *lcmt1* varied among the experiments as the plant's age were not similar. Vermiculite used to grow the plants could also be an important factor behind this.

The plants in the first experiment (Figure 3.1 A, Appendix figure A.1) grew better than in later experiments (Figure 3.1 B and C, Appendix figure A.2 and A.3). When repeating, plants had to be harvested earlier than 5 weeks as they started to suffer much earlier. The reason behind this could possibly be due to soil remnants still left with the roots while transferring the plants from soil to vermiculite in the first experiment. On the other hand, the soil was cleaned properly from the roots, while transferring to vermiculite in later experiments. The leftover soil could be an important factor behind the differences in growth between the plants in the first and later experiments.

3.1.2 Arabidopsis transferred in rockwool

Arabidopsis WT and *lcmt1* plants were grown on rockwool and treated with regular Hoagland solution (2 mM $MgSO_4$) and Hoagland solution with 2 mM $MgCl_2$ at 8 h light/16 h dark cycle for 5 weeks. The shoot weight of WT and mutant plants were measured to determine the phenotypic difference between them. Five WT and *lcmt1* plants were used for each treatment and 4 representative plants from each type of Arabidopsis were chosen to measure shoot weight. Pictures were taken before measuring (Appendix figure A.5) and bar graphs (figure 3.3) were made to display the data.

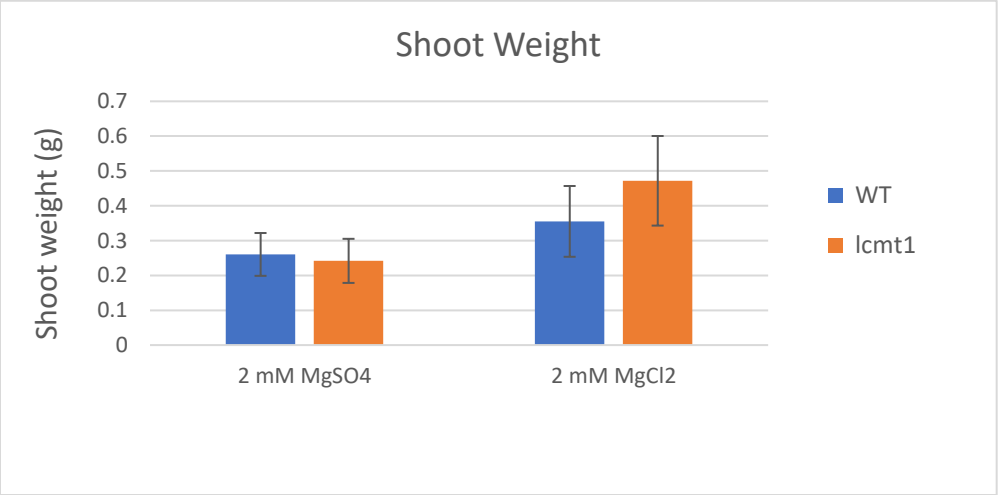

Figure 3.3. Shoot weight of WT and *lcmt1* plants in rockwool. Four WT and mutants (representative plants) were encountered for each 2 mM $MgSO_4$ and 2 mM $MgCl_2$ treatment. Five WT and mutant plants were treated with 2 mM $MgSO_4$ and 2 mM $MgCl_2$ in rockwool and kept at 8 h light/16 h darkness for 5 weeks. SE is given as vertical bars.

The root weights of WT and *lcmt1* were not significantly different either in 2 mM $MgSO_4$ or 2 mM $MgCl_2$ treatment. However, the shoots of *lcmt1* were visually slightly bigger and greener than WT in $MgCl_2$ treatment (Appendix figure A.5).

3.2 Stress experiments

3.2.1 Sulphur experiment

Shoot weight measurement

The WT and *lcmt1* shoots (15 WT and 15 *lcmt1* per treatment) were measured after treating them with different concentrations of Hoagland media such as 0 mM $MgSO_4/MgCl_2$, 2 mM $MgSO_4$ (control), 10 mM $MgSO_4$, 2 mM $MgCl_2$ and 10 mM $MgCl_2$. There were 3 replicates for each treatment. All the shoots of WT and mutant from each replicate (5 WT and 5 *lcmt1* per plate) were measured for each concentration. A bar diagram (Figure 3.4) was made to represent the difference in shoot weight between WT and mutant when they were treated with different concentration of sulphate and chloride.

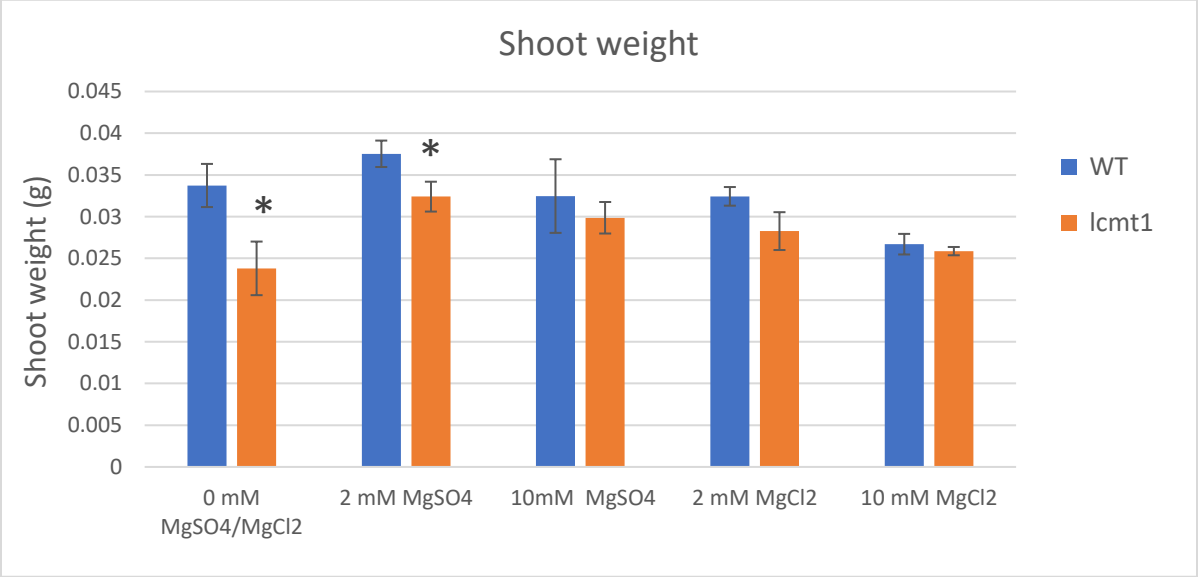

Figure 3.4. Shoot weight of WT and *lcmt1* seedlings. The WT and mutant seedlings (15 WT and 15 *lcmt1* per treatment) were treated with 0 mM (without $MgSO_4$ and $MgCl_2$), 2 mM $MgSO_4$ (control), 10 mM $MgSO_4$, 2 mM $MgCl_2$ and 10 mM $MgCl_2$ at dark for 3 d and at 16 h light/8 h darkness for 5 d. The seedlings were transferred to new plates with respective concentrations of Hoagland media and kept at a16 h light/8 h darkness scheme for additional 7 d. SE is given as vertical bars. P-values below 0.05 is denoted by * where WT is significantly different from *lcmt1*.

Root length measurement

Pictures were taken after treating the WT and *lcmt1* seedlings with different concentrations of Hoagland media such as 0 mM $MgSO_4/MgCl_2$, 2 mM $MgSO_4$ (control), 10 mM $MgSO_4$, 2 mM $MgCl_2$ and 10 mM $MgCl_2$ at 16 h light/8 h dark cycle for 7 d. The root lengths of WT and mutant seedlings were measured from the pictures (Appendix figure B.1) by using ImageJ software. A bar

diagram (shown in figure 3.5) demonstrates the difference in root length between WT and *lcmt1* treated with different concentrations of sulphate and chloride.

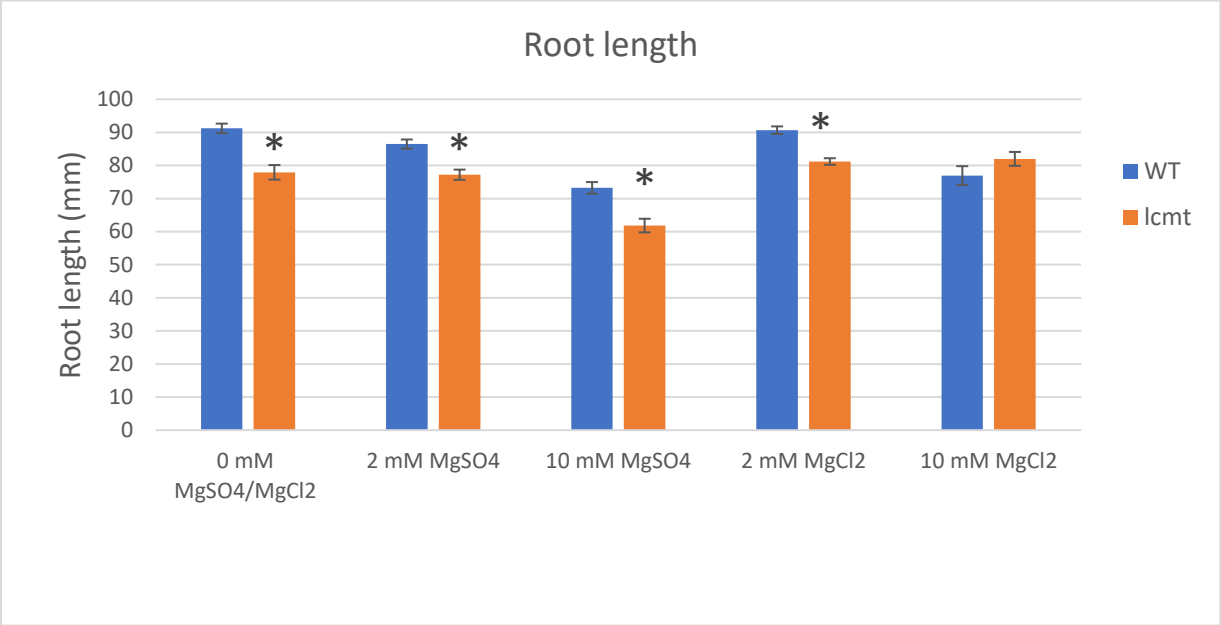

Figure 3.5. Root length of WT and *lcmt1* seedlings. The seedlings (15 WT and 15 *lcmt1* per treatment) were treated with 0 mM (without $MgSO_4$ and $MgCl_2$), 2mM $MgSO_4$ (control), 10 mM $MgSO_4$, 2 mM $MgCl_2$ and 10 mM $MgCl_2$ at dark for 3 d and at 16 h light/8 h darkness for 5 d. The seedlings were transferred to new plates with respective concentrations of Hoagland media and kept at 16 h light/8 h darkness for additional 7 d. SE is given as vertical bars. P-values below 0.05 is denoted by * where WT is significantly different from *lcmt1*.

Chlorophyll assay

A chlorophyll assay was conducted with the shoots of WT and *lcmt1* seedlings (15 WT and 15 *lcmt1* per treatment) grown in different concentrations of Hoagland media at 16 h light/8 h darkness scheme for 7 d. There were 3 replicates for each treatment. The WT and mutant shoots of 3 replicates of each treatment (15 WT and 15 mutant) were encountered to measure the absorbance at 654 nm (Figure 3.6).

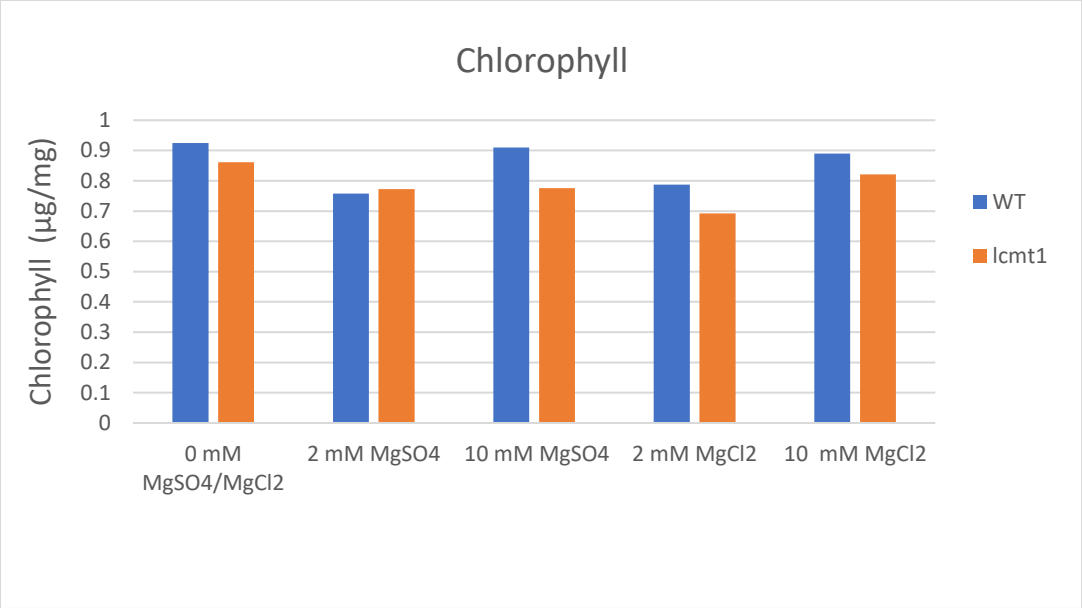

Figure 3.6. Chlorophyll assay of WT and *lcmt1* shoots. The WT and *lcmt1* seedlings (15 WT and 15 *lcmt1* per treatment) were treated with 0 mM (without $MgSO_4$ and $MgCl_2$), 2mM $MgSO_4$ (control), 10 mM $MgSO_4$, 2 mM $MgCl_2$ and 10 mM $MgCl_2$ at dark for 3 d and at 16 h light/8 h darkness for 5 d. Arabidopsis seedlings were transferred to new plates with respective concentrations of Hoagland media and kept at 16 h light/8 h darkness for additional 7 d.

The Hoagland solution with 0 mM $MgSO_4$/$MgCl_2$ and 2 mM $MgSO_4$ significantly inhibited the shoot weight of *lcmt1* compared to WT (P-values = 0.0368 and 0.049, respectively) (Figure 3.4). Whereas no significant difference in shoot weight was observed between WT and mutants treated with other treatments (10 mM $MgSO_4$, 2 mM $MgCl_2$ and 10 mM $MgCl_2$). The tendency of *lcmt1* shoot weights was lower than WT in all the Hoagland treatments but in presence of the highest concentration of chloride (10 mM $MgCl_2$), both WT and *lcmt1* tended to be lower than other treatments. Visually no difference was observed between WT and mutant in any of the treatments (Appendix figure B.1).

The pattern of root length in figure 3.5 followed a similar tendency in presence of control (2 mM $MgSO_4$), 0 mM $MgSO_4$/$MgCl_2$, 10 mM $MgSO_4$ and 2 mM $MgCl_2$. The root length in *lcmt1* was significantly shorter than WT in all the treatments except 10 mM $MgCl_2$. The P-values for 0 mM $MgSO_4$/$MgCl_2$, 2 mM $MgSO_4$, 10 mM $MgSO_4$ and 2 mM $MgCl_2$ are 1.27E-05, 6.20E-05, 0.0001 and 4.68E-07, respectively. The bar diagram displays that the highest concentration of sulphate (10 mM $MgSO_4$) provided more stress to both WT and *lcmt1* roots compared to control. Regarding the 2 mM $MgCl_2$, the root lengths of both WT and *lcmt1* were almost similar as the control treatment. However, the highest concentration of $MgCl_2$ (10 mM) slightly inhibited the root length of WT than *lcmt1* (Figure 3.5, Appendix figure B.1).

In Figure 3.6, the chlorophyll content of both WT and *lcmt1* varied in the treatments of 0 mM $MgSO_4$/$MgCl_2$, 10 mM $MgSO_4$, 2 mM $MgCl_2$ and 10 mM $MgCl_2$ when compared to control (2

mM $MgSO_4$). The chlorophyll content of the mutant seemed to be lower than WT in all the treatments except control. In this experiment, shoots from all replicates in each treatment (15 WT and 15 *lcmt1* per treatment) were crushed to extract the chlorophyll. As a result, the p-value could not be calculated.

3.2.2 NaCl experiment

Shoot weight measurement

The WT and *lcmt1* shoots (5 WT and 5 *lcmt1* per plate) were measured after treating them with different concentrations of NaCl and control (only ½ MS agar media, no NaCl). There were 3 replicates for each treatment. During the shoot weight measurement, all the WT and *lcmt1* shoots from each replicate (5 WT and 5 *lcmt1*) were measured to determine the mean shoot weight of WT and *lcmt1* for each NaCl concentration. This experiment was performed 3 times. In the first experiment, one replicate of control (0 mM NaCl) was deducted from the experimental data due to fungal growth inside the plate. A graph of average shoot weight assay obtained from three experiments is shown in figure 3.7.

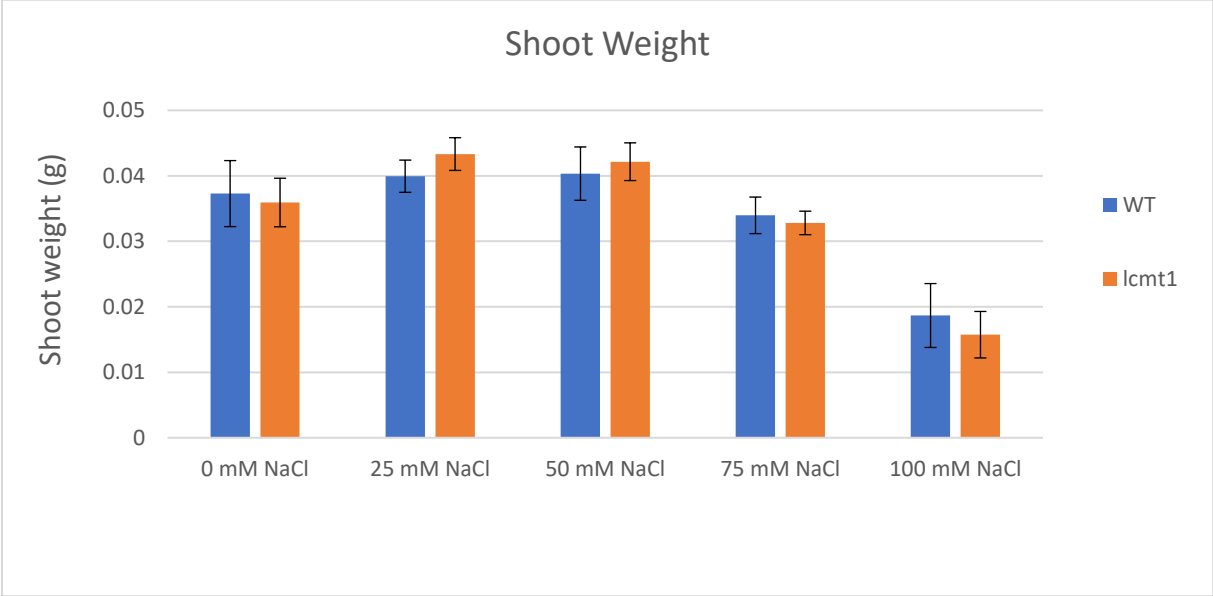

Figure 3.7. Average shoot weight of WT and *lcmt1* seedlings from three NaCl experiments. Here, 45 WT and 45 mutant seedlings were encountered for all NaCl treatments, except 0 mM NaCl where 44 WT and 44 *lcmt1* were accounted. In each experiment, there were 3 replicates for each treatment (total 15 WT and 15 *lcmt1* per treatment). The WT and *lcmt1* seedlings were grown in ½ MS media for 8 d (3 d at dark and 5 d at 16 h light/8 h dark). After 8 d, the seedlings were treated with control (only ½ MS media, no NaCl), 25 mM, 50 mM, 75 mM, and 100 mM NaCl at 16 h light/8 h darkness for additional 7 d. SE is given as vertical bars.

Root length measurement

The root lengths of WT and mutant (5 WT and 5 *lcmt1* per plate) were measured by using ImageJ. Pictures of all the plates (Appendix figure B.2, B.3 and B.4)were taken after treating the WT and *lcmt1* seedlings with different concentrations of NaCl (25 mM, 50 mM, 75 mM and 100 mM) and control (only ½ MS media, no NaCl) for 7 d at 16 h light/8 h dark cycle. Here, 3 replicates from each treatment (15 WT and 15 *lcmt1* per treatment) were accounted to determine the mean root length of WT and *lcmt1* individually. This experiment was performed 3 times. A diagram of average root length assay obtained from three NaCl experiments is shown in figure 3.8.

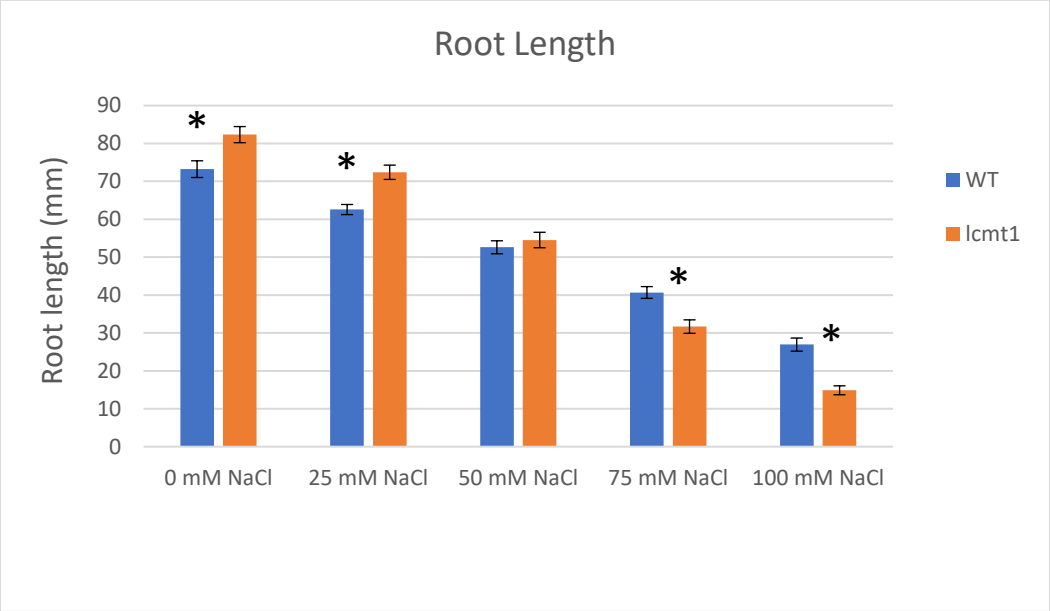

Figure 3.8. Average root length of WT and *lcmt1* seedlings obtained from three NaCl experiments. In the diagram, 45 WT and 45 mutant seedlings were encountered for all NaCl treatments, except 0 mM NaCl where 44 WT and 44 *lcmt1* were accounted. In each experiment, there were 3 replicates for each treatment (total 15 WT and 15 *lcmt1* per treatment). The WT and *lcmt1* seedlings were grown in ½ MS media for 8 d (3 d at dark and 5 d at 16 h light/8 h dark). After 8 d, the seedlings were treated with control (only ½ MS media, no NaCl), 25 mM, 50 mM, 75 mM, and 100 mM NaCl at 16 h light/8 h darkness for additional 7 d. SE is given as vertical bars. P-values below 0.05 are denoted by * when *lcmt1* is significantly different from WT.

Chlorophyll assay

The shoots were collected from WT and mutant seedlings (5 WT and 5 *lcmt1* per plate) treated with different concentrations of NaCl (25 mM, 50 mM, 75 mM and 100 mM) and control (only ½ MS media, no NaCl) at 16 h light/8 h darkness scheme for 7 d. A chlorophyll assay was carried out with all the shoots of WT and *lcmt1* (3 replicates of each treatment included, total 15 WT and 15 mutant shoots per treatment) for each NaCl concentration as well as control to determine the

absorbance. The chlorophyll assay in NaCl experiment was repeated 3 times. A bar graph of average chlorophyll content accomplished from three experiments is displayed in figure 3.9.

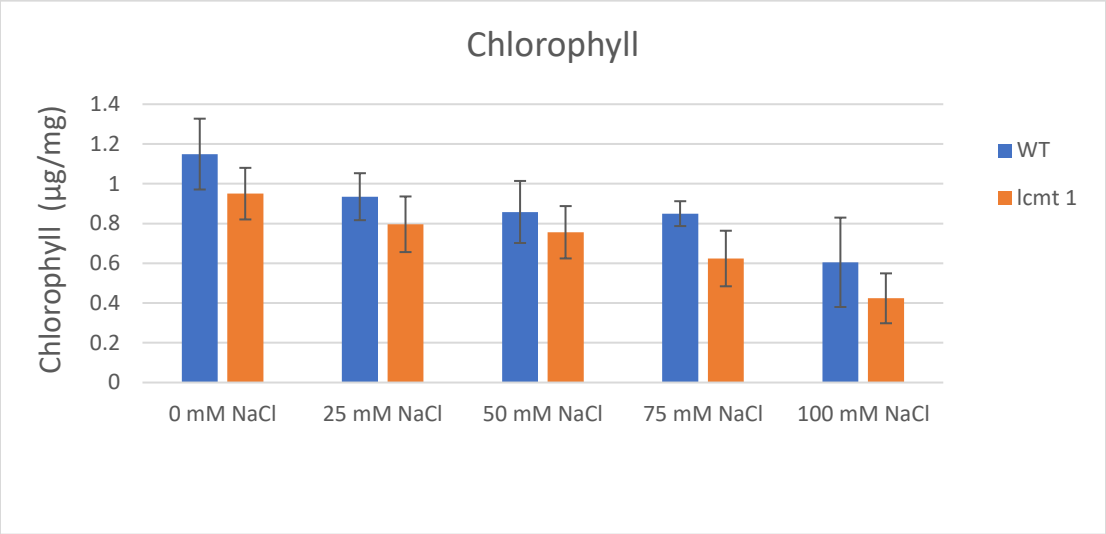

Figure 3.9. Average chlorophyll content of WT and *lcmt1* shoots obtained from three repeated experiments. Here, 45 WT and 45 mutant seedlings were encountered for all NaCl treatments, except 0 mM NaCl where 44 WT and 44 *lcmt1* were accounted. In each experiment, there were 3 replicates for each treatment (total 15 WT and 15 *lcmt1* per treatment). The WT and *lcmt1* seedlings were grown in ½ MS media for 8 d (3 d at dark and 5 d at 16 h light/8 h dark). After 8 d, the seedlings were treated with control (only ½ MS media, no NaCl), 25 mM, 50 mM, 75 mM, and 100 mM NaCl at 16 h light/8 h darkness for additional 7 d. SE is given as vertical bars.

The differences in shoot weights between WT and *lcmt1* were not significant in figure 3.7. In general, from the diagram, the shoot weight of both WT and *lcmt1* in 25 mM and 50 mM NaCl was higher when comparing to WT and *lcmt1* in control. On the other hand, 75 mM and 100 mM NaCl stress seemed to impair the shoot weight of both WT and mutant compared to control. The *lcmt1* shoot weights were slightly inhibited than WT in presence of 75 mM NaCl whereas, it seemed to be more inhibited than WT in 100 mM NaCl stress.

The roots of *lcmt1* in control and 25 mM NaCl (Figure 3.8) were significantly longer than WT (P-values = 0.002 and 2.62E-05, respectively). On the other hand, the root lengths of mutants were significantly shorter than WT, in the presence of increased concentrations of NaCl, e.g., 75 mM and 100 mM NaCl. When NaCl stress is 50 mM, the root length of the mutant was very slightly longer than WT, but the difference was not significant. In the overall diagram, the root lengths of both WT and *lcmt1* seemed to be more impaired than control, with gradually increasing NaCl stress.

There were no significant differences in chlorophyll content between WT and *lcmt1*(Figure 3.9). The chlorophyll content of *lcmt1* tended to be lower than WT in all the treatments of NaCl

including control. This indicates the chlorophyll content in the *lcmt1* mutant is less than WT in standard condition. The *lcmt1* chlorophyll contents were gradually lowered with increasing concentrations of salt which means the *lcmt1* is stressed with higher concentrations of NaCl. Similarly, the tendency of WT chlorophyll contents was gradually decreased like *lcmt1* with increasing salt concentrations but in 50 mM and 75 mM NaCl treatments, the WT chlorophyll contents were almost similar.

3.2.3 H_2O_2 experiment

Shoot weight measurement

The WT and *lcmt1* shoots (5 WT and 5 *lcmt1* per plate) were measured after treating them with different concentrations of H_2O_2 and control (only ½ MS agar media, no H_2O_2). There were 3 replicates for each treatment. During the shoot weight measurement, all the WT and *lcmt1* shoots from each replicate (5 WT and 5 *lcmt1*) were measured to determine the mean shoot weight of WT and *lcmt1* for each H_2O_2 concentration. This experiment was performed 3 times. A bar diagram (Figure 3.10) was made from the average shoot weight obtained from three experiments.

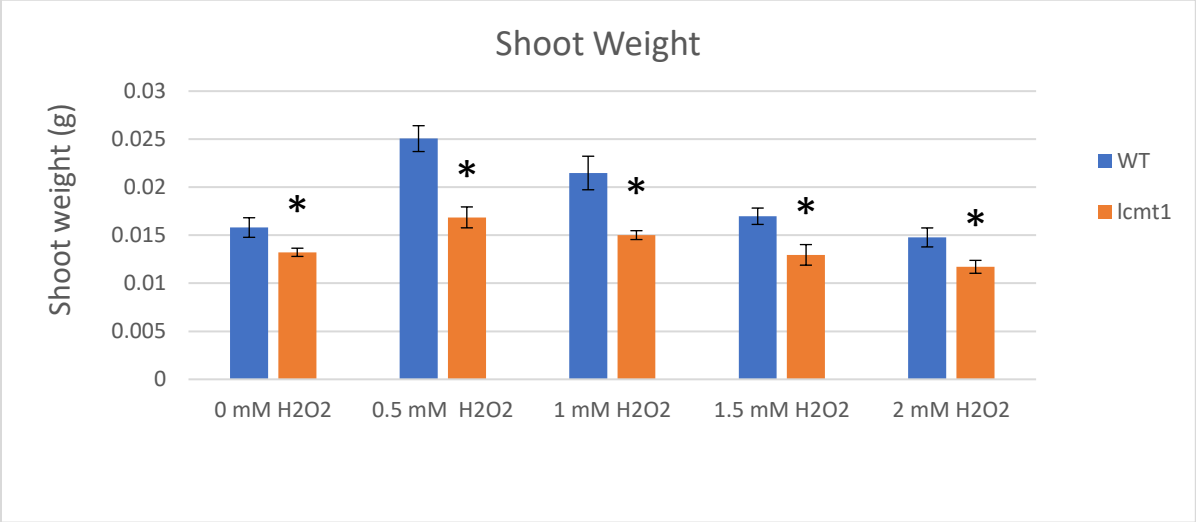

Figure 3.10. Average shoot weight of WT and *lcmt1* seedlings from three H_2O_2 experiments. Here, 45 WT and 45 mutant seedlings were encountered for all H_2O_2 treatment. In each experiment, there were 3 replicates for each treatment (total 15 WT and 15 *lcmt1* per treatment). The WT and *lcmt1* seedlings were grown in ½ MS media for 8 d (3 d at dark and 5 d at 16 h light/8 h dark). After 8 d, the seedlings were treated with control (only ½ MS media, no H_2O_2), 0.5 mM, 1 mM, 1.5 mM, and 2 mM H_2O_2 at 16 h light/8 h darkness for additional 7 d. SE is given as vertical bars. P-values below 0.05 are denoted by * when *lcmt1* is significantly different from WT.

Root length measurement

The root lengths of WT and mutant (5 WT and 5 *lcmt1* per plate) were measured by using ImageJ. Pictures of all the small plates (Figure 3.11, Appendix figure B.5, B.6) were taken after treating the WT and *lcmt1* seedlings with different concentrations of H_2O_2 (0.5 mM, 1 mM, 1.5 mM and 2 mM) and control (only ½ MS media, no H_2O_2) for 7 d at 16 h light/8 h darkness scheme. Here, 3 replicates from each treatment (15 WT and 15 *lcmt1* per treatment) were accounted to determine the mean root length of WT and *lcmt1* individually. This experiment was performed 3 times. A diagram of average root length obtained from three H_2O_2 experiments is shown in figure 3.12.

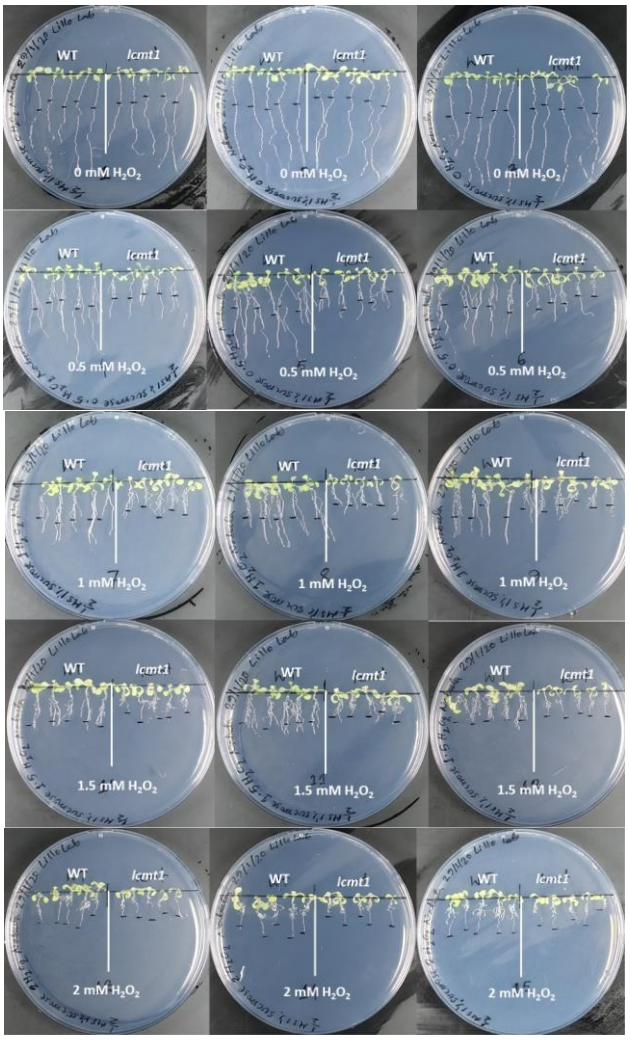

Figure 3.11. Arabidopsis seedlings grown in petri dishes containing ½ MS media and different H_2O_2 treatments. The seedlings (5 WT and 5 *lcmt1* per plate) were grown in ½ MS media for 8 d (3 d at dark and 5 d at 16 h light/8 h dark). After 8 d, the seedlings were treated with control (only ½ MS media, no H_2O_2), 0.5 mM, 1 mM, 1.5 mM, and 2 mM H_2O_2 at 16 h light/8 h darkness for additional 7 d. Three biological replicates were made for each treatment.

Observation from the image of petri dishes (figure 3.11) shows that the *lcmt1* stopped growing at 1 mM H_2O_2, whereas WT was still able to grow. However, during 1.5 mM H_2O_2 treatment, both WT and *lcmt1* root growths were stopped.

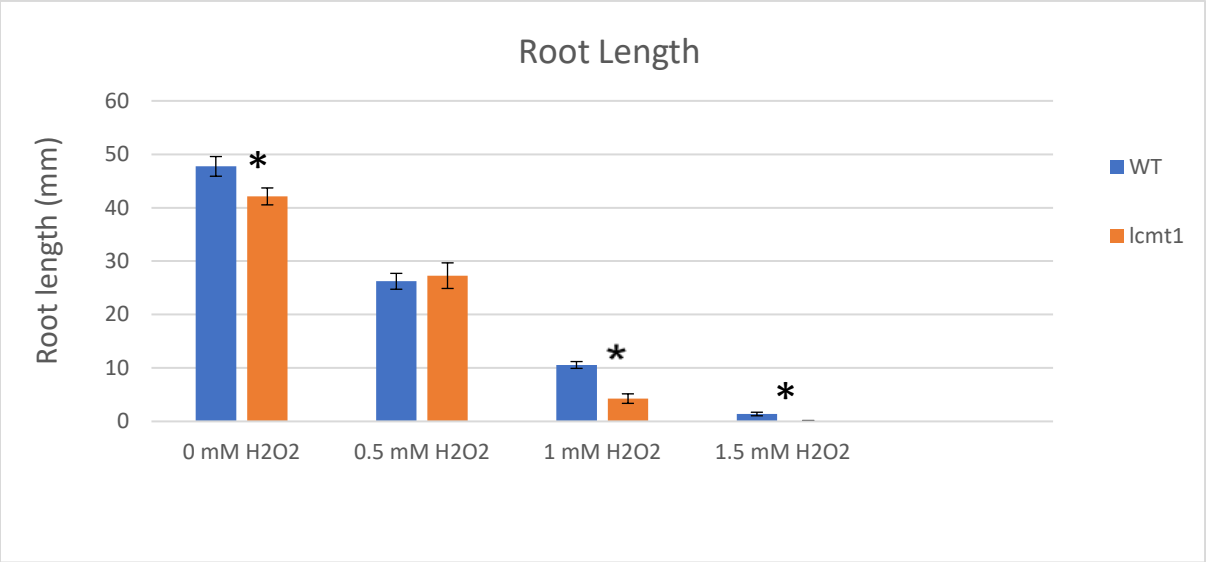

Figure 3.12. Average root length of WT and *lcmt1* seedlings obtained from three H_2O_2 experiments. In the diagram, 45 WT and 45 mutant seedlings were encountered for all H_2O_2 treatments. In each experiment, there were 3 replicates for each treatment (total 15 WT and 15 *lcmt1* per treatment). The WT and *lcmt1* seedlings were grown in ½ MS media for 8 d (3 d at dark and 5 d at 16 h light/8 h dark). After 8 d, the seedlings were treated with control (only ½ MS media, no H_2O_2), 0.5 mM, 1 mM, 1.5 mM, and 2 mM H_2O_2 at 16 h light/8 h darkness for additional 7 d. SE is given as vertical bars. P-values below 0.05 are denoted by * when *lcmt1* is significantly different from WT.

Chlorophyll assay

The shoots were collected from WT and mutant seedlings (5 WT and 5 *lcmt1* per plate) treated with different concentrations of H_2O_2 (0.5 mM, 1 mM, 1.5 mM and 2 mM) and control (only ½ MS media, no H_2O_2) at 16 h light/8 h darkness scheme for 7 d. A chlorophyll assay was carried out with all the shoots of WT and *lcmt1* (3 replicates of each treatment included, total 15 WT and 15 mutant shoots per treatment) for each H_2O_2 concentration as well as control to determine the absorbance. The chlorophyll assay in H_2O_2 experiment was repeated 3 times. A bar graph of average chlorophyll content accomplished from three experiments is displayed in figure 3.13.

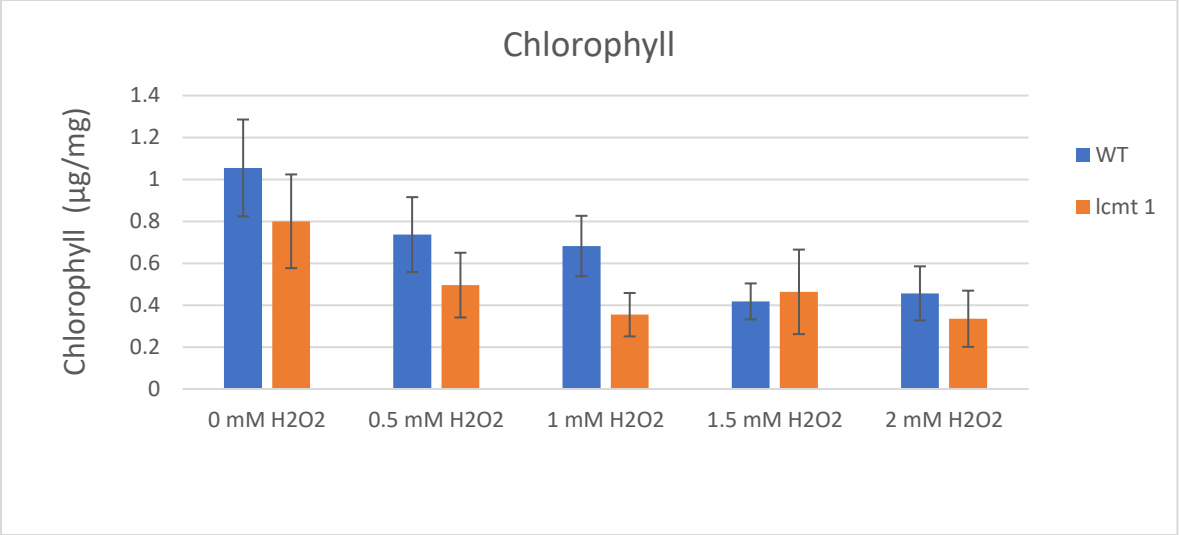

Figure 3.13. Average chlorophyll content of WT and *lcmt1* shoots obtained from three repeated experiments. Here, 45 WT and 45 mutant seedlings were encountered for all H_2O_2 treatments. In each experiment, there were 3 replicates for each treatment (total 15 WT and 15 *lcmt1* per treatment). The WT and *lcmt1* seedlings were grown in ½ MS media for 8 d (3 d at dark and 5 d at 16 h light/8 h dark). After 8 d, the seedlings were treated with control (only ½ MS media, no H_2O_2), 0.5 mM, 1 mM, 1.5 mM, and 2 mM H_2O_2 at 16 h light/8 h darkness for additional 7 d. SE is given as vertical bars.

The shoot weights of *lcmt1* were significantly shorter than WT in all the H_2O_2 treatments including control (Figure 3.10). The P-values in control, 0.5 mM, 1 mM, 1.5 mM and 2 mM H_2O_2 treatments are 0.0165, 0.0001, 0.0013, 0.0048 and 0.0106, respectively. The shoot weights of both WT and mutants gradually decreased with the increasing concentrations of H_2O_2, whereas the shoot weights of WT and *lcmt1* in control seemed to be lower than the stressed WT and *lcmt1* shoots in other treatments.

The root lengths of both WT and *lcmt1* seemed to be gradually impaired with increasing concentrations of H_2O_2 (Figure 3.12). The mutant root lengths were significantly shorter than WT in both control and 1 mM H_2O_2 treatment (P-value = 0.012 and 6.15E-08, respectively). In presence of 1.5 mM H_2O_2, *lcmt1* seedlings stopped to grow compared with WT and a significant difference in root lengths was observed between them. On the other hand, the *lcmt1* root lengths were slightly longer than WT in 0.5 mM H_2O_2, but the difference between them was not significant. However, the treatment of both WT and *lcmt1* seedlings with the highest concentrations of H_2O_2 (2 mM H_2O_2) completely inhibited their root growths.

There were no significant differences in chlorophyll content between WT and *lcmt1* (Figure 3.13). Apart from this, the tendency of chlorophyll content in both WT and mutants were moving toward a lower level with increasing concentrations of H_2O_2. Moreover, chlorophyll level of *lcmt1* tended to be lower than WT in control and other treatments except for 1.5 mM H_2O_2.

3.3 Gene expression analysis

3.3.1 In-gel analysis

3.3.1.1 RNA extraction

RNA was extracted from the roots and shoots of WT and *lcmt1* plants treated with 2 mM $MgSO_4$ and 2 mM $MgCl_2$ in vermiculite for 5weeks. After extraction, the purity of RNA was measured by using NanoDrop One. The concentrations of isolated RNA are represented in table 3.1.

Table 3.1. Concentrations and purity measurement of isolated RNA by NanoDrop One.

Sample	Concentration (ng/µL)	A260/A280	A260/A230
WT shoot $MgSO_4$	303.3	2.13	2.28
WT root $MgSO_4$	416.5	2.13	2.23
lcmt1 shoot $MgSO_4$	471.2	2.11	2.24
lcmt1 root $MgSO_4$	312.9	2.13	2.37
WT shoot $MgCl_2$	221.8	2.10	2.36
WT root $MgCl_2$	238.0	2.12	1.96
lcmt1 shoot $MgCl_2$	256.1	2.13	2.11
lcmt1 root $MgCl_2$	96.2	2.12	1.20

3.3.1.2 PCR and gel analysis

After RNA extraction, cDNA was made from the roots and shoots of WT and mutant plants treated with 2 mM $MgSO_4$ and 2 mM $MgCl_2$. A second PCR was run to amplify several genes in the cDNA samples. The successful amplifications of the genes were tested by running the PCR samples in 1% Agarose bioreagent (Sigma-Aldrich) gel. The band images for different genes, obtained from ChemiDoc™ Touch imaging system (BIO-RAD) are represented in figure 3.14 (A and C), 3.15(A and C), 3.16 (A and C) and 3.17 (A and C). ImageJ software was used to measure the band intensities. All the gene amplifications were compared with *ACTIN* in WT $MgSO_4$. Graphs were also made from the expression values to get a better overview of gene expression that are shown in figure 3.14 (B and D), 3.15 (B and D), 3.16 (B and D) and 3.17 (B and D).

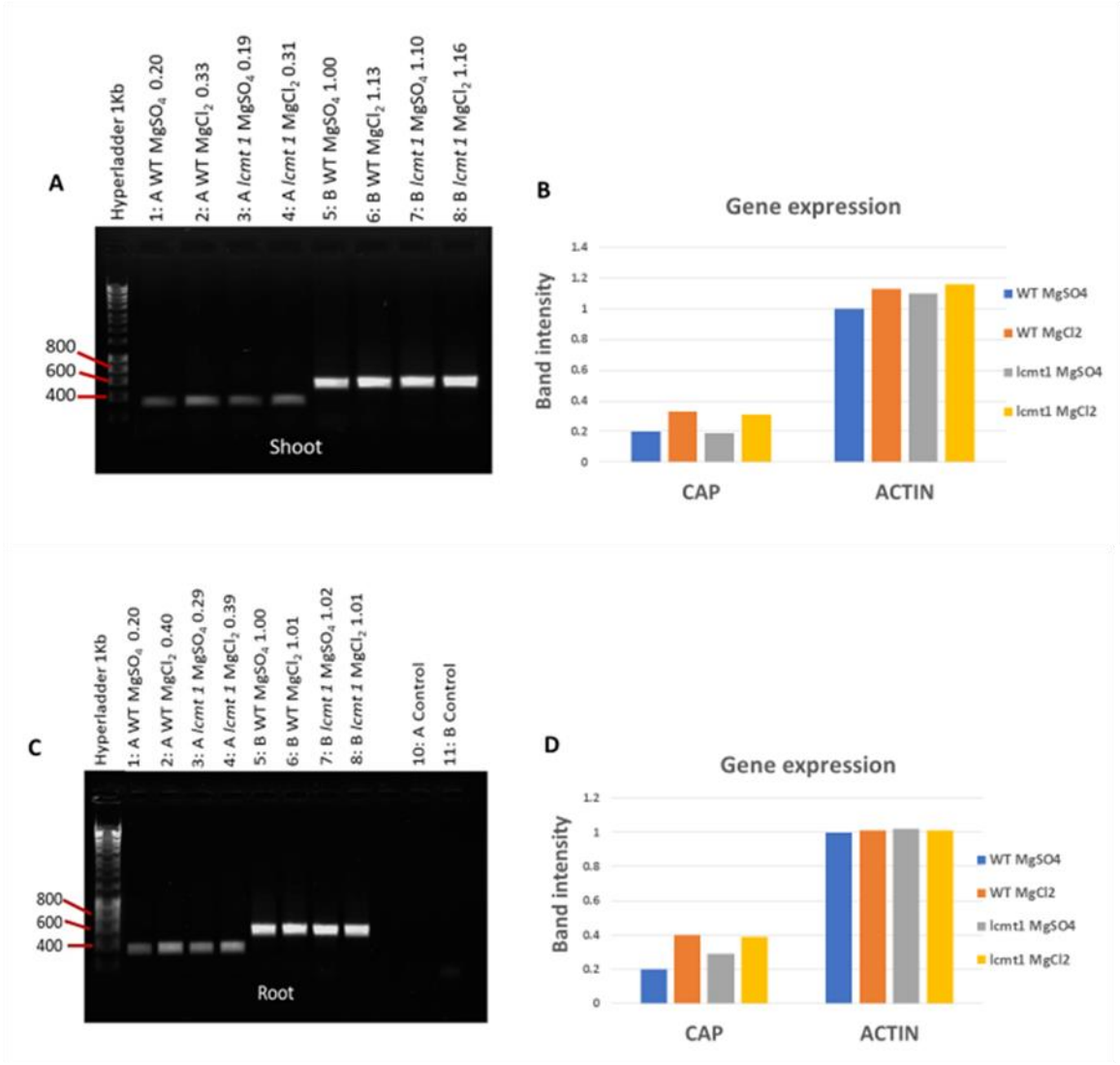

Figure 3.14. In-gel expression analysis on roots and shoots of WT and *lcmt1*. The WT and mutant seedlings were treated with 2 mM $MgSO_4$ and 2 mM $MgCl_2$ for 5 weeks in 8 h light. PCR was run using 50 ng cDNA per 10 µL reaction mixture at 55^0C annealing temperature and 34 cycles. Band intensities were measure by ImageJ software. *CAP* and *ACTIN* are represented as 'A' and 'B', respectively. The numbers are shown above each lane (Fig. **A** and **C**) are relative to *ACTIN* in WT $MgSO_4$.

The amplification of *CAP* seemed to be successful as all the samples (shoots and roots) with *CAP* had clear bands at around 278 bp (lane 1 to lane 4, figure 3.14 A and C). The gene expressed more in shoot samples (Figure 3.14 A and B) treated with $MgCl_2$ (WT = 0.33 and *lcmt1* = 0.31) than the corresponding samples treated with $MgSO_4$ (WT = 0.20 and *lcmt1* =0.19) while compared to the control (*ACTIN* in WT shoot $MgSO_4$). No visible difference in band intensity was observed between WT and mutant treated with either $MgSO_4$ or $MgCl_2$.

The gene (*CAP*) expression in roots (Figure 3.14, C and D) of both WT and *lcmt1* treated with $MgCl_2$ (WT = 0.40 and *lcmt1* = 0.39) was higher than the corresponding samples treated with

$MgSO_4$ (WT = 0.20 and *lcmt1* = 0.29) while compared to control (*ACTIN* in WT root $MgSO_4$). In presence of $MgSO_4$, the band intensity in WT was less than *lcmt1* (Figure 3.14 D).

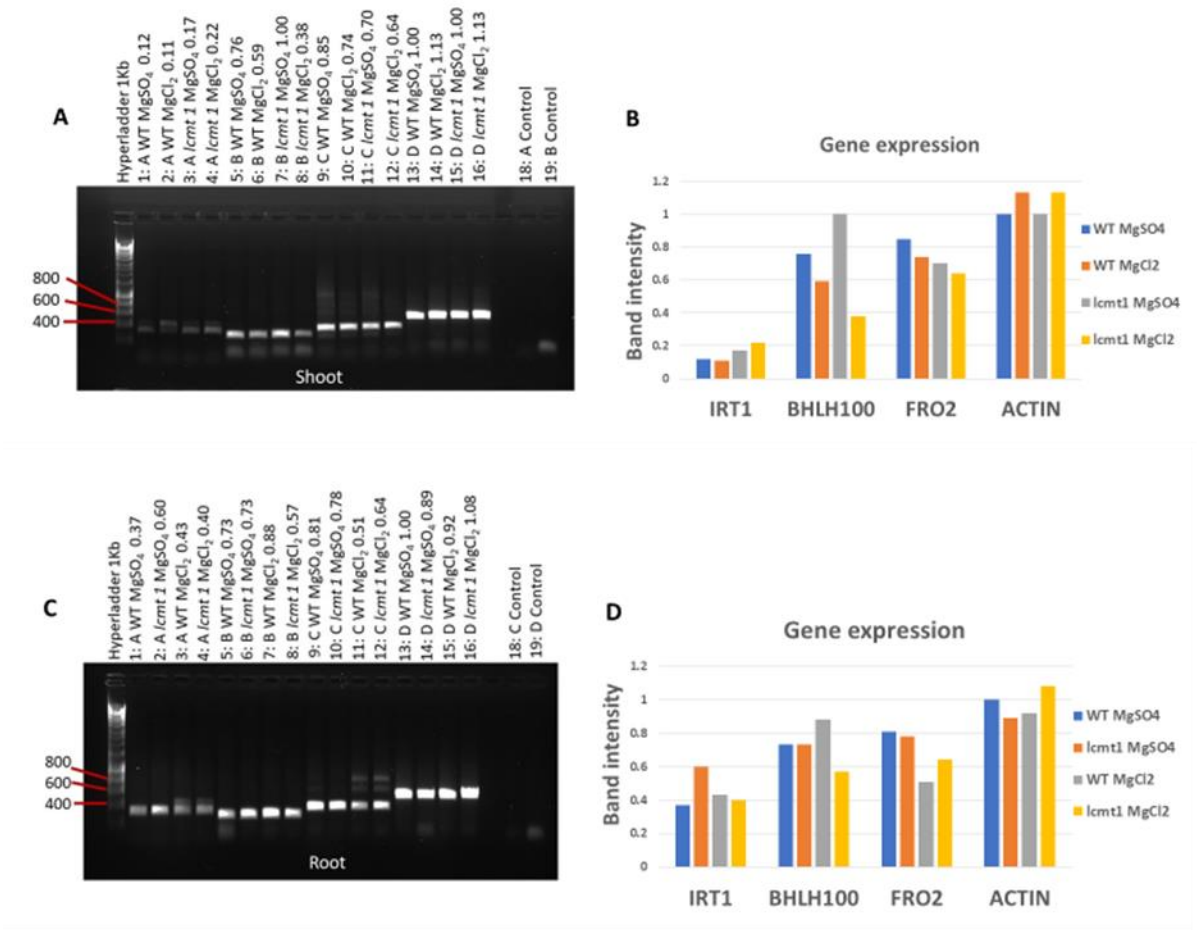

Figure 3.15. In-gel expression analysis on roots and shoots of WT and *lcmt1*. The WT and mutant seedlings were treated with 2 mM $MgSO_4$ and 2 mM $MgCl_2$ for 5 weeks in 8 h light. PCR was run using 50 ng cDNA per 10 µL reaction mixture at 55^0C annealing temperature and 34 cycles. Band intensities were measured by ImageJ software. *IRT1*, *BHLH100*, *FRO2*, and *ACTIN* are represented as A, B, C and D, respectively. The numbers are shown above each lane (Fig. **A** and **C**) are relative to *ACTIN* in WT $MgSO_4$.

Arabidopsis shoot and root samples showed bands at 445 bp (lane 1 to lane 4, figure 3.15 A and C) which indicated successful amplification of *IRT1*. Some double bands also appeared. It might be due to the primer of the gene. Among the shoot samples, *lcmt1* (lane 3 and 4, figure 3.15 A) had slightly higher band intensity than WT in presence of $MgSO_4$ and $MgCl_2$ treatments (lane 1 and 2, figure 3.15 A). Regarding the root samples (Figure 3.15 C and D), the gene expressed more in *lcmt1* with $MgSO_4$ (0.60) treatment than WT with the same treatment (0.37) compared to that of control (lane 13, figure 3.15 C).

In *BHLH100* expression analysis (lane 5 to 8, figure 3.15 A and B), the shoots of *lcmt1* showed highest band intensity (1.00) than WT (0.76) in presence of $MgSO_4$, whereas *BHLH100* expressed more in WT (0.59) than *lcmt1* (0.38) in presence of $MgCl_2$. All the values were compared with the control (lane 13, figure 3.15 A). In general, band intensity in both WT (0.59) and mutant shoots (0.38) treated with $MgCl_2$ is less than the corresponding samples with $MgSO_4$ treatment (WT = 0.76, *lcmt1* = 1.00). In root samples (lane 5 to 8, figure 3.15 C and D), the gene expressed equally in both WT and mutant with $MgSO_4$ treatment (lane 5 and 6, figure 3.15 C and D). On the other hand, *BHLH100* expression in *lcmt1* roots (0.57) is less than WT roots (0.88) in presence of $MgCl_2$ while compared to that of control (lane 13, figure 3.15 C).

The clear bands at 322 bp indicate successful amplification of *FRO2* in shoot and root samples (lane 9 to 12, figure 3.15 A and C). The analysis of shoot samples (Figure 3.15 A and B) showed that gene expression in WT was higher than *lcmt1* in presence of both MgSO4 and $MgCl_2$ treatments. On the other hand, WT and *lcmt1* had higher band intensities in the presence of $MgSO_4$ treatment, while compared respectively with $MgCl_2$ treatment. In case of roots (Figure 3.15 C and D), *FRO2* expressed higher in the samples (WT and *lcmt1* both) treated with $MgSO_4$ than the corresponding samples in $MgCl_2$. The mutant with $MgCl_2$ treatment had a higher intense band (0.64) than WT with the similar treatment (0.51).

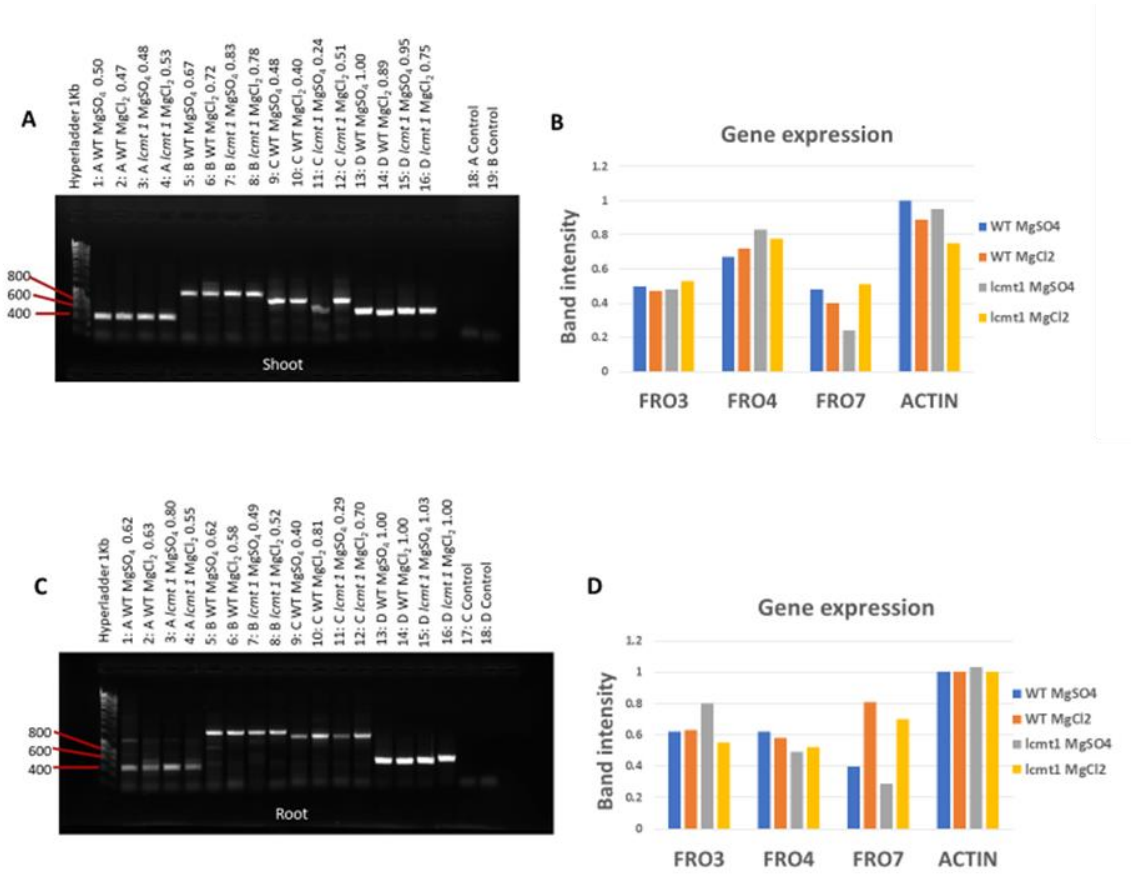

Figure 3.16. In-gel expression analysis on roots and shoots of WT and *lcmt1*. The WT and mutant seedlings were treated with 2 mM $MgSO_4$ and 2 mM $MgCl_2$ for 5 weeks in 8 h light. PCR was run using 50 ng cDNA per 10 µL reaction mixture at 55^0C annealing temperature and 34 cycles. Band intensities were measure by ImageJ software. *FRO3*, *FRO4*, *FRO7*, and *ACTIN* are represented as A, B, C and D, respectively. The numbers are shown above each lane (Fig. **A** and **C**) are relative to *ACTIN* in WT $MgSO_4$.

Arabidopsis shoots and roots had clear bands at 361 bp, pointing out of successful amplification of *FRO3* (lane 1 to 4, figure 3.16 A and C). The gene expression among the shoot samples differed non significantly. In the presence of $MgSO_4$, WT shoots showed a slightly more intense band than *lcmt1* shoots (Figure 3.16 A and B). Conversely, *lcmt1* shoots had a slightly more intense band than WT shoots in $MgCl_2$ treatment in comparison with control (lane 13, figure 3.16 A). The expressions of *FRO3* in WT roots (Figure 3.16 C and D) were almost similar between $MgSO_4$ and $MgCl_2$ treatments. On the other hand, the gene expressed more in *lcmt1* roots with $MgSO_4$ (0.80) than $MgCl_2$ treatment (0.55) compared to that of control (lane 13, figure 3.16 C).

The clear and strong bands for all the samples (shoots and roots) at 944 bp specifying to successful amplification of *FRO4* (lane 5 to 8, figure 3.16 A and C). In presence of both $MgSO_4$ and $MgCl_2$ treatments, shoots of *lcmt1* had higher intense bands than WT (Figure 3.16, A and B) compared to control (lane 13, figure 3.16 A). On the contrary, *FRO4* expressed more in WT roots treated with

either $MgSO_4$ or $MgCl_2$ than the roots of *lcmt1* treated with corresponding treatments (Figure 3.16 C and D). The values of band intensity were compared to the control (lane 13, figure 3.16 C).

It is observed from the gel images that *FRO7* successfully amplified in the samples (shoots and roots) as strong bands were noticed at 795 bp (lane 9 to 12, figure 3.16; A and C). In lane 11 (Figure 3.16 A), the band appeared slightly lower than 795 bp as some sample was lost during pipetting. It was observed in shoot samples (Figure 3.16 A and B) that the gene expression was higher in Arabidopsis WT (0.48) than mutant (0.24) in presence of $MgSO_4$. In this case, sample loss from the mutant treated with $MgSO_4$ might be a reason behind lower band intensity in *lcmt1*. Differently, the band intensity was higher in the mutant (0.51) rather than WT (0.40) while treated with $MgCl_2$. During root analysis, *FRO7* expressed more in both WT and *lcmt1* roots in presence of $MgCl_2$ (WT = 0.81 and *lcmt1* = 0.70) than the corresponding samples treated with $MgSO_4$ (WT = 0.40 and *lcmt1* = 0.29) (Figure 3.16 C and D). While comparing between the WT and mutant, the band intensity seemed to be higher in roots of WT than *lcmt1* in presence of both $MgSO_4$ and $MgCl_2$ treatments.

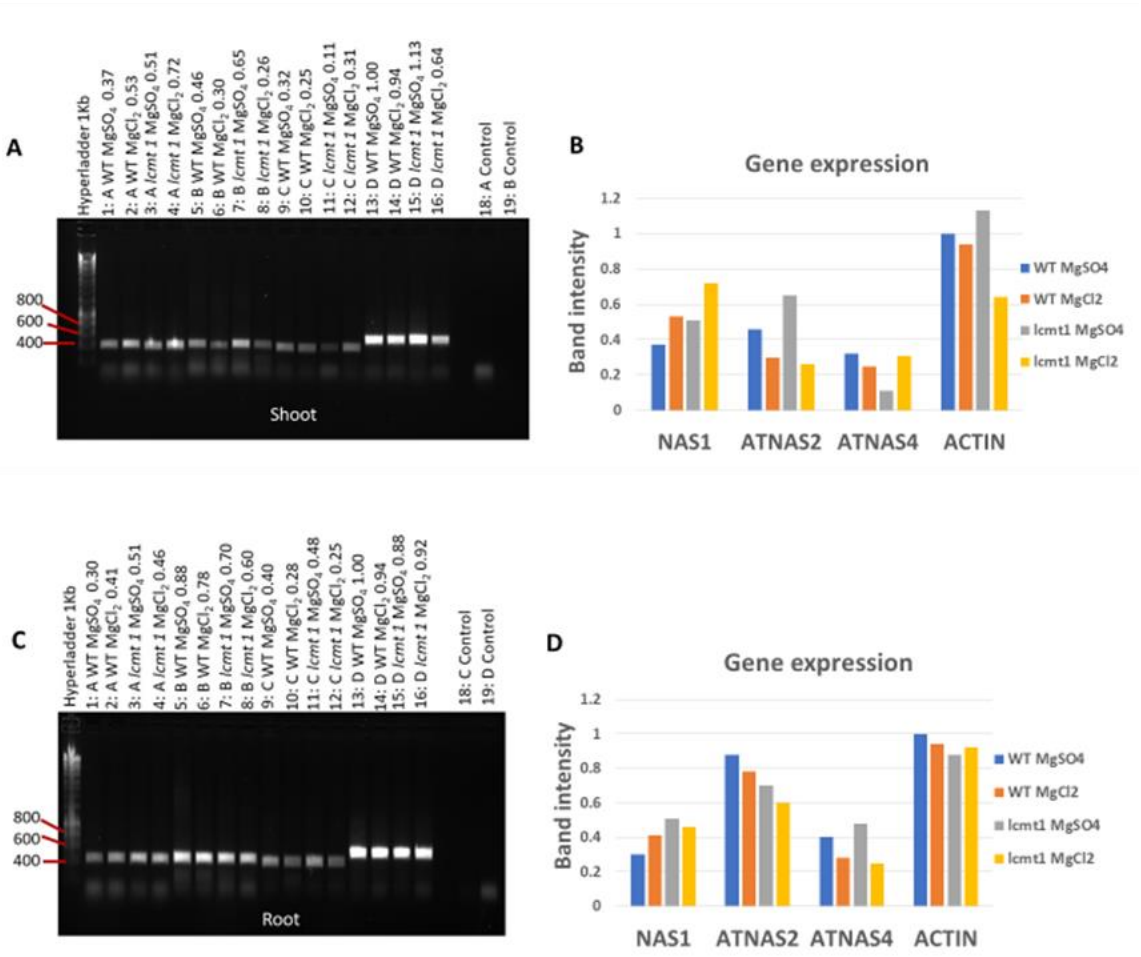

Figure 3.17. In-gel expression analysis on roots and shoots of WT and *lcmt1*. The WT and mutant seedlings were treated with 2 mM $MgSO_4$ and 2 mM $MgCl_2$ for 5 weeks in 8 h light. PCR was run using 50 ng cDNA per 10 µL reaction mixture at 55^0C annealing temperature and 34 cycles. Band intensities were measure by ImageJ software. *NAS1*, AT*NAS2*, *ATNAS4*, and *ACTIN* are represented as A, B, C and D, respectively. The numbers are shown above each lane (Fig. **A** and **C**) are relative to *ACTIN* in WT $MgSO_4$.

The gel images showed clear and strong bands at 388 bp indicating a successful amplification of *NAS1* in both shoot and root samples of Arabidopsis (lane 1 to 4, figure 3.17 A and C). The gel image and graphical overview of shoots (Figure 3.17 A and B) specified that the gene expression in shoot samples (both WT and *lcmt1*) with $MgSO_4$ (WT = 0.37 and *lcmt1* = 0.51) were lower than the corresponding samples with $MgCl_2$ (WT = 0.53 and *lcmt1* = 0.72). Interestingly, the band intensity in *lcmt1* shoot was higher than WT in the presence of any of the Hoagland treatments ($MgSO_4$/$MgCl_2$). In the figure 3.17 (C and D), the expression of *NAS1* seemed to be slightly higher in *lcmt1* roots than WT roots in presence of both $MgSO_4$ (WT = 0.30 and *lcmt1* = 0.51) and $MgCl_2$ (WT = 0.41 and *lcmt1* = 0.46) treatments.

Arabidopsis shoot and root samples had clear bands at 397 bp that specified a successful amplification of *ATNAS2* (lane 5 to 8, figure 3.17 A and C). The gene expression was higher in

the shoots of both WT and *lcmt1* treated with $MgSO_4$ (WT = 0.46 and *lcmt1* = 0.65) than the corresponding samples treated with $MgCl_2$ (WT = 0.30 and *lcmt1* = 0.26) (Figure 3.17 A and B). The gene expression also differed between WT and mutant according to the treatment solution, e.g., in the presence of $MgSO_4$, the gene expressed higher in mutant shoots (0.65) than WT shoots (0.46). On the other hand, slightly higher band intensity was observed in WT (0.30) than *lcmt1* shoots (0.26) while treated with $MgCl_2$. All the values compared with the control (lane 13, figure 3.17, A). In case of roots (Figure 3.17 C and D), the WT and *lcmt1* samples treated with $MgSO_4$ (WT = 0.88 and *lcmt1* = 0.70) seemed to have higher band intensity than the corresponding samples with $MgCl_2$ (WT = 0.78 and *lcmt1* = 0.60). *ATNAS2* highly expressed in roots of WT than *lcmt1* while treated with $MgSO_4$. Similarly, WT roots seemed to have high band intensity than *lcmt1* in presence of $MgCl_2$ treatment compared to that of control (lane 13, figure 3.17 C).

The gel image of Arabidopsis shoots and roots displayed clear bands at 366 bp, pointing out of successful amplification of *ATNAS4* (lane 9 to 12, figure 3.17 A and C). The overall gene expression in shoot samples (Figure 3.17 A and B) was less in compared to that of control (*ACTIN* in WT $MgSO_4$). The gene expressed higher in shoots of WT (0.32) than *lcmt1* (0.11) while treated with $MgSO_4$. On the other hand, in the presence of $MgCl_2$, slightly high band intensity was observed in the mutant (0.31) shoot than that of WT (0.25). Regarding the root samples (Figure 3.17 C and D), the gene highly expressed in WT with $MgSO_4$ (0.40) treatment than the WT treated with $MgCl_2$ (0.28). In the same way, *lcmt1* seemed to have higher gene expression in $MgSO_4$ (0.48) treatment than $MgCl_2$ (0.25). The values compared with the control (lane 13, figure 3.17 C).

3.3.2 Real-time PCR

3.3.2.1 RNA extraction

The RNA was extracted from shoots of WT and *lcmt1* grown on rockwool and treated with Hoagland solution of 2 mM $MgSO_4$ (control) and 2 mM $MgCl_2$ at 8 h light for 5 weeks. The ratio of absorbance (Table 2.12) was measured by using NanoDrop One to assess the purity of RNA and concentrations (Table 2.12) of that isolated RNA were also calculated.

Table 3.2. Concentrations and purity measurement of isolated RNA.

Sample	**Concentration (ng/µL)**	**A260/A280**	**A260/A230**
$MgSO_4$ WT shoot	699.5	2.15	1.94
$MgSO_4$ *lcmt1* shoot	517.2	2.16	1.81
$MgCl_2$ WT shoot	681.4	2.15	2.42
$MgCl_2$ *lcmt1* shoot	519.9	2.14	2.18

3.3.2.2 RT-PCR data analysis

The cDNAs were synthesized from the extracted RNA of WT and mutant shoots grown on rockwool and treated with Hoagland solutions of 2 mM $MgSO_4$ (control) and 2 mM $MgCl_2$ at 8 h light for 5 weeks. Taq-Man assay was used to perform RT-PCR with the cDNA of samples (WT and *lcmt1* shoots). The data (RQ-value and average Ct value) obtained from RT-PCR were used to analyze the samples. Bar diagrams of Relative Quantification (RQ) (Figure 3.18 and Figure 3.20) and Cycle Threshold (Ct) (Figure 3.19 and Figure 3.21) represent specific gene expressions in the samples.

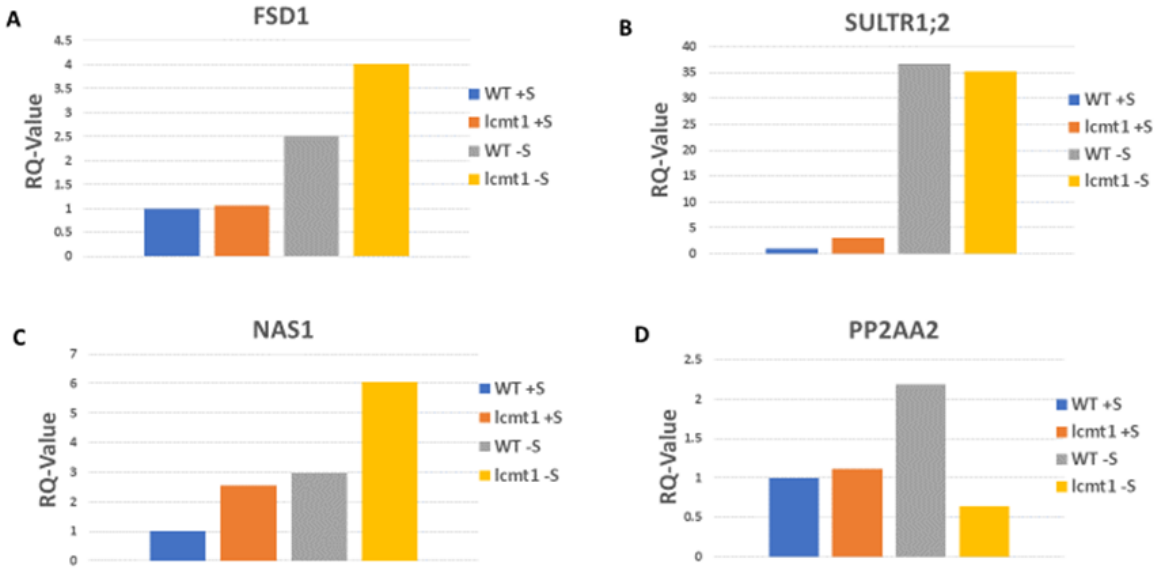

Figure 3.18. RQ-values of Arabidopsis WT compared with *lcmt1* mutant for *FSDI* (**A**), *SULTR1;2* (**B**), *NAS1* (**C**) and *PP2AA2* (**D**). The WT and *lcmt1* plants (4 WT and 4 *lcmt1* shoots per treatment) grown on rockwool and treated with Hoagland solutions of 2 mM $MgSO_4$ and 2 mM $MgCl_2$ at 8 h light for 5 weeks. RQ-values were measured by using Ubiquitin (*UBC35*) as an endogenous control and WT+S (WT treated with 2 mM $MgSO_4$) as a calibrator.

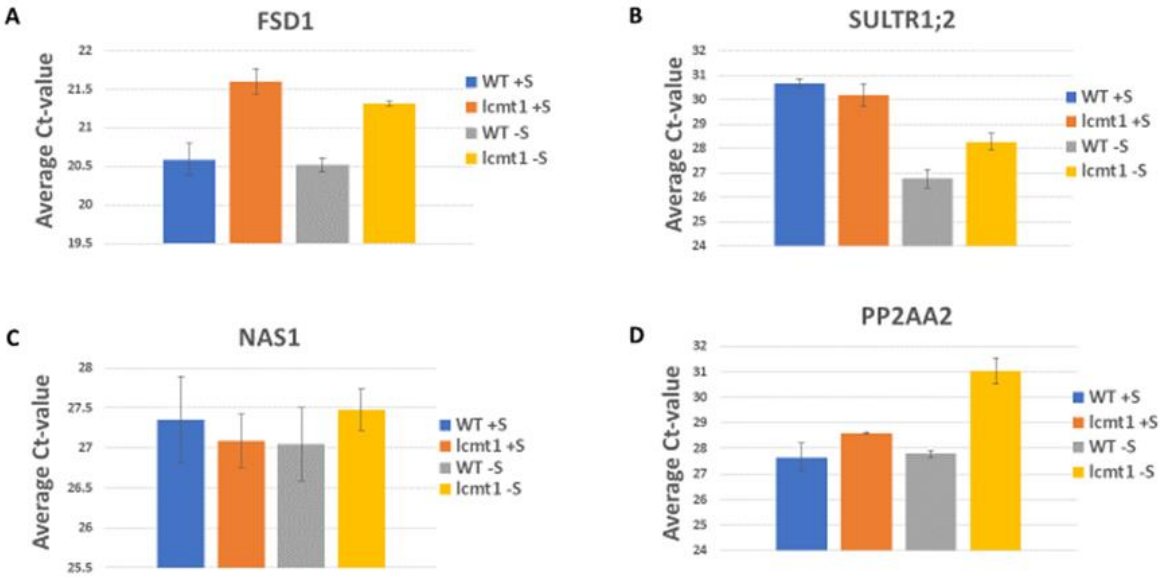

Figure 3.19. Average Ct-value of Arabidopsis WT compared with *lcmt1* mutant for *FSDI* (**A**), *SULTR1;2* (**B**), *NAS1* (**C**) and *PP2AA2* (**D**). The WT and *lcmt1* plants (4 WT and 4 *lcmt1* shoots per treatment) grown on rockwool and treated with Hoagland solutions of 2 mM $MgSO_4$ and 2 mM $MgCl_2$ at 8 h light for 5 weeks. Ct-values were averaged for 3 replicates of WT and *lcmt1* each.

In figure 3.19 (A), both *lcmt1*+S and *lcmt1*-S had higher Ct values compared to WT+S (calibrator). This means the fluorescent signals from the two corresponding samples crossed the threshold later than WT+S. It indicates that a small amount of *FSD1* was present at the starting point in *lcmt1*+S and *lcmt1*-S. This result of Ct values does not correlate with the RQ values as figure 3.18 (A) shows that the gene expression was very slightly higher in *lcmt1*+S and about 4-fold higher in *lcmt1*-S compared to the calibrator (WT+S). On the other hand, the Ct value (Figure 3.19 A) of WT -S associates with its RQ value (Figure 3.18 A) while comparing to that of WT+S. The reason behind higher *FSD1* expression in *lcmt1-S* could be the gene response to oxidative stress during -S.

In figure 3.19 (B), the Ct values of all the samples were lower than the calibrator (WT+S). Here, *lcmt1*+S had very slightly and the other two samples (WT-S and *lcmt1*-S) had distinctly lower Ct values compared to that of WT+S. These Ct values of the samples represent that *SULTR1;2* gene was present at the starting point from highest to lowest level in WT-S, *lcmt1*-S and *lcmt1*+S, respectively, in respect of WT+S. This result is completely corresponding with the result of RQ value (Figure 3.18 B) where highest to lowest *SULTR1;2* expressions were observed in WT-S, *lcmt1*-S and *lcmt1*+S, respectively, compared with the calibrator (WT+S). The distinct higher level of gene expression in both WT-S and *lcmt1*-S appeared due to the response of *SULTR1;2* toward Sulphur starvation.

The lower Ct values of *lcmt1*+S and WT-S for *NAS1* (Figure 3.19 C) indicate that at the starting point, the gene products were more in the corresponding samples than WT+S. This result matches up with the individual RQ values of *lcmt1*+S and WT-S (Figure 3.18 C) where the gene expressed about 2 to 3 fold more in those two samples compared to that with WT+S. In case of *lcmt1*-S, though the presence of the target gene was less, RQ value of the sample was sharply higher than that of the calibrator. It specifies that the Ct value of *lcmt1*-S (Figure 3.19 C) does not correlate with its RQ value (Figure 3.18 C) while compared it with WT+S (calibrator).

The presence of minimal target gene (*PP2AA2*) in *lcmt1*-S sample (Figure 3.19 D) was leading to a lowest level of gene expression (Figure 3.18 D) compared to other samples. This indicates that the Ct value of *lcmt1*-S completely correlates with its RQ value. Regarding the WT+S and WT-S, the amount of *PP2AA2* was almost similar in both samples (Figure 3.19 D), but the gene expression in WT-S was about 2 fold higher compared to WT+S (Figure 3.18 D). Similarly, a slightly lower gene was present at the starting point in *lcmt1*+S compared to the calibrator. However, the RQ value was similar in both *lcmt1*+S and WT+S. This observation indicates that the Ct values of *lcmt1*+S, WT-S and the calibrator did not correlate with their respective RQ values.

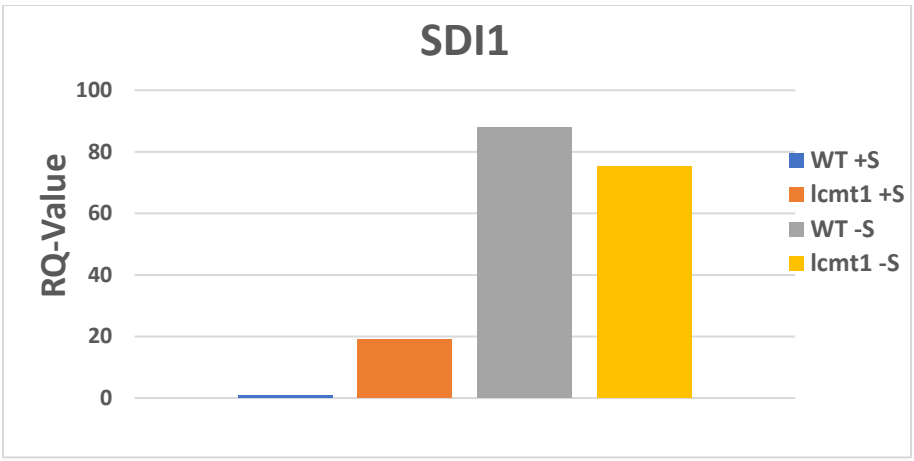

Figure 3.20. RQ-values of Arabidopsis WT compared with *lcmt1* mutant for SDI1. The WT and *lcmt1* plants (4 WT and 4 *lcmt1* shoots per treatment) grown on rockwool and treated with Hoagland solutions of 2 mM $MgSO_4$ and 2 mM $MgCl_2$ at 8 h light for 5 weeks. RQ-values were measured by using Ubiquitin (*UBC35*) as an endogenous control and WT+S (WT treated with 2 mM $MgSO_4$) as a calibrator.

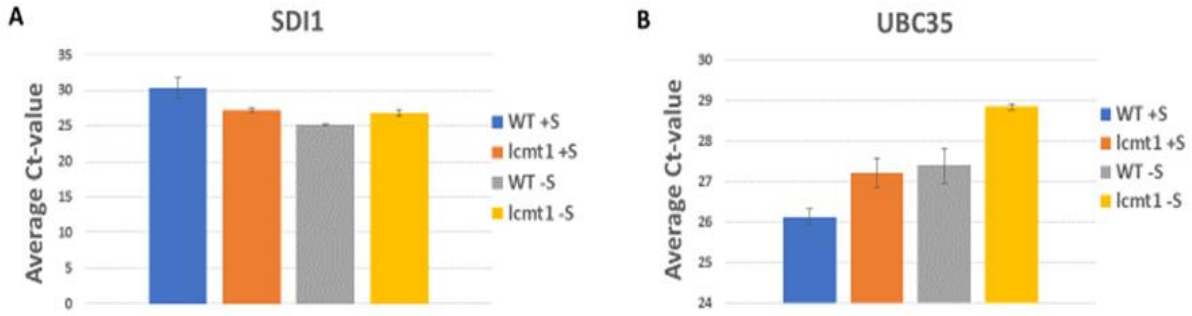

Figure 3.21. Average Ct-value of Arabidopsis WT compared with *lcmt1* mutant for **(A)** *SDI1* and **(B)** *UBC35*. The WT and *lcmt1* plants (4 WT and 4 *lcmt1* shoots per treatment) grown on rockwool and treated with Hoagland solutions of 2 mM $MgSO_4$ and 2 mM $MgCl_2$ at 8 h light for 5 weeks. Ct-values were averaged for 3 replicates of WT and *lcmt1* each.

In the figure 3.21 (A), the fluorescent signal from WT-S crossed the threshold line earlier than WT+S (calibrator), indicating a larger amount of *SDI1* was present in WT-S before starting the reaction. In figure 3.20, the highest RQ value was observed in WT-S compared to other samples that appropriately matches its specific Ct value. The gene expressions were about 20 and 90 fold higher in *lcmt1*+S and *lcmt1*-S, respectively when compared to the calibrator (Figure 3.20). Here, the lower Ct values of both *lcmt1*+S and *lcmt1*-S (Figure 3.21 A) than that of WT+S match with their respective RQ values in figure 3.20. In this case, the highest level of *SDI1* expression in the samples without Sulphur (WT-S and *lcmt1*-S) justifies the involvement of the gene in the cellular response to Sulphur starvation.

In the RT-PCR, Ubiquitin (*UBC35*) was used as an endogenous control to measure the RQ-value of other genes. Figure 3.21 (B) represents that the fluorescent signal from the calibrator (WT+S) crossed the threshold line earlier than other samples, whereas the signal emitted from *lcmt1* mutant upon -S later than other samples. This signifies that a larger amount of *UBC35* was present in WT+S at the starting point, yet least amount of gene was present in the mutant under -S. However, the Ct-value of WT-S (27.4) were very slightly higher than *lcmt1*+S (27.2).

4 Discussion

PP2A activity is essential for the life cycle of plants. The knockout of all the members from any of the catalytic subgroups of PP2A has serious effects on plants (Ballesteros et al., 2013). However, knocked out of LCMT1, regulating enzyme for methylation of PP2A, is not detrimental to plant growth and development under standard conditions. This indicates that LCMT1 is not a prerequisite for plant survival (Wu et al., 2011). Interestingly, strong conservation of LCMT1 in plants indicates that this gene may serve important functions during evolution and be essential for plant survival in harsh or stressed conditions (Chen et al., 2014; Creighton et al., 2017). In the present study, several stress conditions were provided to WT and lcmt1 mutant (knockout of LCMT1) to identify the roles of the gene in competitive conditions.

In absence of methylation, the overall growth of *lcmt1* did not show any serious growth difficulties when treated with regular Hoagland solution, but the pattern of leaves was visually different from the WT. When the plants cultivated in either vermiculite or rockwool, *lcmt1* showed elongated petioles than WT (Appendix figure A.1, A.2, A.3, A.4, A.5). When the plants were grown in vermiculite and kept in 8 h light/ 16 h darkness for 5 weeks (Appendix figure A.1), early flowering was also observed in the mutant. These observations agree with the study by Creighton et al., 2017. In other experiments in vermiculite (Appendix figure A.2, A.3, A.4, A.5), plants were kept in 8 h light/16 h darkness for a shorter time, and flowering could not be observed.

4.1 S-deficiency induced chlorosis

As expected, S-depletion induced chlorosis (pale yellow or pale green color of the leaves) was observed in the first experiment where plants grown for 5 weeks in vermiculite and treated with sulfur deficient Hoagland solution (2 mM $MgCl_2$) (Appendix figure A.1). The purple coloring of the S-deficient plant leaves in this experiment (5 weeks incubation in 8 h light/ 16 h dark) signifies the accumulation of secondary metabolite, anthocyanin. This observation corresponds to the studies by Lillo et al., 2007 where nutrient deficiency resulted in a reduced level of chlorophyll and production of anthocyanin. Similarly, in the fourth experiment, the chlorosis was observed in the plants (3 weeks incubation in 8 h light/ 16 h dark) during S deficiency (Appendix figure A.4). However, in the third experiment (Appendix figure A.3), neither chlorosis nor anthocyanin production was observed in the plants under S deficiency. The plants upon -S looked bigger and healthier compared to the plants treated with control solution. The same response was observed in the plants grown in rockwool (Appendix figure A.5). Precipitation of stock Hoagland solution could possibly be a reason behind these.

4.2 Effects of S-deficiency in absence of methylation

Regarding the visual appearance of Arabidopsis, the petioles of the *lcmt1* rosette seemed to be more crippled than WT upon -S that could be explained by lower PP2A activity in *lcmt1* during -S (Appendix figure A.1). This interpretation corresponds to the study by Creighton et al., 2017. On the other hand, in the control solution, the petioles of *lcmt1* were way bigger and healthier than WT. Likewise, in the fourth experiment (Appendix figure A.4), *lcmt1* had more crippled leaves, thinner and shorter roots compared to WT when treated with S-deficient Hoagland solution for 3 weeks. However, in the second experiment (Appendix figure A.2), no visible changes in shoot morphology were observed between WT and mutant in presence of $MgCl_2$. This might be due to the early harvesting of plants. Surprisingly, in the third experiment (Appendix figure A.3), only one *lcmt1* survived in control, whereas shoots and roots both looked healthy, as WT, in presence of S-deficient solution. Similarly, the *lcmt1* grown on rockwool were not affected by S-deficiency when compared to WT. As stated before, the formation of precipitate in the Hoagland nutrient solution might be a factor behind this.

According to the graphical overview of first and second experiments in vermiculite, no significant differences were observed between WT and *lcmt1* regarding shoot weight (Figure 3.2 A and 3.2 B) during S deficiency. While, in the second experiment, *lcmt1* root weight was significantly lowered than WT upon -S (Figure 3.1 B). This indicates a strong correlation with the function of LCMT1 enzyme of the plants in order to cope with stress conditions such as S-deficiency. However, in the third experiment, increased root and shoot weight were observed in the mutant than WT during -S which matches the visual analysis of this experiment.

4.3 Arabidopsis seedlings grown in Hoagland media

In absence of both $MgSO_4$ and $MgCl_2$, the shoot weights of WT and *lcmt1* seedlings were retarded more than in control (2 mM $MgSO_4$) treatment (Figure 3.4). This finding supports the study by Gruber et al., 2013 where dry shoot weight of Arabidopsis was drastically inhibited in absence of Mg and S. The shoot weight of *lcmt1* was significantly more stunted than WT, and indicated that the removal of essential macronutrients (Mg and S) and micronutrients (Cl) have a more negative effect on the shoots of *lcmt1* compared to WT. However, minimal changes were observed between WT and *lcmt1* when they were treated with 10 mM $MgSO_4$, 2 mM $MgCl_2$ and 10 mM $MgCl_2$.

During 0 mM $MgSO_4$/$MgCl_2$ (S, Cl and Mg deficient) and 2 mM $MgCl_2$ (S deficient) treatments, the root lengths of both WT and *lcmt1* were almost similar as for control (Figure 3.5). This observation supports the study on the Arabidopsis root system under nutrient deficiencies by Gruber et al., 2013, where Arabidopsis roots were found not to be affected by S and Cl depletion. On the other hand, the root lengths of both WT and *lcmt1* were greatly reduced in the presence of excess S and Mg (10 mM $MgSO_4$) compared to the control and other treatments. This observation can be correlated with the study by Niu et al., 2014, where primary root elongation of Arabidopsis was observed under 10 mM $MgSO_4$ treatment. Regarding the effect of PP2A methylation during

stress, *lcmt1* was observed to be significantly retarded than WT in the stress conditions, e.g., 0 mM $MgSO_4/MgCl_2$, 10 mM $MgSO_4$ and 2 mM $MgCl_2$. This observation specified that methylation of PP2A seemed to be important for the survival of plant in harsh conditions that matches with the study by Chen et al., 2014. However, during 10 mM $MgCl_2$ (excess Mg and Cl) treatment, the difference between WT and mutant root length were very small which indicates a little or no effect of PP2A methylation on this treatment.

According to several studies, the chlorophyll content of Arabidopsis was reduced during removal of Mg and S (Guo et al., 2015; Garai and Tripathy 2018), whereas in this study (Figure 3.6), the chlorophyll content during stresses was higher or similar compared to that of control. Interestingly, the mutant had lower chlorophyll content than WT in all the stress treatments, while slightly increased chlorophyll content was observed in the control treatment. The findings from this chlorophyll assay did not correlate with the above-mentioned studies might be due to the usage of different culture systems, e.g. solid or liquid nutritional medium.

4.4 Arabidopsis response to salt stress

According to Álvarez-Aragón et al., 2015, gradually increasing NaCl concentration inhibited the shoot weight of WT Arabidopsis. Conversely, in this study of salt stress, the shoot weights of both WT and lcmt1 were increased (Figure 3.7) compared to that of control, when treated with either 25 mM or 50 mM NaCl. However, reduced shoot weights were observed in both WT and *lcmt1* compared with control during 75 mM and 100 mM salt stresses. When comparing WT and *lcmt1* during salt stresses, insignificant differences were observed compared to the control.

In the study of root length (Figure 3.8), gradual retardation of root lengths were observed with increasing NaCl concentration which supports the study by Jiang et al., 2016, where changes in Arabidopsis root meristem structure and development were studied in presence of varied NaCl concentrations. Regarding the absence of methylation, the *lcmt1* root lengths were seemed to be significantly higher than WT in both control and 25 mM salt treatment. A slight elongation was observed in *lcmt1* root compared with WT in presence of 50 mM salt treatment. Interestingly, during higher salt concentrations (75 mM and 100 mM NaCl), a sharp and significant reduction of *lcmt1* compared with WT was observed. These observations indicate that *lcmt1* root lengths might not be affected by mild salt stress, but it was affected devastatingly at higher salt concentrations that is corresponding to the finding of Chen et al., 2014.

A gradual decrease of chlorophyll content was observed for the seedlings with increasing concentrations of NaCl (Figure 3.9) compared to that of control which correlates with the study by Stepien and Johnson 2009, where a reduced chlorophyll content was observed in Arabidopsis with increasing salt concentrations. In this study, the chlorophyll content of WT was almost the same in presence of 50 mM and 75 mM NaCl. Regarding the absence of methylation, reduced chlorophyll content in *lcmt1* compared to WT was noticed during increasing salt concentrations, yet the difference between WT and the mutant was not significant. This indicates that the absence

of PP2A methylation somewhat hampers the photosynthesis of plants under high salt concentration.

4.5 H_2O_2 induced oxidative stress

According to the study by Zhu et al., 2007, H_2O_2 induced oxidative stress reduced the seedling fresh weight in Arabidopsis WT and its several mutants. In the current study (Figure 3.10), a converse result was found regarding Arabidopsis shoot weight, when they were treated with different concentrations of H_2O_2. Instead of shoot weight reduction, a noticeable higher shoot weight was observed both in WT and *lcmt1* in presence of 0.5 mM H_2O_2 compared to that of control. The further increasing concentration of H_2O_2 followed by a linear shoot weight reduction in both WT and *lcmt1* relative to the shoot weight in 0.5 mM H_2O_2. Accordingly, a gradually impaired shoot weight was found in *lcmt1* during increasing oxidative stress relative to the *lcmt1* that was treated with 0.5 mM H_2O_2. The reason for impaired shoot weight of both WT and *lcmt1* in control is a bit unclear. When comparing WT and the mutant, *lcmt1* shoot weight was significantly retarded compared with WT in all the treatments including control. This observation brings light on the importance of PP2A methylation during stress conditions which is perfectly compatible with the study by Chen et al., 2014.

Claeys et al., 2014 pointed out that H_2O_2 induced oxidative stress produced a sharp reduction on the root length of *Arabidopsis thaliana* which is completely corresponding to the findings of this current study (Figure 3.12). In this study, a striking inhibitory effect of oxidative stress was observed in both WT and *lcmt1* with increasing concentrations of H_2O_2, when compared with control. Moreover, at the maximum oxidative stress (2 mM H_2O_2), root elongation of seedlings was totally stopped for both WT and the mutant. Regarding the sensitivity of *lcmt1* to oxidative stress, significant root reduction was observed in higher H_2O_2 concentrations as well as in control that supports the study by Chen et al., 2014. However, *lcmt1* had slight and nonsignificant elongated roots than WT during 0.5 mM H_2O_2 stress. The root lengths in 0.5 mM H_2O_2 varied among the repeated H_2O_2 experiments (Appendix figure B.5 and B.6) and might produce an overlapping result.

In the study by Claeys et al., 2014, a binary trait of bleaching on Arabidopsis shoots was observed between 1 to 1.25 mM H_2O_2, e.g., some seedlings were fully bleached, whereas some appeared as normal. Conversely, in this study, bleaching did not appear in any repeated experiments of oxidative stress (Appendix figure B.5, B.6). The seedlings maintained a gradual chlorophyll reduction followed by increasing stress (Figure 3.13). Furthermore, a lower chlorophyll level was observed in the mutant than in WT for the control and H_2O_2 stresses (0.5 mM, 1 mM and 2 mM H_2O_2), indicating that methylation status has an important impact on Arabidopsis tolerance to oxidative stress. This finding can be matched with Chen et al., 2014. On the contrary, *lcmt1* had a slightly higher chlorophyll level than WT during 1.5 mM H_2O_2 stress. As the chlorophyll content in WT and *lcmt1* minorly differed from each other in this treatment, it possibly occurred due to slightly overlapping sensitivity to stress between them at this point.

4.6 In-gel gene expression analysis of Arabidopsis

Forieri et al., 2013 pointed out the coregulation between the metabolism of two essential nutrients, S and Fe. According to that study, Fe mainly conjugates with S to form Fe-S cluster and thus one nutrient strongly influences the uptake of the other one. Later in another study by Forieri et al., 2017 opposing regulation, e.g., induced gene at -Fe and reduced at -S, or vice versa, upon S deficiency, was observed in Arabidopsis for several genes involved in the Fe assimilation pathway. Thus, it is interesting to analyze the expression of Fe uptake genes in the S depleted Arabidopsis in this current study.

The expressions of *IRT1* varied between roots and shoots of Arabidopsis (Figure 3.15), where the gene expression was more induced in roots rather than shoots. This observation is expected, as *IRT1* is a primary iron uptake transporter in roots and expression mainly occurs in the external cell layers of roots. The differences in gene expression in both WT and *lcmt1* shoots were very small during -S compared to that in control (Figure 3.15 A and B). Regarding the roots, *IRT1* expression in *lcmt1* was reduced 1.5 times during -S compared with *lcmt1* in control. However, the gene expression in both WT and the mutant was almost same upon -S. This indicates that PP2A methylation might have no effect on *IRT1* during S deficiency.

A lower expression of *BHLH100* was observed in both WT and *lcmt1* shoots (Figure 3.15 A and B) upon -S compared with that in control which is correlated with the study by Forieri et al., 2017. When comparing between WT and *lcmt1*, about 1.5 times intense gene expressions were observed in both roots and shoots of WT compared with *lcmt1* upon -S (Figure 3.15). This observation might be explained by having more Sulfur depletion and a decreased requirement of Fe in the mutant for Fe-S cluster synthesis under -S condition. Regarding *CAP* expression, the shoots and roots of both WT and *lcmt1* upon -S had higher gene expression compared to that in +S (Figure 3.14). When comparing WT and *lcmt1* during -S, minor changes in gene expression were observed. This indicates PP2A methylation might have no effect on *CAP* expression.

Arabidopsis employ a strategy I mechanism for effective Fe acquisition under iron stress. This strategy I includes reduction of Fe (III) to Fe (II) on the root surface and transport of Fe (II) across the root epidermal cell membrane. The genes of FRO gene family encodes ferric chelate reductase that serves to reduce Fe (III) chelates to form soluble Fe^{2+} which is needed for the assimilation of Fe in cells of leaves and other tissues. The response of these genes of FRO family induces in Fe limiting stress (Bienfait et al., 1983; Fox et al., 1996). As mentioned above Fe and S metabolism has coregulation in plants, thus S deficiency might have influences on the expression of these genes.

The reduced expression of *FRO2* was observed in both WT and *lcmt1* shoots and roots during S deficiency compared to those in control (Figure 3.15). This observation agrees with the study by Forieri et al., 2017, where *FRO2* was 4-fold down-regulated in Arabidopsis during -S. When comparing between WT and the mutant, an induced expression of *FRO2* was observed in *lcmt1* roots compared with WT roots upon -S. This indicates a greater need for Fe supply in the mutant

even under S depletion which might cause Fe toxicity in *lcmt1*. However, a minor difference was observed between the shoots of WT and *lcmt1* during -S.

In shoot samples, the expressions of *FRO3* and *FRO4* slightly changed in both WT and *lcmt1* during -S compared with their control condition. While, in *lcmt1* roots, a lower expression of *FRO3* was observed during -S compared to that in +S. When comparing between WT and *lcmt1* in both root and shoot samples, the changes in gene expression (*FRO3* and *FRO4*) were very small. This observation denotes that the PP2A methylation might have small or no effect on *FRO3* and *FRO4* expression during -S. Regarding the *FRO7* expression level upon -S, induced expression was observed in the roots of both WT and *lcmt1*. This indicates increased Fe (III) chelate reductase activity in the chloroplast of Arabidopsis to supply enough iron to the pigmentation chlorophyll during Fe deficiency which is co-regulated by S deficiency (Jeong et al., 2008). Interestingly, in absence of sulfur, the gene (*FRO7*) expression was reduced in the mutant compared to WT. Thereby, indicating a less active Fe^{3+} reduction at chloroplast and lower level of chlorophyll production in the mutant compared with WT during -S. The shoots of mutant had similar induced gene expression upon -S compared with that in +S (Figure 3.16).

The higher expression of *NAS1* in *lcmt1* shoot compared with WT upon -S indicates an induced accumulation of nicotianamine (NA) and thus elevated transport of Fe in the mutant during S deficiency (Figure 3.17). On the other hand, during *ATNAS2* expression analysis, significantly reduced NA synthesis and NA-Fe formation were observed in both WT and *lcmt1* shoots under -S compared to that in +S. This observation agrees with the study by Forieri et al., 2017, where *ATNAS2* was 4-fold repressed in Arabidopsis during -S. However, in root samples, very small differences were observed between WT and the mutant upon -S regarding *NAS1* and *ATNAS2* expressions. Similarly, the expression of *ATNAS4* slightly varied between WT and *lcmt1* roots and shoots upon -S. Thereby, these observations signify that PP2A methylation might have small or no effect on *NAS1*, *ATNAS2* and *ATNAS4*.

4.7 Gene expression analysis by RT-PCR

According to the study by Waters et al., 2012, Fe superoxide dismutase 1 (*FSD1*) was down regulated during Fe deficiency in Arabidopsis. In this current study (Figure 3.18 A), a highly induced expression of *FSD1* was observed in both WT and *lcmt1* upon -S. This could imply that Fe uptake was present during S depletion. As a result, excess Fe could be produced rather than the formation of Fe-S clusters during -S. This might cause Fe toxicity, ROS production and ultimately leading to induced expression of *FSD1* in both WT and *lcmt1* during -S. Interestingly, *lcmt1* showed the highest *FSD1* expression upon -S might be due to higher Fe uptake and increased Fe toxicity compared to WT. However, no strong conclusion could be drawn without further experimentations.

The increased expression of *SULTR1;2* (Figure 3.18 B) in both WT and *lcmt1* during -S was expected as this gene is responsible for sulfur uptake during S deficiency. In WT, about 36 times

induced gene expression was observed upon -S compared with control. Conversely, *SULTR1;2* expression was about 12 times up regulated in *lcmt1* during -S compared with that in +S, indicating a great impact of PP2A methylation on the Arabidopsis during sulfur deficiency. This observation would signify that *lcmt1* might have less capability regarding the S uptake than WT upon -S.

The induced *NAS1* expression (Figure 3.18 C) during sulfur starvation in both WT and *lcmt1* indicates higher Fe uptake and nicotianamine accumulation in the plants. Interestingly this observation completely correlates with the analysis of Arabidopsis shoots obtained from In-gel expression. As relatively little is known about the correlation between sulfur depletion and *NAS1* expression, perhaps in future, determination of Fe concentration in sulfur depleted Arabidopsis might enlighten some interesting facts.

The expressions of *SDI1* were highly induced in both WT and *lcmt1* upon -S according to expectations (Figure 3.20). It was interesting to analyze that this gene expression was about 88-fold higher upon -S in WT compared to that in control. On the other hand, only 4-fold higher expression was observed in *lcmt1* upon -S than that in +S. This analysis underpins that the utilization of stored sulfate was much weaker when PP2A methylation was absent, which might lead to a poor surviving capability of Arabidopsis during S starvation. Regarding the *PP2AA2*, the highest expression was observed in WT upon -S, while the mutant had the lowest gene expression (Figure 3.18 D). This observation denotes approximately 3 times weaker expresssion of *PP2AA2* in absence of PP2A methylation during -S compared to that of WT.

4.8 Confounding variables and sources of errors

The results obtained from vermiculite could not be compared with each other, as the cultivation lengths were different. The plants in the first experiment (Appendix figure A.1) were cultivated in vermiculite for 5 weeks. However, in other experiments, plants were harvested earlier than 5 weeks as they could not survive longer. Due to these differences, root and shoot weights also varied among the experiments. In addition to this, the plants were not transferred to vermiculite from the soil after exactly the same number of days from sowing seeds. This might cause differences in the size of the plants at the starting point of cultivation in the vermiculite and could potentially affect the plant growth rate. Apart from these, the formation of precipitate inside the Hoagland solution might also affect the result obtained from the plants cultivated in vermiculite.

During harvesting, three representative plants of WT and *lcmt1* were harvested from vermiculite for further experiments. In this case, the healthy appeared plants were collected and sometimes the plants were suffering most were avoided. This might influence the gene expression analysis and also the measurement of root and shoot weight.

Moreover, it was not always possible to maintain a similar size of seedlings during transferring the seedlings from nutritional MS media to the stress condition. Thus, the effect of stress on the seedlings might vary which could ultimately influence the stress analysis.

Furthermore, different Ct values represented a varied amount of genes at the starting point of the cycle. This might indicate a pipetting error during mixing the PCR samples or loading the samples in the plate, which could affect the gene expression analysis. Additionally, the gene expression analysis from gel electrophoresis and RT-PCR were conducted only one time. As a result, no strong conclusion could be drawn regarding that analysis without further experimentations.

5 Conclusion and future perspective

5.1 Conclusion

The study aimed to reveal the importance of the *LCMT1* gene and associated methylation of PP2A under different environmental conditions. The findings of the thesis are:

- The petioles of *lcmt1* rosettes were more crippled compared to WT upon -S when the plants were cultivated for 5 weeks in vermiculite.
- Reduced root and shoot weight were observed in *lcmt1* upon -S, where the root weights were more affected by the stress than shoots.
- During triple nutrient deficiency (Mg, S and Cl), *lcmt1* growth, e.g., shoot weight and root length, were significantly retarded compared to WT. On the other hand, sulfur deficiency and sulfur toxicity remarkably reduced the root length of the mutant.
- At higher salt concentration (75 mM and 100 mM NaCl), notable differences were observed between WT and *lcmt1*.
- The increasing concentrations of oxidative stress devastatingly hampered the overall growth of *lcmt1* compared to WT.
- Lower chlorophyll content was observed in *lcmt1* than WT under salt and oxidative stresses, but the differences were very small between them.
- The *SULTR1;2* and *SDI1* expressions indicated that sulfur uptake by *lcmt1* was less than WT under sulfur starvation. It resembled less adaptation capability of the mutant during the competitive environment.
- Expression data of the ROS scavenging gene (*FSD1*) showed ROS production was higher in the mutant compared with WT during -S.
- Upon -S the protein phosphatase PP2A-A2 subunit was weaker in *lcmt1* compared to WT.

5.2 Future perspective

A study about the correlation between sulfur deficiency and iron uptake in the mutant would be a of special interest as it has been hardly studied. Determination of iron content in sulfur deficient *lcmt1* would enlighten some new facts in future. Additional experiments regarding the impact of these tested genes in absence of methylation would establish a strong statistical basis to build a future conclusion. Furthermore, the impact of oxidative stress and the functionality of additional ROS scavenging genes on the *lcmt1* would be a very attractive study to take on.

6 References

Aarabi, F., Kusajima, M., Tohge, T., Konishi, T., Gigolashvili, T., Takamune, M., Sasazaki, Y., Watanabe, M., Nakashita, H., Fernie, A. R., Saito, K., Takahashi, H., Hubberten, H., Hoefgen, R., & Maruyama-Nakashita, A. (2016). Sulfur deficiency–induced repressor proteins optimize glucosinolate biosynthesis in plants. *Science Advances*, *2*(10), e1601087. https://doi.org/10.1126/sciadv.1601087

Alberts, B., Johnson, A., Lewis, J., Raff, M., Roberts, K., & Walter, P. (2013). *Essential Cell Biology* (4th ed.). Garland Science.

Alonso, J. M. (2003). Genome-wide insertional mutagenesis of arabidopsis thaliana. *Science*, 301(5633), 653-657. https://doi.org/10.1126/science.1086391

Álvarez-Aragón, R., Haro, R., Benito, B., & Rodríguez-Navarro, A. (2015). Salt intolerance in Arabidopsis: shoot and root sodium toxicity, and inhibition by sodium-plus-potassium overaccumulation. *Planta*, *243*(1), 97-114. https://doi.org/10.1007/s00425-015-2400-7

Amundsen, I. (2011). *Analysis of the Arabidopsis PP2A regulatory subunit B´θ* [Unpublished master's thesis]. University of Stavanger.

Antolín-Llovera, M., Leivar, P., Arró, M., Ferrer, A., Boronat, A., & Campos, N. (2011). Modulation of plant HMG-CoA reductase by protein phosphatase 2A: positive and negative control at a key node of metabolism. *Plant Signaling & Behavior*, *6*(8), 1127-1131. https://doi.org/10.4161/psb.6.8.16363

Apel, K., & Hirt, H. (2004). Reactive oxygen species: metabolism, oxidative stress, and signal transduction. *Annual Review of Plant Biology*, *55*, 373-399. https://doi.org/10.1146/annurev.arplant.55.031903.141701

Apse, M. P., & Blumwald, E. (2007). Na^+ transport in plants. *FEBS Letters*, *581*(12), 2247-2254. https://doi.org/10.1016/j.febslet.2007.04.014

Ballesteros, I., Domínguez, T., Sauer, M., Paredes, P., Duprat, A., Rojo, E., Sanmartín, M., & Sánchez-Serrano, J. J. (2013). Specialized functions of the PP2A subfamily II catalytic subunits PP2A-C3 and PP2A-C4 in the distribution of auxin fluxes and development in Arabidopsis. *The Plant Journal*, *73*(5), 862-872. https://doi.org/10.1111/tpj.12078

Bienfait, H. F., Bino, R. J., Bliek, A. M., Duivenvoorden, J. F., & Fontaine, J. M. (1983). Characterization of ferric reducing activity in roots of Fe-deficient Phaseolus vulgaris. *Physiologia Plantarum*, *59*(2), 196-202. https://doi.org/10.1111/j.1399-3054.1983.tb00757.x

Brautigan, D. L. (2013). Protein ser/ Thr phosphatases--the ugly ducklings of cell signalling. *FEBS Journal*, *280*(2), 324-345. https://doi.org/10.1111/j.1742-4658.2012.08609.x

Brumbarova, T., Bauer, P., & Ivanov, R. (2015). Molecular mechanisms governing Arabidopsis iron uptake. *Trends in Plant Science*, *20*(2), 124-133. https://doi.org/10.1016/j.tplants.2014.11.004

Camilleri, C., Azimzadeh, J., Pastuglia, M., Bellini, C., Grandjean, O., & Bouchez, D. (2002). The Arabidopsis TONNEAU2 gene encodes a putative novel protein phosphatase 2A regulatory subunit essential for the control of the cortical cytoskeleton. *The Plant Cell*, *14*, 833-845. https://doi.org/10.1105/tpc.010402

Cassin, G., Mari, S., Curie, C., Briat, J., & Czernic, P. (2009). Increased sensitivity to iron deficiency in Arabidopsis thaliana overaccumulating nicotianamine. *Journal of Experimental Botany*, *60*(4), 1249-1259. https://doi.org/10.1093/jxb/erp007

Castermans, D., Somers, I., Kriel, J., Louwet, W., Wera, S., Versele, M., Janssens, V., & Thevelein, J. M. (2012). Glucose-induced posttranslational activation of protein phosphatases PP2A and PP1 in yeast. *Cell Research*, *22*(6), 1058-1077. https://doi.org/10.1038/cr.2012.20

Chen, J., Hu, R., Zhu, Y., Shen, G., & Zhang, H. (2014). Arabidopsis phosphotyrosyl phosphatase activator is essential for protein phosphatase 2A holoenzyme assembly and plays important roles in hormone signaling, salt stress response, and plant development. *Plant Physiology*, *166*(3), 1519-1534. https://doi.org/10.1104/pp.114.250563

Claeys, H., Van Landeghem, S., Dubois, M., Maleux, K., & Inzé, D. (2014). What is stress? dose-response effects in commonly used in vitro stress assays. *Plant Physiology*, *165*(2), 519-527. https://doi.org/10.1104/pp.113.234641

Cohen, P. (2001). The role of protein phosphorylation in human health and disease. *European Journal of Biochemistry*, *268*(19), 5001-5010. https://doi.org/10.1046/j.0014-2956.2001.02473.x

Colucci, G., Apone, F., Alyeshmerni, N., Chalmers, D., & Chrispeels, M. J. (2002). GCR1, the putative Arabidopsis G protein-coupled receptor gene is cell cycle-regulated, and its overexpression abolishes seed dormancy and shortens time to flowering. *Proceedings of the National Academy of Sciences*, *99*(7), 4736-4741. https://doi.org/10.1073/pnas.072087699

Cramer, G. R., Urano, K., Delrot, S., Pezzotti, M., & Shinozaki, K. (2011). Effects of abiotic stress on plants: a systems biology perspective. *BMC Plant Biology*, *11*(1), 163. https://doi.org/10.1186/1471-2229-11-163

Creighton, M. T., Kolton, A., Kataya, A. R., Maple-Grødem, J., Averkina, I. O., Heidari, B., & Lillo, C. (2017). Methylation of protein phosphatase 2A-influence of regulators and environmental stress factors. *Plant, Cell & Environment*, *40*(10), 2347-2358. https://doi.org/10.1111/pce.13038

De Baere, I., Derua, R., Janssens, V., Van Hoof, C., Waelkens, E., Merlevede, W., & Goris, J. (1999). Purification of porcine brain protein phosphatase 2A leucine carboxyl methyltransferase and cloning of the human homologue. *Biochemistry*, *38*(50), 16539-16547. https://doi.org/10.1021/bi991646a

DeLong, A. (2006). Switching the flip: protein phosphatase roles in signaling pathways. *Current Opinion in Plant Biology*, *9*(5), 470-477. https://doi.org/10.1016/j.pbi.2006.07.015

Deruere, J., Jackson, K., Garbers, C., Soll, D., & DeLong, A. (1999). The RCN1-encoded a subunit of protein phosphatase 2A increases phosphatase activity in vivo. *The Plant Journal*, *20*(4), 389-399. https://doi.org/10.1046/j.1365-313x.1999.00607.x

Epstein, E., & Bloom, A. J. (2005). *Mineral nutrition of plants. Principles and perspectives* (2nd ed.). Sinauer Associates.

Farkas, I., Dombrádi, V., Miskei, M., Szabados, L., & Koncz, C. (2007). Arabidopsis PPP family of serine/threonine phosphatases. *Trends in Plant Science*, *12*(4), 169-176. https://doi.org/10.1016/j.tplants.2007.03.003

Forieri, I., Sticht, C., Reichelt, M., Gretz, N., Hawkesford, M. J., Malagoli, M., Wirtz, M., & Hell, R. (2017). System analysis of metabolism and the transcriptome in Arabidopsis thaliana roots reveals differential co-regulation upon iron, sulfur and potassium deficiency. *Plant, Cell & Environment*, *40*(1), 95-107. https://doi.org/10.1111/pce.12842

Forieri, I., Wirtz, M., & Hell, R. (2013). Toward new perspectives on the interaction of iron and sulfur metabolism in plants. *Frontiers in Plant Science*, *4*. https://doi.org/10.3389/fpls.2013.00357

Fox, T. C., Shaff, J. E., Grusak, M. A., Norvell, W. A., Chen, Y., Chaney, R. L., & Kochian, L. V. (1996). Direct measurement of 59Fe-labeled Fe^{2+} influx in roots of pea using a chelator buffer system to control free Fe^{2+} in solution. https://doi.org/ 10.1104/pp.111.1.93

Garai, S., & Tripathy, B. C. (2018). Alleviation of nitrogen and sulfur deficiency and enhancement of photosynthesis in Arabidopsis thaliana by overexpression of uroporphyrinogen III methyltransferase (UPM1). *Frontiers in Plant Science*, *9*. https://doi.org/10.3389/fpls.2018.01365

Garbers, C., DeLong, A., Deruére, J., Bernasconi, P., & Söll, D. (1996). A mutation in protein phosphatase 2A regulatory subunit A affects auxin transport in Arabidopsis. *The EMBO Journal*, *15*(9), 2115-2124. https://doi.org/10.1002/j.1460-2075.1996.tb00565.x

Groves, M. R., Hanlon, N., Turowski, P., Hemmings, B. A., & Barford, D. (1999). The structure of the protein Phosphatase 2A PR65/A subunit reveals the conformation of its 15 tandemly repeated HEAT motifs. *Cell*, *96*(1), 99-110. https://doi.org/10.1016/s0092-8674(00)80963-0

Gruber, B. D., Giehl, R. F., Friedel, S., & Von Wirén, N. (2013). Plasticity of the Arabidopsis root system under nutrient deficiencies. *Plant Physiology*, *163*(1), 161-179. https://doi.org/10.1104/pp.113.218453

Guo, W., Chen, S., Hussain, N., Cong, Y., Liang, Z., & Chen, K. (2015). Magnesium stress signaling in plant: just a beginning. *Plant Signaling & Behavior*, *10*(3), e992287.

Gupta, B., & Huang, B. (2014). Mechanism of salinity tolerance in plants: physiological, biochemical, and molecular characterization. *International Journal of Genomics*, *2014*, 1-18. https://doi.org/10.1155/2014/701596

He, X., Anderson, J. C., Pozo, O. D., Gu, Y., Tang, X., & Martin, G. B. (2004). Silencing of subfamily I of protein phosphatase 2A catalytic subunits results in activation of plant defense responses and localized cell death. *The Plant Journal*, *38*(4), 563-577. https://doi.org/10.1111/j.1365-313x.2004.02073.x

Heidari, B., Matre, P., Nemie-Feyissa, D., Meyer, C., Rognli, O. A., Møller, S. G., & Lillo, C. (2011). Protein phosphatase 2A B55 and A regulatory subunits interact with nitrate reductase and are essential for nitrate reductase activation. *Plant Physiology*, *156*(1), 165-172. https://doi.org/10.1104/pp.111.172734

Heidari, B., Nemie-Feyissa, D., Kangasjärvi, S., & Lillo, C. (2013). Antagonistic regulation of flowering time through distinct regulatory subunits of protein phosphatase 2A. *PLoS ONE*, *8*(7), e67987. https://doi.org/10.1371/journal.pone.0067987

Hernández, J. A., Ferrer, M. A., Jiménez, A., Barceló, A. R., & Sevilla, F. (2001). Antioxidant systems and $O_2^{\cdot -}/H_2O_2$ production in the apoplast of pea leaves. Its relation with salt-induced necrotic lesions in minor veins. *Plant Physiology*, *127*(3), 817-831. https://doi.org/10.1104/pp.010188

Hoagland, D. R., & Arnon, D. I. (1950). The water-culture method for growing plants without soil. *Circular California Agricultural Experiment Station*, *347*, 1-32. https://doi.org/10.5962/bhl.title.60957http://hdl.handle.net/2027/uc2.ark:/13960/t51g1sb8j

Hu, R., Zhu, Y., Wei, J., Chen, J., Shi, H., Shen, G., & Zhang, H. (2016). Overexpression of PP2A-C5 that encodes the catalytic subunit 5 of protein phosphatase 2A in Arabidopsis confers better root and shoot development under salt conditions. *Plant, Cell & Environment*, *40*(1), 150-164. https://doi.org/10.1111/pce.12837

Humphrey, S. J., James, D. E., & Mann, M. (2015). Protein phosphorylation: a major switch mechanism for metabolic regulation. *Trends in Endocrinology & Metabolism*, *26*(12), 676-687. https://doi.org/10.1016/j.tem.2015.09.013

Janssens, V., & Goris, J. (2001). Protein phosphatase 2A: a highly regulated family of serine/threonine phosphatases implicated in cell growth and signalling. *Biochemical Journal*, *353*, 417-439. https://doi.org/10.1042/0264-6021:3530417

Janssens, V., Longin, S., & Goris, J. (2008). PP2A holoenzyme assembly: in Cauda venenum (the sting is in the tail). *Trends in Biochemical Sciences*, *33*(3), 113-121. https://doi.org/10.1016/j.tibs.2007.12.004

Jeong, J., & Connolly, E. L. (2009). Iron uptake mechanisms in plants: functions of the FRO family of ferric reductases. *Plant Science*, *176*(6), 709-714. https://doi.org/10.1016/j.plantsci.2009.02.011

Jeong, J., Cohu, C., Kerkeb, L., Pilon, M., Connolly, E. L., & Guerinot, M. L. (2008). Chloroplast Fe(III) chelate reductase activity is essential for seedling viability under iron limiting conditions. *Proceedings of the National Academy of Sciences*, *105*(30), 10619-10624. https://doi.org/10.1073/pnas.0708367105

Jiang, K., Moe-Lange, J., Hennet, L., & Feldman, L. J. (2016). Salt stress affects the redox status of Arabidopsis root meristems. *Frontiers in Plant Science*, *7*. https://doi.org/ 10.3389/fpls.2016.00081

Jonassen, E. M., Heidari, B., Nemie-Feyissa, D., Matre, P., & Lillo, C. (2011). Protein phosphatase 2A regulatory subunits are starting to reveal their functions in plant metabolism and development. *Plant Signaling & Behavior*, *6*(8), 1216-1218. https://doi.org/10.4161/psb.6.8.16180

Kalhor, H. R., Luk, K., Ramos, A., Zobel-Thropp, P., & Clarke, S. (2001). Protein phosphatase methyltransferase 1 (Ppm1p) is the sole activity responsible for modification of the major forms of protein phosphatase 2A in yeast. *Archives of Biochemistry and Biophysics*, *395*, 239-245. https://doi.org/10.1006/abbi.2001.2558

Kerk, D., Bulgrien, J., Smith, D. W., Barsam, B., Veretnik, S., & Gribskov, M. (2002). The complement of protein phosphatase catalytic subunits encoded in the genome of Arabidopsis. *Plant Physiology*, *129*(2), 908-925. https://doi.org/10.1104/pp.004002

Kerk, D., Templeton, G., & Moorhead, G. B. (2008). Evolutionary radiation pattern of novel protein phosphatases revealed by analysis of protein data from the completely sequenced genomes of humans, green algae, and higher plants. *Plant Physiology*, *146*(2), 351-367. https://doi.org/10.1104/pp.107.111393

Kimura, Ushiwatari, Suyama, Tominaga-Wada, Wada, & Maruyama-Nakashita. (2019). Contribution of root hair development to sulfate uptake in Arabidopsis. *Plants*, *8*(4), 106. https://doi.org/10.3390/plants8040106

Koen, E., Besson-Bard, A., Duc, C., Astier, J., Gravot, A., Richaud, P., Lamotte, O., Boucherez, J., Gaymard, F., & Wendehenne, D. (2013). Arabidopsis thaliana nicotianamine synthase 4 is required for proper response to iron deficiency and to cadmium exposure. *Plant Science*, *209*, 1-11. https://doi.org/10.1016/j.plantsci.2013.04.006

Kwak, J. M., Moon, J., Murata, Y., Kuchitsu, K., Leonhardt, N., DeLong, A., & Schroeder, J. I. (2002). Disruption of a guard cell-expressed protein phosphatase 2A regulatory subunit, RCN1, confers abscisic acid insensitivity in Arabidopsis. *The Plant Cell*, *14*(11), 2849-2861. https://doi.org/10.1105/tpc.003335

Larsen, P. B., & Cancel, J. D. (2003). Enhanced ethylene responsiveness in the Arabidopsis eer1 mutant results from a loss-of-function mutation in the protein phosphatase 2A A regulatory subunit, RCN1. *The Plant Journal*, *34*(5), 709-718. https://doi.org/10.1046/j.1365-313x.2003.01762.x

Lee, J. A., & Pallas, D. C. (2007). Leucine carboxyl methyltransferase-1 is necessary for normal progression through mitosis in mammalian cells. *Journal of Biological Chemistry*, *282*, 30974-30984. https://doi.org/10.1074/jbc.m704861200

Lillo, C., Kataya, A. R., Heidari, B., Creighton, M. T., Nemie-Feyissa, D., Ginbot, Z., & Jonassen, E. M. (2014). Protein phosphatases PP2A, PP4 and PP6: mediators and regulators in development and responses to environmental cues. *Plant, Cell & Environment*, *37*(12), 2631-2648. https://doi.org/10.1111/pce.12364

Lillo, C., Lea, U. S., & Ruoff, P. (2007). Nutrient depletion as a key factor for manipulating gene expression and product formation in different branches of the flavonoid pathway. *Plant, Cell & Environment*, *31*(5), 587-601. https://doi.org/10.1111/j.1365-3040.2007.01748.x

Limon Pacheco, J. H., Carballo, M. A., & Gonsebatt, M. E. (2017). Antioxidants against environmental factor-induced oxidative stress. In *Nutritional Antioxidant Therapies: Treatments and Perspective* (pp. 189-215). Springer.

Luan, S. (2003). Protein phosphatases in plants. *Annual Review of Plant Biology*, *54*(1), 63-92. https://doi.org/10.1146/annurev.arplant.54.031902.134743

Maselli, G. A., Slamovits, C. H., Bianchi, J. I., Vilarrasa-Blasi, J., Caño-Delgado, A. I., & Mora-García, S. (2014). Revisiting the evolutionary history and roles of protein phosphatases with kelch-like domains in plants. *Plant Physiology*, *164*(3), 1527-1541. https://doi.org/10.1104/pp.113.233627

Meimoun, P., Ambard-Bretteville, F., Colas-des Francs-Small, C., Valot, B., & Vidal, J. (2007). Analysis of plant phosphoproteins. *Analytical Biochemistry*, *371*(2), 238-246. https://doi.org/10.1016/j.ab.2007.08.022

Moorhead, G., De Wever, V., Templeton, G., & Kerk, D. (2009). Evolution of protein phosphatases in plants and animals. *Biochemical Journal*, *417*(2), 401-409. https://doi.org/10.1042/bj20081986

Mumby, M. (2007). The 3D structure of protein phosphatase 2A: new insights into a ubiquitous regulator of cell signaling. *ACS Chemical Biology*, *2*(2), 99-103. https://doi.org/10.1021/cb700021z

Munns, R., & Tester, M. (2008). Mechanisms of salinity tolerance. *Annual Review of Plant Biology*, *59*(1), 651-681. https://doi.org/10.1146/annurev.arplant.59.032607.092911

Murashige, T., & Skoog, F. (1962). A revised medium for rapid growth and bio assays with tobacco tissue cultures. *Physiologia Plantarum*, *15*(3), 473-497. https://doi.org/10.1111/j.1399-3054.1962.tb08052.x

Myouga, F., Hosoda, C., Umezawa, T., Iizumi, H., Kuromori, T., Motohashi, R., Shono, Y., Nagata, N., Ikeuchi, M., & Shinozaki, K. (2008). A heterocomplex of iron superoxide dismutases defends chloroplast nucleoids against oxidative stress and is essential for chloroplast development in Arabidopsis. *The Plant Cell*, *20*(11), 3148-3162. https://doi.org/10.1105/tpc.108.061341

Niu, Y., Jin, G., & Zhang, Y. S. (2014). Root development under control of magnesium availability. *Plant Signaling & Behavior*, *9*(9), e29720. https://doi.org/10.4161/psb.29720

Noctor, G., Mhamdi, A., & Foyer, C. H. (2016). Oxidative stress and antioxidative systems: recipes for successful data collection and interpretation. *Plant, Cell and Environment*, *39*, 1140-1160. https://doi.org/ 10.1111/pce.12726

Okamura, H., Yoshida, K., Morimoto, H., Teramachi, J., Ochiai, K., Haneji, T., & Yamamoto, A. (2017). Role of protein phosphatase 2A in osteoblast differentiation and function. *Journal of Clinical Medicine*, *6*(3), 23. https://doi.org/10.3390/jcm6030023

Olsen, J. V., Blagoev, B., Gnad, F., Macek, B., Kumar, C., Mortensen, P., & Mann, M. (2006). Global, in vivo, and site-specific phosphorylation dynamics in signaling networks. *Cell*, *127*(3), 635-648. https://doi.org/10.1016/j.cell.2006.09.026

Parida, A. K., & Das, A. B. (2005). Salt tolerance and salinity effects on plants: a review. *Ecotoxicology and Environmental Safety*, *60*(3), 324-349. https://doi.org/10.1016/j.ecoenv.2004.06.010

Park, H., Lee, K., Park, E. S., Oh, S., Yan, R., Zhang, J., Beach, T. G., Adler, C. H., Voronkov, M., Braithwaite, S. P., Stock, J. B., & Mouradian, M. M. (2016). Dysregulation of protein phosphatase 2A in parkinson disease and dementia with lewy bodies. *Annals of Clinical and Translational Neurology*, *3*(10), 769-780. https://doi.org/10.1002/acn3.337

Pérez-Callejón, E., Casamayor, A., Pujol, G., Camps, M., Ferrer, A., & Ariño, J. (1998). Molecular cloning and characterization of two phosphatase 2A catalytic subunit genes from Arabidopsis thaliana. *Gene, 209*(1-2), 105-112. https://doi.org/10.1016/s0378-1119(98)00013-4

Pernas, M., García-Casado, G., Rojo, E., Solano, R., & Sánchez-Serrano, J. J. (2007). A protein phosphatase 2A catalytic subunit is a negative regulator of abscisic acid signalling. *The Plant Journal*, *51*(5), 763-778. https://doi.org/10.1111/j.1365-313x.2007.03179.x

Pesaresi, P., Pribil, M., Wunder, T., & Leister, D. (2011). Dynamics of reversible protein phosphorylation in thylakoids of flowering plants: The roles of STN7, STN8 and TAP38. *Biochimica et Biophysica Acta (BBA) - Bioenergetics*, *1807*(8), 887-896. https://doi.org/10.1016/j.bbabio.2010.08.002

Qados, A., & S, A. M. (2011). Effect of salt stress on plant growth and metabolism of bean plant Vicia faba (L.). *Journal of the Saudi Society of Agricultural Sciences*, *10*(1), 7-15. https://doi.org/10.1016/j.jssas.2010.06.002

Rahnama, A., James, R. A., Poustini, K., & Munns, R. (2010). Stomatal conductance as a screen for osmotic stress tolerance in durum wheat growing in saline soil. *Functional Plant Biology*, *37*(3), 255-263. https://doi.org/10.1071/fp09148

Raimi, O. G., Hammed, A. M., Alaebo, P. O., Fajana, A. A., & Fashina-Bombata, H. A. (2014). Partial characterization of alkaline phosphatase in some species of fresh water Cichlids ('Wesafu', Oreochromis niloticus and Sarotherodon melanotheron). *International Journal of Modern Biochemistry*, *3*(1), 7-17.

Robinson, N. J., Procter, C. M., Connolly, E. L., & Guerinot, M. L. (1999). A ferric-chelate reductase for iron uptake from soils. *Nature*, *397*(6721), 694-697. https://doi.org/10.1038/17800

Sharma, P., & Dubey, R. S. (2005). Drought induces oxidative stress and enhances the activities of antioxidant enzymes in growing rice seedlings. *Plant Growth Regulation, 46,* 209-221. https://doi.org/10.1007/s10725-005-0002-2

Sharma, P., Jha, A. B., Dubey, R. S., & Pessarakli, M. (2012). Reactive oxygen species, oxidative damage, and antioxidative defense mechanism in plants under stressful conditions. *Journal of Botany, 2012,* 1-26. https://doi.org/10.1155/2012/217037

Shrivastava, P., & Kumar, R. (2015). Soil salinity: a serious environmental issue and plant growth promoting bacteria as one of the tools for its alleviation. *Saudi Journal of Biological Sciences 22, 123-131 , 22*(2), 123-131. https://doi.org/10.1016/j.sjbs.2014.12.001

Sontag, E. (2001). Protein phosphatase 2A: the Trojan Horse of cellular signaling. *Cell Signal, 13*(1), 7-16. https://doi.org/10.1016/s0898-6568(00)00123-6

Sontag, J., Wasek, B., Taleski, G., Smith, J., Arning, E., Sontag, E., & Bottiglieri, T. (2014). Altered protein phosphatase 2A methylation and Tau phosphorylation in the young and aged brain of methylenetetrahydrofolate reductase (MTHFR) deficient mice. *Frontiers in Aging Neuroscience, 6*. https://doi.org/10.3389/fnagi.2014.00214

Sperotto, R. A., Ricachenevsky, F. K., Williams, L. E., Vasconcelos, M. W., & Menguer, P. K. (2014). From soil to seed: micronutrient movement into and within the plant. *Frontiers in Plant Science, 5*. https://doi.org/10.3389/fpls.2014.00438

Stanevich, V., Jiang, L., Satyshur, K. A., Li, Y., Jeffrey, P. D., Li, Z., Menden, P., Semmelhack, M. F., & Xing, Y. (2011). The structural basis for tight control of PP2A methylation and function by LCMT-1. *Molecular Cell, 41*(3), 331-342. https://doi.org/10.1016/j.molcel.2010.12.030

Stepien, P., & Johnson, G. N. (2009). Contrasting responses of photosynthesis to salt stress in the glycophyte Arabidopsis and the halophyte Thellungiella: role of the plastid terminal oxidase as an alternative electron sink. *Plant Physiology, 149*(2), 1154-1165. https://doi.org/10.1104/pp.108.132407

Taiz, L., & Zeiger, E. (2010). Mineral nutrition. In *Plant physiology* (5th ed., pp. 108-130).

Taiz, L., & Zeiger, E. (2010). Responses and adaptations to abiotic stress. In *Plant physiology* (5th ed., pp. 756-782).

Tang, W., Yuan, M., Wang, R., Yang, Y., Wang, C., Oses-Prieto, J. A., Kim, T., Zhou, H., Deng, Z., Gampala, S. S., Gendron, J. M., Jonassen, E. M., Lillo, C., DeLong, A., Burlingame, A. L., Sun, Y., & Wang, Z. (2011). PP2A activates brassinosteroid-responsive gene expression and plant growth by dephosphorylating BZR1. *Nature Cell Biology, 13*(2), 124-131. https://doi.org/10.1038/ncb2151

Tanou, G., Molassiotis, A., & Diamantidis, G. (2009). Induction of reactive oxygen species and necrotic death-like destruction in strawberry leaves by salinity. *Environmental and Experimental Botany, 65*(2-3), 270-281. https://doi.org/10.1016/j.envexpbot.2008.09.005

Terol, J., Bargues, M., Carrasco, P., Pérez-Alonso, M., & Paricio, N. (2002). Molecular characterization and evolution of the protein phosphatase 2A B′ regulatory subunit family in plants. *Plant Physiology, 129*, 808-822. https://doi.org/10.1104/pp.020004

Torres-Ruiz, R. A., & Jurgens, G. (1994). Mutations in the FASS gene uncouple pattern formation and morphogenesis in Arabidopsis development. *Development (Cambridge, England), 120*, 2967-2978.

Tran, H. T., Nimick, M., Uhrig, R. G., Templeton, G., Morrice, N., Gourlay, R., DeLong, A., & Moorhead, G. B. (2012). Arabidopsis thaliana histone deacetylase 14 (HDA14) is an αlpha-tubulin deacetylase that associates with PP2A and enriches in the microtubule fraction with

the putative histone acetyltransferase ELP3. *The Plant Journal*, *71*(2), 263-272. https://doi.org/10.1111/j.1365-313x.2012.04984.x

Tsai, M., Cronin, N., & Djordjevic, S. (2011). The structure of human leucine carboxyl methyltransferase 1 that regulates protein phosphatase PP2A. *Acta Crystallographica Section D Biological Crystallography*, *67*(1), 14-24. https://doi.org/10.1107/s0907444910042204

Uhrig, R. G., Kerk, D., & Moorhead, G. B. (2013a). Evolution of bacterial-like phosphoprotein phosphatases in photosynthetic eukaryotes features ancestral mitochondrial or archaeal origin and possible lateral gene transfer. *PLANT PHYSIOLOGY*, *163*(4), 1829-1843. https://doi.org/10.1104/pp.113.224378

Uhrig, R. G., Labandera, A., & Moorhead, G. B. (2013b). Arabidopsis PPP family of serine/threonine protein phosphatases: Many targets but few engines. *Trends in Plant Science*, *18*(9), 505-513. https://doi.org/10.1016/j.tplants.2013.05.004

Vert, G., Grotz, N., Dédaldéchamp, F., Gaymard, F., Guerinot, M. L., Briat, J., & Curie, C. (2002). IRT1, an Arabidopsis transporter essential for iron uptake from the soil and for plant growth. *The Plant Cell*, *14*(6), 1223-1233. https://doi.org/10.1105/tpc.001388

Wang, H. U., Chevalier, D., Larue, C., Cho, S. K., & Walker, J. C. (2007). The protein phosphatases and protein kinases of Arabidopsis thaliana. *The Arabidopsis Book*. https://doi.org/10.1199/tab.0106

Waters, B. M., McInturf, S. A., & Stein, R. J. (2012). Rosette iron deficiency transcript and microRNA profiling reveals links between copper and iron homeostasis in Arabidopsis thaliana. *Journal of Experimental Botany*, *63*(16), 5903-5918. https://doi.org/10.1093/jxb/ers239

Wei, H., Ashby, D. G., Moreno, C. S., Ogris, E., Yeong, F. M., Corbett, A. H., & Pallas, D. C. (2001). Carboxymethylation of the PP2A catalytic subunit in Saccharomyces cerevisiae is required for efficient interaction with the B-type subunits Cdc55p and Rts1p. *Journal of Biological Chemistry*, *276*(2), 1570-1577. https://doi.org/10.1074/jbc.m008694200

Winter, D., Vinegar, B., Nahal, H., Ammar, R., Wilson, G. V., & Provart, N. J. (2007). An "Electronic Fluorescent Pictograph" browser for exploring and analyzing large-scale biological data sets. *PLoS ONE*, *2*(8), e718. https://doi.org/10.1371/journal.pone.0000718

Wu, G., Wang, X., Li, X., Kamiya, Y., Otegui, M. S., & Chory, J. (2011). Methylation of a phosphatase specifies dephosphorylation and degradation of activated brassinosteroid receptors. *Science Signaling*, *4*(172), ra29. https://doi.org/10.1126/scisignal.2001258

Wu, J., Tolstykh, T., Lee, J., Boyd, K., Stock, J. B., & Broach, J. R. (2000). Carboxyl methylation of the phosphoprotein phosphatase 2A catalytic subunit promotes its functional

association with regulatory subunits in vivo. *The EMBO Journal*, *19*(21), 5672-5681. https://doi.org/10.1093/emboj/19.21.5672

Xie, X., He, Z., Chen, N., Tang, Z., Wang, Q., & Cai, Y. (2019). The roles of environmental factors in regulation of oxidative stress in plant. *BioMed Research International*, *2019*, 1-11. https://doi.org/10.1155/2019/9732325

Zhao, F., Tausz, M., & De Kok, L. J. (2008). Role of sulfur for plant production in agricultural and natural ecosystems. *Sulfur Metabolism in Phototrophic Organisms*, 417-435. https://doi.org/10.1007/978-1-4020-6863-8_21

Zhou, H., Nussbaumer, C., Chao, Y., & DeLong, A. (2004). Disparate roles for the regulatory A subunit isoforms in Arabidopsis protein phosphatase 2A. *The Plant Cell*, *16*, 709-722. https://doi.org/10.1105/tpc.018994

Zhu, J., Fu, X., Koo, Y. D., Zhu, J., Jenney, F. E., Adams, M. W., Zhu, Y., Shi, H., Yun, D., Hasegawa, P. M., & Bressan, R. A. (2007). An enhancer mutant of Arabidopsis salt overly sensitive 3 mediates both ion homeostasis and the oxidative stress response. *Molecular and Cellular Biology*, *27*(14), 5214-5224. https://doi.org/10.1128/mcb.01989-06

Zolnierowicz, S., & Bollen, M. (2000). Protein phosphorylation and protein phosphatases. De panne, Belgium, September 19–24, 1999. *The EMBO Journal*, *19*(4), 483-488. https://doi.org/10.1093/emboj/19.4.483

APPENDIX

A. Phenotypic difference between WT and *lcmt1*

A.1 Arabidopsis grown in vermiculite

A.1.1 First experiment

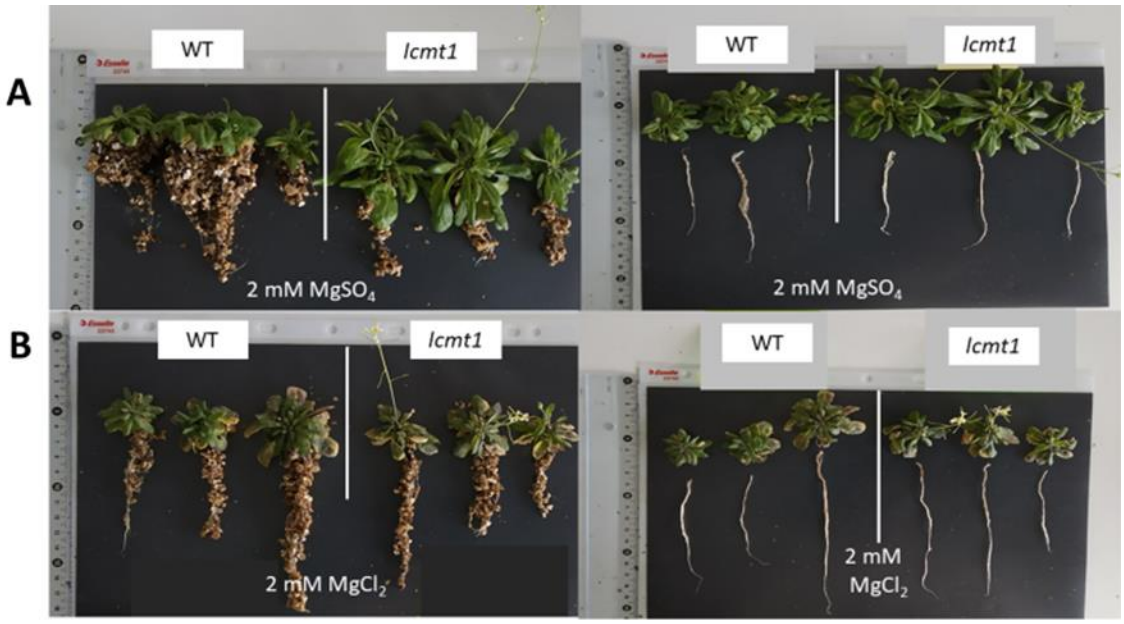

Figure A.1. Phenotype of Arabidopsis WT and *lcmt1* (5 plants of each) grown in vermiculite. Here, 3 representative plants from both WT and *lcmt1*, with and without vermiculite are shown in the images. **A.** Plants were treated with regular Hoagland solutions (2 mM $MgSO_4$) in 8 h light/16 h darkness for 5 weeks. **B.** WT and *lcmt1* treated with 2 mM $MgCl_2$ in 8 h light/16 h darkness for 5 weeks.

A.1.2 Second experiment

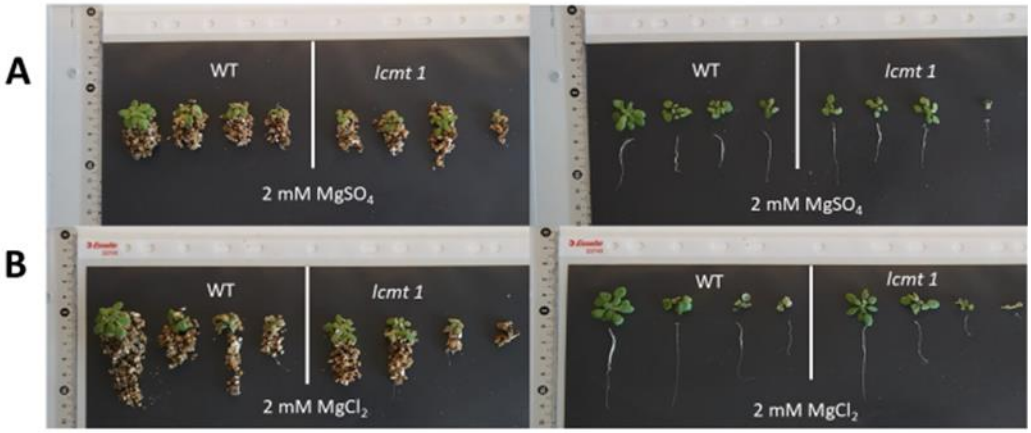

Figure A.2. Phenotype of Arabidopsis WT and *lcmt1* (5 plants of each) grown in vermiculite. Here, 4 representative plants from both WT and *lcmt1*, with and without vermiculite are shown in the images. **A.** Plants were treated with regular Hoagland solutions (2 mM $MgSO_4$) in 8 h light/16 h darkness for 2 weeks. **B.** WT and *lcmt1* treated with 2 mM $MgCl_2$ in 8 h light/16 h darkness for 2 weeks.

A.1.3 Third experiment

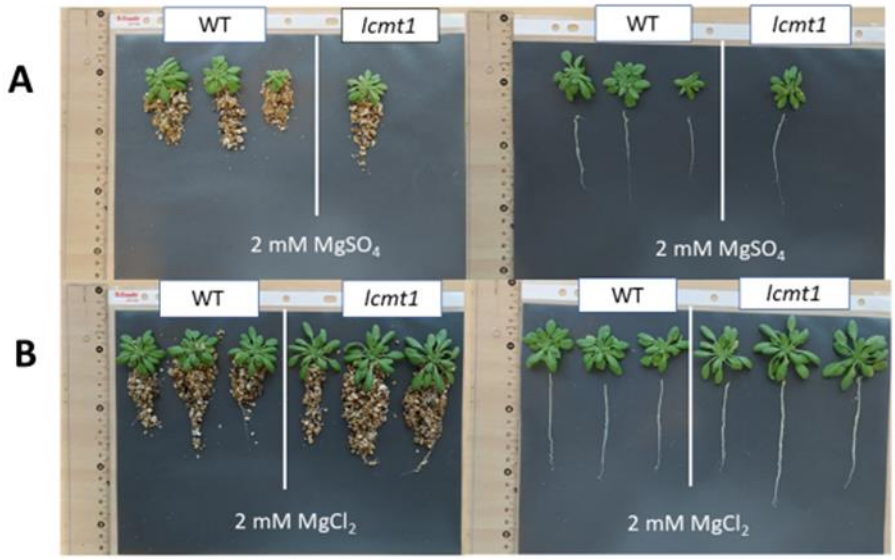

Figure A.3. Phenotype of Arabidopsis WT and *lcmt1* (5 plants of each) grown in vermiculite. The plants with and without vermiculite are shown in the images. **A.** Three representatives of WT and *lcmt1* were treated with Hoagland solutions of 2 mM $MgSO_4$ at 8 h light/16 h darkness for 4 weeks. **B.** Three representatives from both WT and *lcmt1* were treated with Hoagland solutions of 2 mM $MgCl_2$ at 8 h light/16 h darkness for 4 weeks.

A.1.4 Fourth experiment

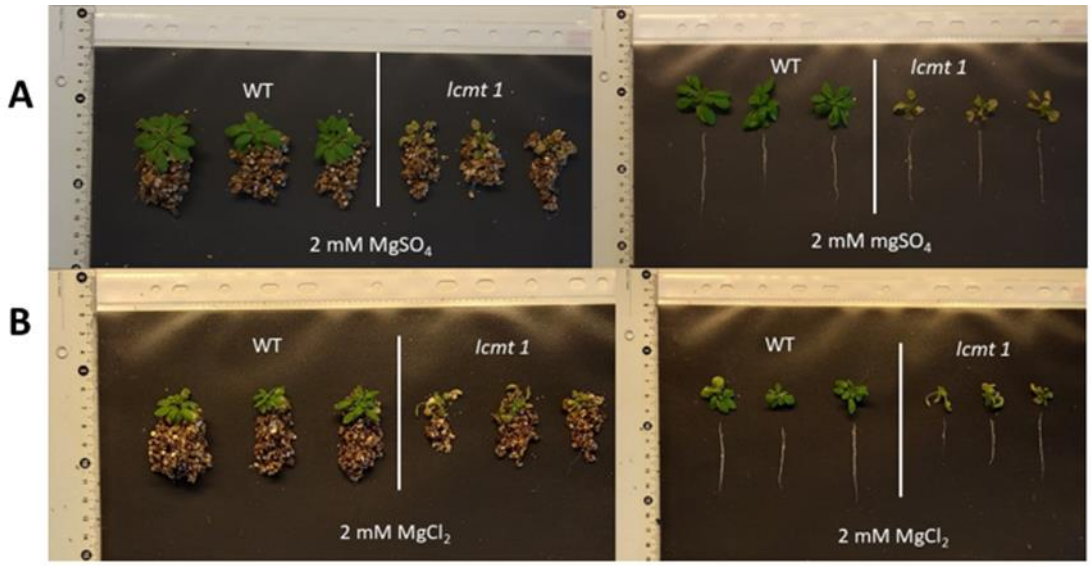

Figure A.4. Phenotype of Arabidopsis WT and *lcmt1* (5 plants of each) grown in vermiculite. Three representative plants from both WT and *lcmt1*, with and without vermiculite are shown in the images. **A.** Plants were treated with regular Hoagland solutions (2 mM $MgSO_4$) in 8 h light/16 h darkness for 3 weeks. **B.** WT and *lcmt1* treated with 2 mM $MgCl_2$ in 8 h light/16 h darkness for 3 weeks.

A.2. Arabidopsis grown in rockwool

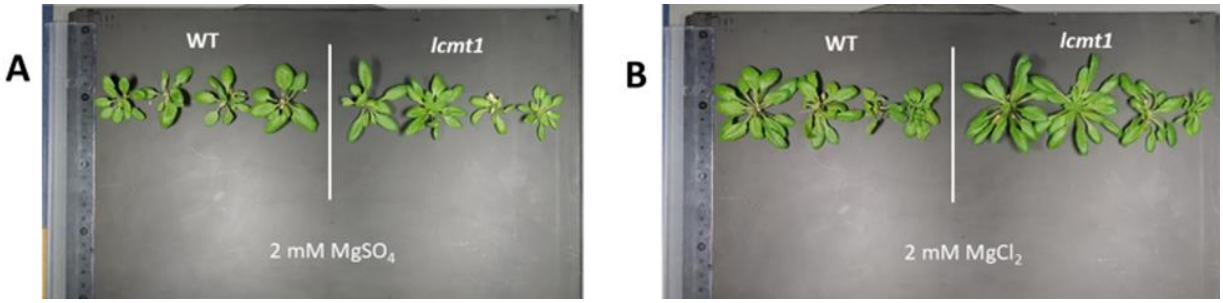

Figure A.5. Arabidopsis WT and *lcmt1* grown on rockwool. The plants were treated with Hoagland solutions at 8 h light/16 h darkness for 5 weeks. **A.** WT and mutant treated with regular Hoagland solution (2 mM $MgSO_4$). **B.** WT and mutant treated with Hoagland solutions of 2 mM $MgCl_2$.

B. Stress experiments

B.1. Sulphur experiment

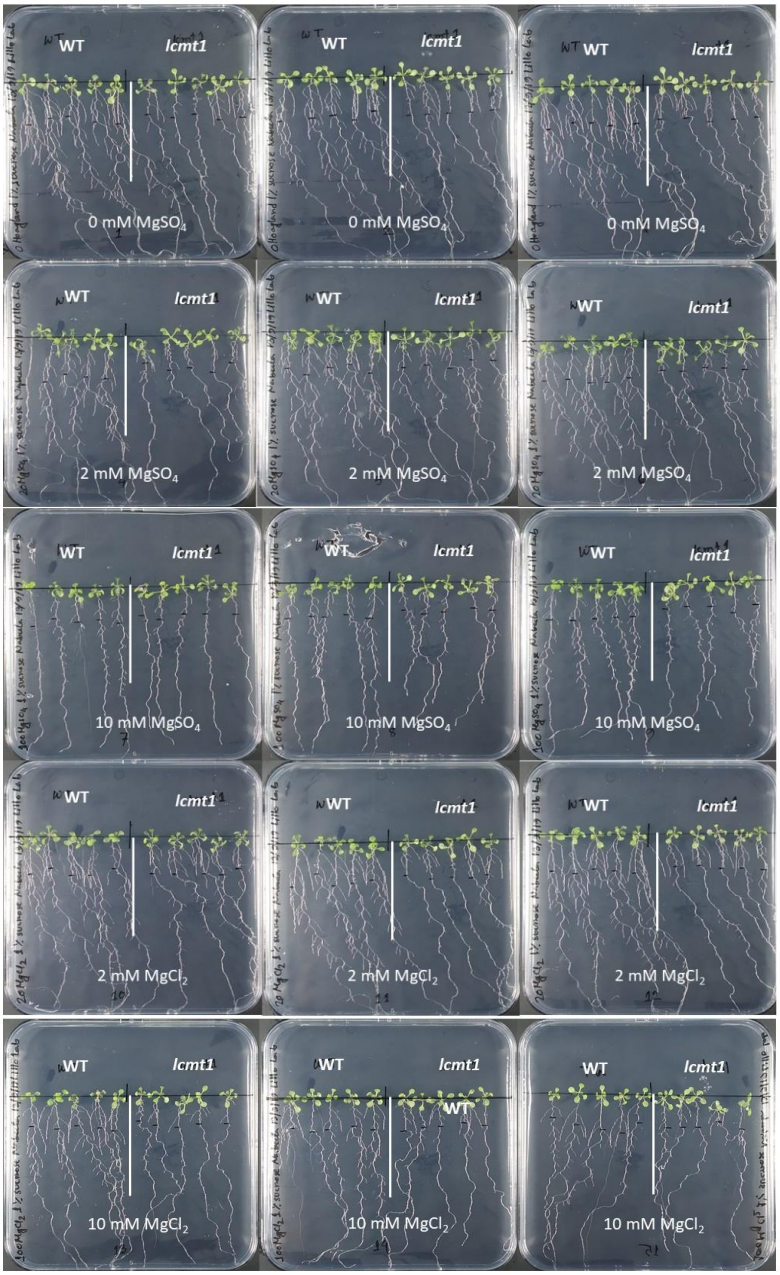

Figure B.1. Arabidopsis WT and *lcmt1* seedlings grown in Hoagland media. The WT and mutant seedlings were treated with 0 mM (without $MgSO_4$ and $MgCl_2$), 2mM $MgSO_4$ (control), 10 mM $MgSO_4$, 2 mM $MgCl_2$ and 10 mM $MgCl_2$ at dark for 3 d and at 16 h light/8 h darkness for 5 d. The seedlings were transferred to new plates with respective concentrations of Hoagland media and kept at 16 h light/8 h darkness for additional 7 d.

B.2. NaCl experiment

B.2.1. First NaCl experiment

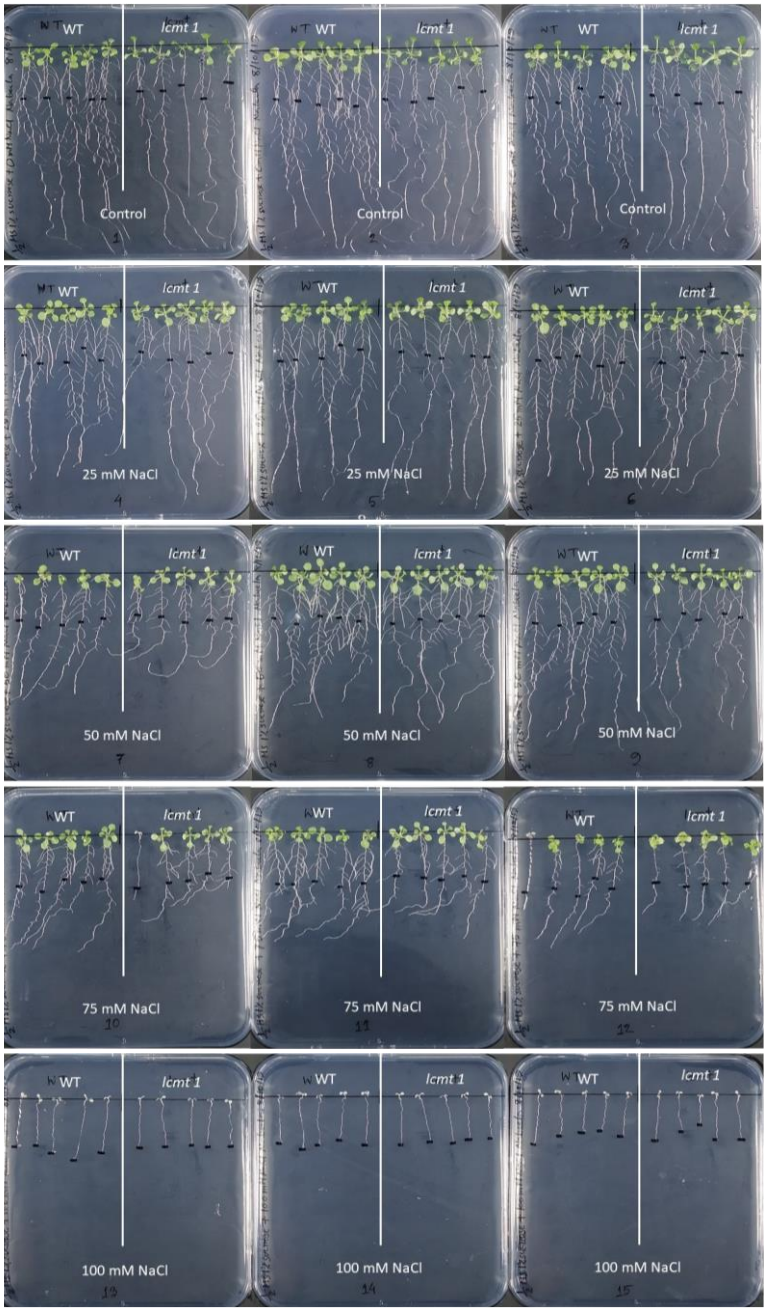

Figure B.2. Arabidopsis WT and *lcmt1* seedlings grown in ½ MS media with different NaCl treatment. The WT and *lcmt1* seedlings were grown in ½ MS media for 8 d (3 d at dark and 5 d at 16 h light/8 h dark). After 8 d, the seedlings were treated with control (only ½ MS media, no NaCl), 25 mM, 50 mM, 75 mM, and 100 mM NaCl at 16 h light/8 h darkness for additional 7 d. Three biological replicates were made for each treatment.

B.2.2. Second NaCl experiment

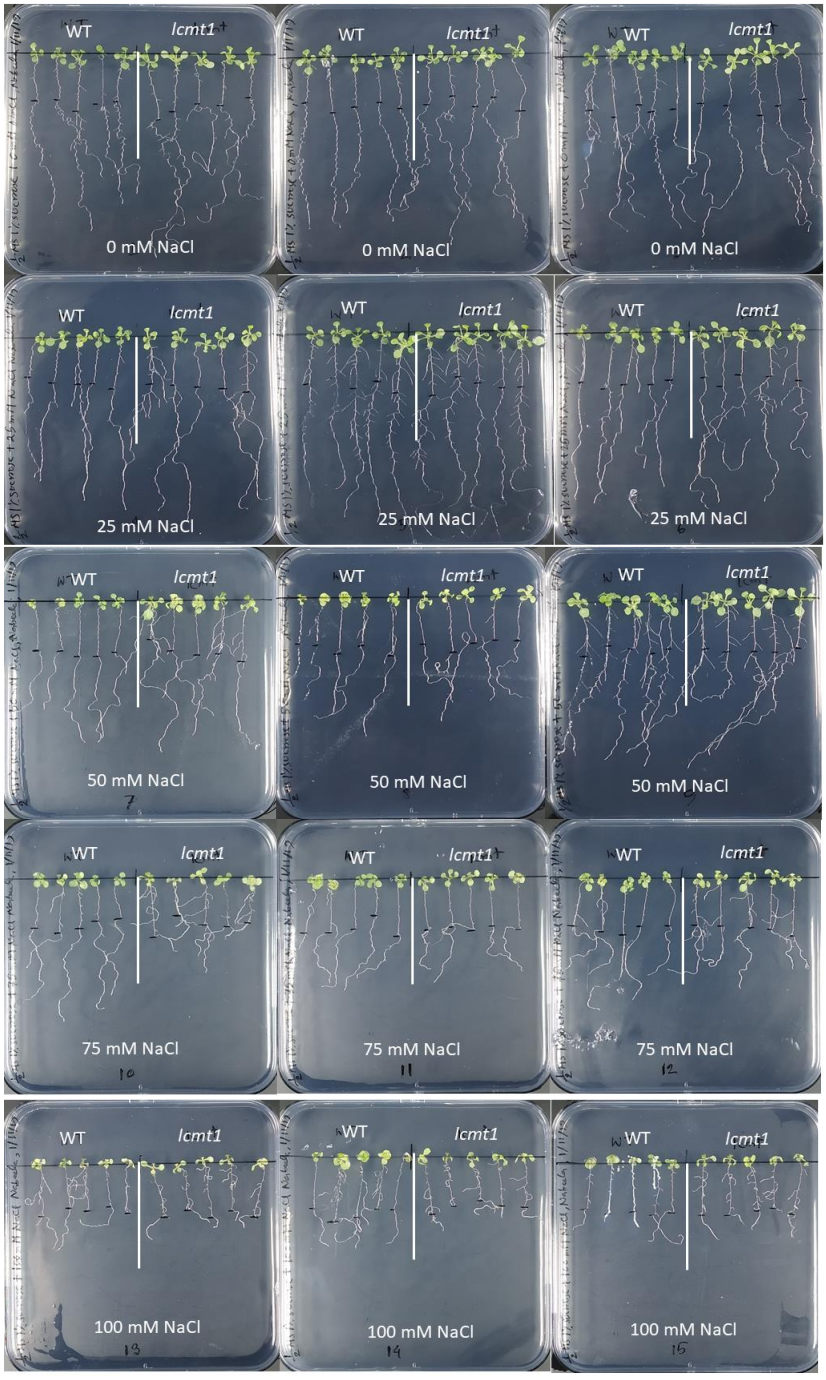

Figure B.3. Arabidopsis WT and *lcmt1* seedlings grown in ½ MS media with different NaCl treatment. The WT and *lcmt1* seedlings were grown in ½ MS media for 8 d (3 d at dark and 5 d at 16 h light/8 h dark). After 8 d, the seedlings were treated with control (only ½ MS media, no NaCl), 25 mM, 50 mM, 75 mM, and 100 mM NaCl at 16 h light/8 h darkness for additional 7 d. Three biological replicates were made for each treatment.

B.2.3. Third NaCl experiment

Figure B.4. Arabidopsis WT and *lcmt1* seedlings grown in ½ MS media with different NaCl treatment. The WT and *lcmt1* seedlings were grown in ½ MS media for 8 d (3 d at dark and 5 d at 16 h light/8 h dark). After 8 d, the seedlings were treated with control (only ½ MS media, no NaCl), 25 mM, 50 mM, 75 mM, and 100 mM NaCl at 16 h light/8 h darkness for additional 7 d. Three biological replicates were made for each treatment.

B.3. H_2O_2 experiment

B.3.1. Second H_2O_2 experiment

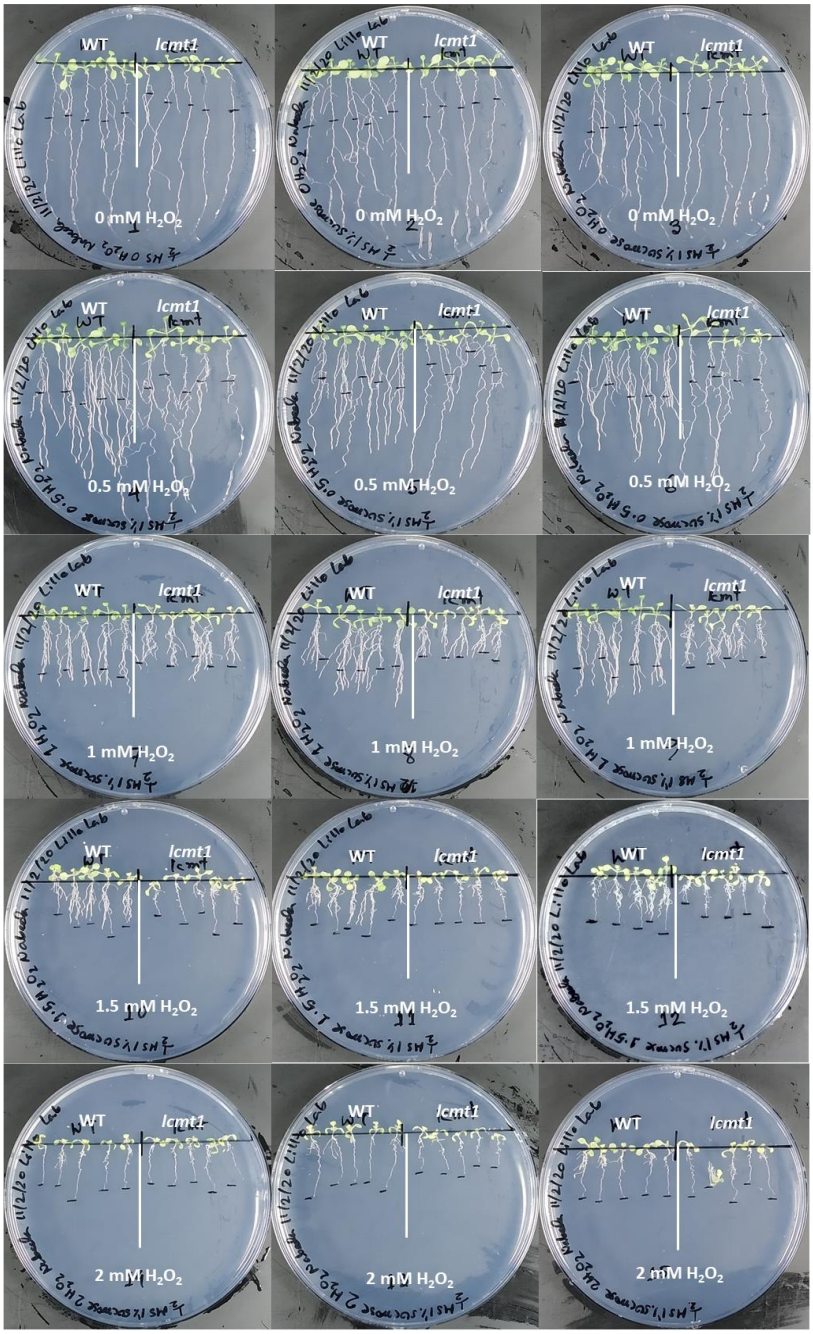

Figure B.5. Arabidopsis seedlings grown in petri dishes containing ½ MS media and different H_2O_2 treatments. The seedlings (5 WT and 5 *lcmt1* per plate) were grown in ½ MS media for 8 d (3 d at dark and 5 d at 16 h light/8 h dark). After 8 d, the seedlings were treated with control (only ½ MS media, no H_2O_2), 0.5 mM, 1 mM, 1.5 mM, and 2 mM H_2O_2 at 16 h light/8 h darkness for additional 7 d. Three biological replicates were made for each treatment.

B.3.2. Third H_2O_2 experiment

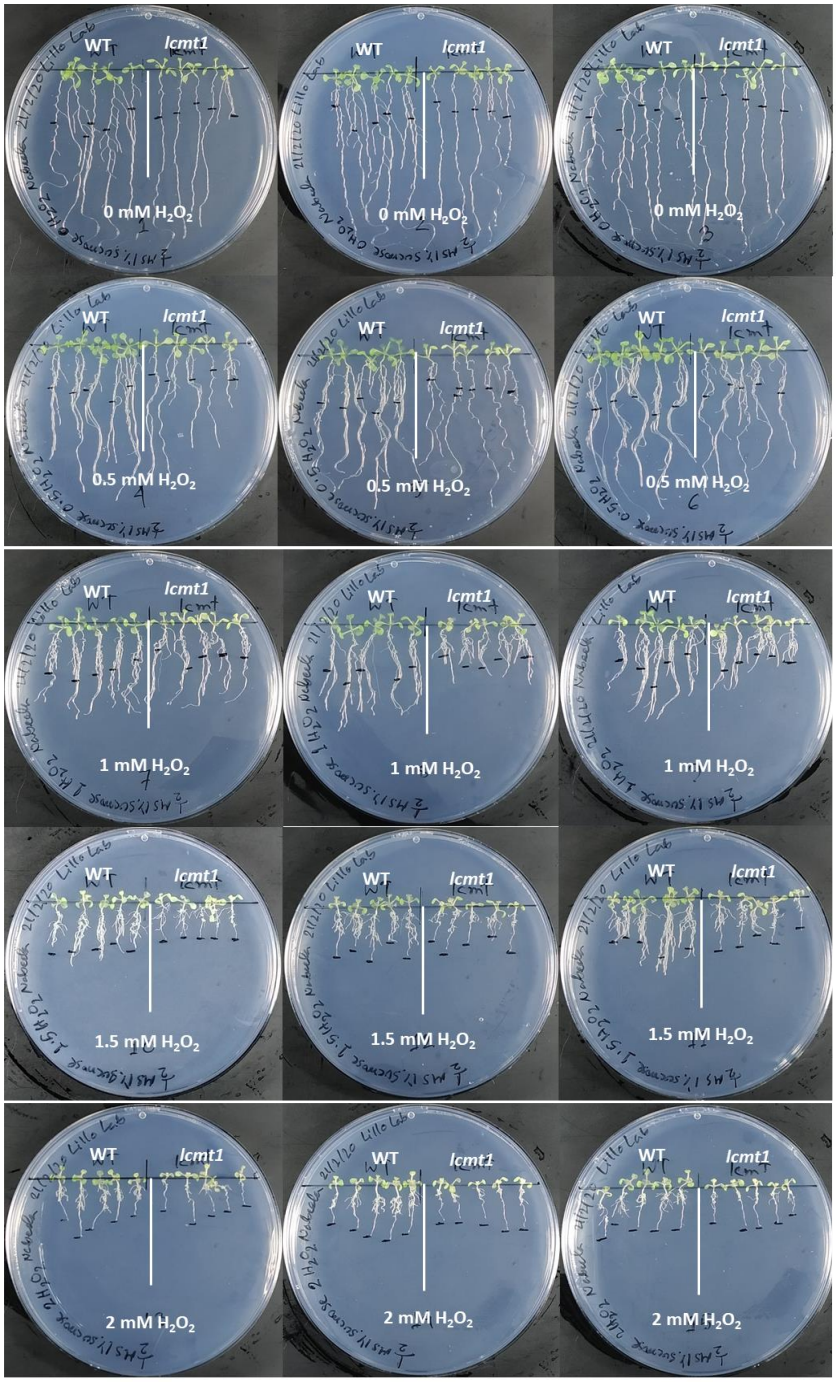

Figure B.6. Arabidopsis seedlings grown in petri dishes containing ½ MS media and different H_2O_2 treatments. The seedlings (5 WT and 5 *lcmt1* per plate) were grown in ½ MS media for 8 d (3 d at dark and 5 d at 16 h light/8 h dark). After 8 d, the seedlings were treated with control (only ½ MS media, no H_2O_2), 0.5 mM, 1 mM, 1.5 mM, and 2 mM H_2O_2 at 16 h light/8 h darkness for additional 7 d. Three biological replicates were made for each treatment.

C. Gene expression analysis

C.1. In-gel analysis

Table C.1. List of genes tested for expression in-gel analysis.

ATG number	Gene	Full name of gene	Description
AT4G19690	*IRT1*	IRON-REGULATED TRANSPORTER 1	Uptake of iron from the rhizosphere across the plasma membrane. Acts as the principal regulator of iron homeostasis. It mediates the heavy metals uptake under iron-deficiency
AT2G41240	*BHLH100*	BASIC HELIX-LOOP-HELIX PROTEIN 100	Cellular response to iron ion starvation, iron ion homeostasis, regulation of transcription by RNA polymerase II, regulation of transcription, DNA-templated, response to water deprivation
AT1G01580	*FRO2*	FERRIC REDUCTION OXIDASE 2	Iron ion homeostasis, oxidation-reduction process, reductive iron assimilation, response to bacterium
AT1G23020	*FRO3*	FERRIC REDUCTION OXIDASE 3	Encodes a ferric chelate reductase whose transcription is regulated by FIT1.
At5g49740	*FRO7*	FERRIC REDUCTION OXIDASE 7	Encodes a chloroplast ferric chelate reductase. Shows differential splicing and has three different mRNA products.
AT5G23980	*FRO4*	FERRIC REDUCTION OXIDASE 4	Encodes a ferric chelate reductase that is expressed at low levels in roots, shoots and cotyledons, but not flowers. Its transcription is regulated by FIT1.

AT4G33720	*CAP*	Cysteine-rich secretory proteins	Cellular response to ethylene stimulus, cellular response to iron ion, cellular response to nitric oxide, nicotianamine biosynthetic process, phloem transport, pollen development, pollen tube growth
AT5G04950	*NAS1*	NICOTIANAMINE SYNTHASE 1	Nicotianamine biosynthetic process, phloem transport, pollen development, pollen tube growth
AT5G56080	*ATNAS2*	NICOTIANAMINE SYNTHASE 2	Cellular response to ethylene stimulus, cellular response to iron ion, cellular response to nitric oxide, nicotianamine biosynthetic process, phloem transport, pollen development, pollen tube growth, response to zinc ion
AT1G56430	*ATNAS4*	NICOTIANAMINE SYNTHASE 4	Nicotianamine biosynthetic process, phloem transport, pollen development, pollen tube growth

C.2. Real-time PCR

Table C.2. List of TaqMan primers (Applied Biosystems, USA).

Accession number	**Gene**	**Full name of gene**	**Description**
At4g25100	*FSD1*	FE SUPEROXIDE DISMUTASE 1	Circadian rhythm, removal of superoxide radicals, response to cadmium ion and copper ion, response to light intensity, oxidative stress and ozone
At1g78000	*SULTR1;2*	SULFATE TRANSPORTER 1;2, SELENATE RESISTANT 1	Cellular response to sulfate starvation, selenate transport, sulfate transport

AT5g04950	*ATNAS1*	ARABIDOPSIS THALIANA NICOTIANAMINE SYNTHASE 1	Nicotianamine biosynthetic process, phloem transport, pollen development, pollen tube growth
At5g48850	*SDI1*	SULPHUR DEFICIENCY INDUCED 1	Cellular response to sulfur starvation, regulation of glucosinolate biosynthetic process, regulation of sulfur utilization
AT3G25800	*PP2AA2*	PROTEIN PHOSPHATASE 2A SUBUNIT A2	Regulates phosphorylation, response to cadmium ion
AT1G78870	*UBC35*	UBIQUITIN-CONJUGATING ENZYME 35	Post replication repair, protein K63-linked ubiquitination, response to cadmium ion, iron ion, root epidermal cell differentiation and ubiquitin-dependent protein catabolic process